

Abstract

Title of dissertation: CHARACTERIZATION OF PATHOGENIC AND NONPATHOGENIC STRAINS OF WEST NILE VIRUS AT THE BLOOD-BRAIN BARRIER

Katherine Louise Pankow Hussmann, Doctor of Philosophy, 2013

Dissertation directed by: Dr. Brenda Fredericksen
Department of Cell Biology and Molecular Genetics

West Nile virus (WNV) is an emerging pathogen that has the potential to cause severe neuropathologies, including encephalitis, acute flaccid paralysis, and meningitis. The severity of WNV infection is highly strain dependent, ranging from avirulent to highly neuropathogenic. Here, we assessed both viral and host-specific factors that contribute to WNV-mediated neuropathogenesis. We initially observed that despite inoculating equivalent levels of virus directly into the blood, mice inoculated with a nonvirulent strain of WNV, WNV-MAD78, exhibited increased survival compared to mice inoculated with a highly pathogenic strain, WNV-NY. Thus, one limitation for nonneuropathogenic WNV may exist at the blood-brain barrier (BBB). Therefore, we investigated the strain-specific contributions to establishing infection in the CNS by comparing the replication of WNV-MAD78 and WNV-NY in neurons, astrocytes, and microvascular endothelial cells, which comprise the neurovascular unit within the CNS. WNV-MAD78 replicated in and traversed brain microvascular endothelial cells as

efficiently as WNV-NY. Similar levels of replication for both strains were detected in neuronal cells. Thus, WNV-MAD78's nonneuropathogenic phenotype is not due to an intrinsic inability to invade the CNS or replicate within neurons. In contrast, WNV-MAD78 replicated to lower levels than WNV-NY in astrocytes. Reduced susceptibility of astrocytes to WNV-MAD78 was a result of a delay in initiating viral replication and an interferon-independent reduction in cell-to-cell spread. Further characterization indicated that the restriction to WNV-MAD78 cell-to-cell spread in astrocytes was due in part to the higher production of defective particles compared to WNV-NY infected astrocytes. To identify regions of the genome that contribute to this restriction, we generated recombinant viruses of WNV-NY and WNV-MAD78. While replication of a recombinant virus consisting of the structural proteins of WNV-NY and the nonstructural proteins of WNV-MAD78 was delayed in astrocytes, the virus reached peak viral titers similar to WNV-NY. In contrast, a recombinant virus comprised of the structural proteins from WNV-MAD78 and nonstructural proteins from WNV-NY replicated at a similar rate and level as WNV-MAD78 in astrocytes. Thus, protein composition of the virion is a determining factor in the level of WNV replication in astrocytes. Therefore, viral processing pathways within astrocytes may be attractive targets for managing WNV-induced neuropathologies.

CHARACTERIZATION OF PATHOGENIC AND NONPATHOGENIC STRAINS
OF WEST NILE VIRUS AT THE BLOOD-BRAIN BARRIER

by

Katherine Louise Pankow Hussmann

Dissertation submitted to the Faculty of the Graduate School of the
University of Maryland, College Park in partial fulfillment
Of the requirements for the degree of
Doctor of Philosophy
2013

Advisory Committee:

Assistant Professor Brenda Fredericksen, Chair
Professor Jeffrey Destefano
Associate Professor Patrick Kanold
Adjunct Professor Bernard Moss
Professor David Mosser

Copyright 2013 Katherine Louise Pankow Hussmann

All Rights Reserved

Dedication

The following dissertation research is dedicated to my husband, Patrick, and our beautiful son, Luke Thomas.

Acknowledgements

Throughout PhD journey, several groups of people were essential in keeping me focused, strengthened, and committed. I would first and foremost like to thank my dissertation research advisor, Dr. Brenda Fredericksen. When I first applied to Maryland, I was incredibly interested in the research being carried out in her lab. Now, over 5 years later, I am even more engaged and find the research fascinating. She has challenged me to develop skills, physical and mental, essential for scientific research. It has been a pleasure working for her, discussing scientific ideas, and being part of the daily grind. In addition, every one of my committee members, Dr. Bernard Moss, Dr. Patrick Kanold, Dr. David Mosser, and Dr. Jeffrey Destefano, have been helpful in developing my research and my training as a scientist. I also would like to thank Amy Beaven for all of her help in the core facilities here at UMD, Ken for help with the flow cytometer.

Of course, there are also the people in the lab who have gone through this all with me, side by side, figuring out all of the little details necessary. Lisa, Rianna, Camilla, and Kang, currently, and past members, Jen, Anna, and Tang- each one I have shared many memorable moments, from science and development as a scientist, to life events. Thank you all for being here to support me and my project, and in providing the nourishment to keep the wheels going.

We often hear horror stories about terrible roommates. However, I was incredibly lucky to have 3 wonderful roommates my first 2 years here. I hit the jackpot, and am thankful to have each one of them as a friend. I would also like

to thank the other graduate students, especially those who participated in the graduate student association and recruitment events. Also, to those who I would regularly work out with, as relieving stress through physical activity no doubt has kept me well-balanced throughout my PhD.

Last but definitely not least, I want to thank my family for supporting me through this. My parents, who brought me up to value education and let me explore with mixtures from nature at a young age, and my brother and sister. And, of course, a very special thank you to my wonderful husband Patrick, whose advice, ideas, and love I value more than anything. He continues to make me a better person daily, and I am so excited to be a new parent with you. Sometime soon, we may actually get to sleep 😊

Table of Contents

1. Dedication	ii
2. Acknowledgements	iii
3. Table of Contents	v
4. List of Tables	ix
5. List of Figures	x
6. List of Abbreviations	xiii
7. Chapter 1: Introduction	1
1.1 The Flaviviridae	1
1.2 WNV Classification and lineages	3
1.3 WNV transmission cycle	5
1.4 WNV Clinical presentation	5
1.5 WNV dissemination pathway	8
1.6 WNV Life cycle	9
1.7 The Blood-brain barrier	16
1.8 The role of Astrocytes in the CNS	21
1.9 Immune responses to WNV within the CNS	25
1.9.1 The cell intrinsic innate immune response	25
1.9.2 Amplification of the antiviral response	29
1.9.3 The proinflammatory response to WNV	33
1.9.4 The adaptive immune response to WNV in the CNS	45
1.10 Significance of PhD Dissertation research	50

8. Chapter 2: Materials and Methods	54
9. Chapter 3: Differential replication for pathogenic and nonpathogenic strains of West Nile virus within astrocytes	
Abstract	75
Introduction	76
Results	
WNV-NY and WNV-MAD78 replicate to similar levels in neuronal cells	78
WNV-MAD78 efficiently infects and traverses human brain endothelial cells	80
WNV-MAD78 replication is restricted in co-cultures of HBMECs and HBCAs.	82
WNV-MAD78 replication within astrocytes is restricted at multiple steps in the virus life cycle	84
The reduced susceptibility of HBCAs to WNV-MAD78 is independent of type-I interferon (IFN)	89
Discussion	93
10. Chapter 4: Role of cellular processing in WNV infection in astrocytes	
Abstract	99
Introduction	100
Results	
WNV-MAD78 replication in astrocytes is not restricted by a secreted host factor	102

Astrocyte-derived WNV-MAD78 particles are less infectious than WNV-NY particles	103
WNV-MAD78 infectious particle production is partially limited by furin activity in astrocytes	108
WNV structural proteins contribute to infectious particle production in astrocytes	111
Discussion	114
11. Chapter 5: Observations on the contribution of cell types at the BBB to WNV neuropathogenesis	
Abstract	121
Introduction	122
Results	
Treatment with type-1 IFN but not TNF α inhibits WNV replication in HBMECs	127
WNV-MAD78 and WNV-NY initiate similar activation kinetics of the innate intracellular antiviral responses in HBMECs and HBCAs	128
CCL2 and CCL5 expression and localization in WNV-infected HBMECs.	135
CCL5 and CCL2 expression in WNV-infected astrocytes	138
Chemokine gradient induction in a co-culture model of the BBB	142
Effect of WNV infection on the integrity of an <i>in vitro</i> model of the BBB	142

WNV-NY-infected HBCAs express higher levels of CAMs	
compared to WNV-MAD78-infected HBCAs	145
WNV-NY and WNV-MAD78 replicate to low levels in THP1 cells	148
In vitro models of WNV infection and neuroinflammation at the	
BBB represent functional model systems	150
Discussion	153
12. Chapter 6: Antiviral responses and detection of virus in mice	
inoculated with a nonneuropathogenic strain of WNV compared to a	
neuropathogenic strain of WNV	
Abstract	159
Introduction	160
Results	
WNV-NY causes greater lethality than WNV-MAD76 in	
intravenously-inoculate mice.	162
Detection of WNV in intravenously-inoculated mice	163
Cytokine and chemokine levels in blood and brains of WNV-	
inoculated mice	167
Discussion	172
13. Chapter 7: Discussion of Dissertation Research	177
14. References	192

List of Tables

1. Table 1: WNV infection in mouse knockout experiments and effects in CNS
2. Table 2: Primers used in qRT-PCR
3. Table 3: Primers and enzymes used in construction of infectious Clones
4. Table 4: Detection of virus in intravenous mouse inoculations

List of Figures

Figure 1: Phylogenetic relationships within Flaviviridae

Figure 2: WNV classification

Figure 3: Map of WNV distribution worldwide

Figure 4: West Nile virus life cycle.

Figure 5: WNV genome

Figure 6: WNV particle processing

Figure 7: The BBB and mechanisms of neuroinvasion

Figure 8: The intracellular innate antiviral response

Figure 9: The IFN signal transduction pathway (the JAK/STAT pathway)

Figure 10: Proinflammatory cytokine synthesis and signalling

Figure 11: The extravasation process

Figure 12: Recognition of a WNV-infected neuron by a CD8⁺ T cell

Figure 13: Schematic for construction of infectious clones

Figure 14: WNV-NY and WNV-MAD78 replication in neuronal cells

Figure 15: WNV-NY and WNV-MAD78 replication in human brain microvascular endothelial cells.

Figure 16: WNV replication in an *in vitro* model of the BBB.

Figure 17: WNV replication in HBCAs.

Figure 18: Infectious virions released per cell and cell-to-cell spread in HBCAs

Figure 19: Role of type I IFN in limited WNV replication and spread in HBCAs.

Figure 20: WNV-MAD78 replication in astrocytes is not restricted via canonical pathways.

Figure 21: WNV-MAD78 particles derived from astrocytes are less infectious than WNV-NY particles derived in astrocytes.

Figure 22: Furin activity in astrocytes is greater than that in endothelial cells and plays a role in inhibiting WNV-MAD78 infectious particle production.

Figure 23: Structural proteins of WNV contribute to infectious particle production in astrocytes.

Figure 24: Treatment of endothelial cells with proinflammatory cytokines.

Figure 25: HBMEC responses to exogenous proinflammatory cytokines

Figure 26: Innate intracellular antiviral responses in HBMECs and HBCAs

Figure 27: CCL2 expression in WNV-infected HBMECs.

Figure 28: Localization and quantification of CCL2 within WNV-infected HBMECs.

Figure 29: CCL5 expression in WNV-infected HBMECs.

Figure 30: Localization and quantification of CCL5 within WNV-infected HBMECs

Figure 31: CCL2 and CCL5 expression in WNV-infected HBCAs

Figure 32: CCL2 localization within the HBMEC monolayer of an *in vitro* model of the BBB.

Figure 33: CCL5 localization within the HBMEC monolayer of an *in vitro* model of the BBB

Figure 34: Effect of WNV infection on the permeability of the HBMEC monolayer.

Figure 35: Expression of cell adhesion molecules (CAMs) in HBMECs and HBCAs.

Figure 36: WNV-NY and WNV-MAD78 replication in THP-1 cells

Figure 37: Attachment and diapedesis of monocytes in BBB models

Figure 38: Survival analysis of mice infected with WNV-NY and WNV-MAD78.

Figure 39: Detection of infectious WNV-NY in intravenously-inoculated mice

Figure 40: Plaque reduction Neutralization test

Figure 41: Cytokine and chemokine responses in the blood and brain of WNV-infected mice

List of Abbreviations

BBB- blood-brain barrier

CAM-cellular adhesion molecule

CD- cluster of differentiation

CLR- C-type lectin receptor

CNS- central nervous system

DC-SIGN-Dendritic Cell-Specific Intercellular adhesion molecule-3-Grabbing Non-integrin)

GAPDH- Glyceraldehyde 3-phosphate dehydrogenase

HBCA-human brain cortical astrocytes

HBMEC-human brain microvascular endothelial cells

HBMVE-human brain microvascular endothelial cells, donor matched

IFIT- IFN-induced protein with tetratricopeptide repeats

IFN- interferon

IL-interleukin

IRF-Interferon regulatory factor

ISG-IFN-stimulated gene

JAK-Janus Kinase

MAPK- Mitogen-activated protein kinases

MDA5- melanoma differentiation associated protein 5

MyD88- Myeloid differentiation primary response gene 88

NFkB- nuclear factor kappa-light-chain-enhancer of activated B cells

NLR- NOD-like receptor

PAMP- Pathogen associated molecular patten

PRR- Pattern recognition receptor

RIGI- retinoic inducible gene-1

RLR-RIG-I-like receptor

STAT- Signal Transducers and Activators of Transcription

TIR- Toll/Interleukin-1 receptor

TLR- Toll-like receptor

TNF- Tumor necrosis factor

TRAIL- TNF-related apoptosis-inducing ligand

TRIF- TIR-domain-containing adapter-inducing interferon- β

WNV- West Nile

Chapter 1: Introduction

1.1 The Flaviviridae

West Nile virus (WNV) is a member of the family Flaviviridae. The Flaviviridae are a family of enveloped, positive strand RNA viruses that replicate in the cytoplasm of host cells. Since many members of Flaviviridae cause significant disease in either humans or livestock, further research into disease mechanisms may lead to improved strategies for treating and preventing disease. The Flaviviridae family are comprised of three main genera: hepaciviruses, pestiviruses, and flaviviruses (**Figure 1**). The hepaciviruses are comprised almost exclusively of hepatitis C virus (HCV) genotypes. HCV infects over 150 million people worldwide. HCV establishes chronic infections in the liver. Complications from HCV infections, such as cirrhosis of the liver or hepatocellular carcinoma, result in ~350,000 hepatitis C-related casualties yearly (19, 114). The closely related pestiviruses include several viruses, such as Borna disease virus (BDV), bovine viral diarrhea virus (BVDV), and classical swine fever virus (CSFV), that infect economically important livestock. Pestiviruses also establish chronic infections that cause diarrhea, hemorrhage, wasting disease, and spontaneous abortion (25, 278). In contrast to Hepaci- and Pestiviruses, Flaviviruses typically cause an acute infection. This genus includes multiple notable human pathogens such as West Nile virus (WNV), Yellow fever virus (YFV), Japanese encephalitis virus (JEV), Tick Born encephalitis virus (TBEV), and Dengue virus (DENV). Flaviviruses are further categorized into serogroups, with WNV categorized in the JEV serogroup.

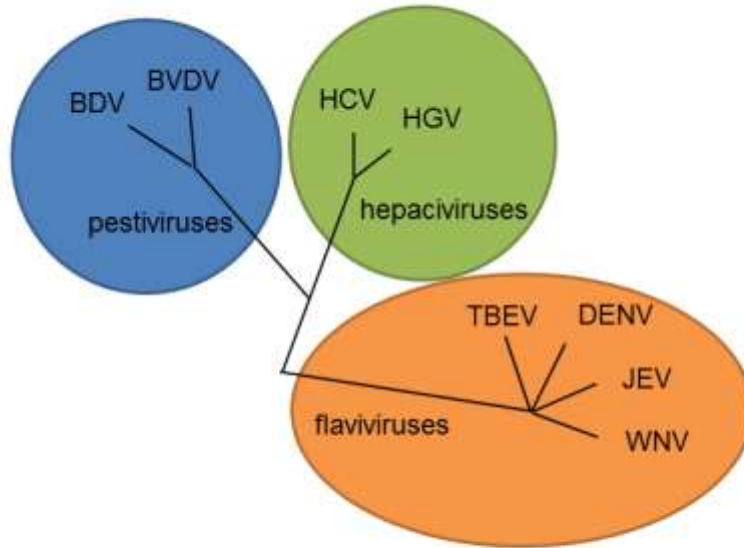


Figure 1. Phylogenetic relationships within the Flaviviridae. Flaviviridae is comprised of hepaciviruses (green), pestiviruses (blue), and flaviviruses (orange). Distances between lines are representative of relatedness of groups (i.e. longer lines describe more distantly related groups than shorter lines), but are not quantitative. Figure adapted from Fields Virology (78).

Flaviviruses are transmitted through tick or mosquito vectors, although the vector for some flaviviruses remains to be determined. Flaviviruses can also be categorized as viscerotropic and neurotropic. Viscerotropic flaviviruses, such as DENV, replicate to high titers in the vasculature and induce pathology such as excessive bleeding, decreased blood pressure, and hemorrhagic fever (174). Neurotropic flaviviruses, such as JEV and WNV, cause severe disease as a result of neuronal damage from both viral replication and bystander cell death from the immune response (44, 122). For example, during WNV infection, a productive CD8⁺ T cell response is necessary for viral clearance from the CNS (248). However, without proper T cell maintenance and resolution of T cell infiltration into the CNS, CD8⁺ T cells can exacerbate pathology (212, 257). Thus, examining which cells within the CNS contribute to activation and resolution of the immune response is an essential step toward understanding the kinetics of immune responses in the CNS and for developing therapies that may aid in viral clearance.

1.2 WNV classification and lineages

WNV is divided into 5 lineages, although most WNV strains reside within 2 main lineages (**Figure 2**). Within lineages, WNV sequences are >90% conserved at the nucleotide level, and >99% conserved at the amino acid level (141). Despite the high level of similarity at the amino acid level, there is substantial variation in pathogenicity among strains. Moreover, experiments in mice indicate virulence is lineage-independent (22, 23). Examining specific

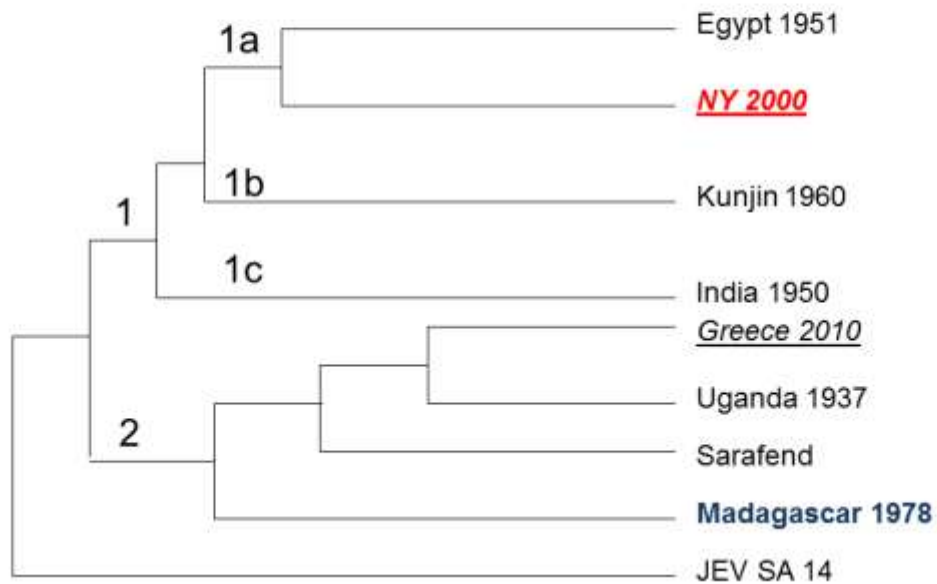


Figure 2. Diagram of the two main lineages of WNV. The select strains of WNV displayed are common experimental strains. Underlined strains have been shown to be highly neuropathogenic. JEV is the common outlier to all strains, residing within the same serogroup as WNV. Colored strains (NY 2000 and Madagascar 1978) are strains used throughout the following experiments. Length of lines qualitatively represents relatedness between strains, but was not experimentally determined. Figure adapted from Lanciotti et. Al (141).

genetic variances among strains that vary greatly in their observed pathology is an effective and necessary approach to identify viral motifs that contribute to WNV neuropathogenesis.

1.3 WNV transmission cycle

In nature, WNV is maintained in a transmission cycle between arthropods, including mosquitoes, and migratory birds. *Culex* mosquitoes are the primary vector of WNV, but other mosquito species can harbor infectious virus (17, 110). In mosquitoes, WNV replicates to high titers without causing pathology (91). Although mosquitoes transmit WNV to a wide range of species, including various mammalian species, migratory birds and reptiles are the only species in which WNV replicates to high enough levels to perpetuate the transmission cycle (132). Because mosquitoes are the transmission vector for WNV, the seasonal emergence of human WNV infections corresponds to mosquito populations and activity. Thus, the overwintering of mosquito populations due to climate change will elongate the WNV season.

1.4 West Nile virus (WNV) clinical presentation

WNV was first identified in sub-Saharan Africa in 1937, with symptoms presenting as a mild, febrile illness, although most cases were asymptomatic (258). Throughout the 1950s and 1960s, WNV evolved and spread from the African continent into the Mediterranean, continuing to cause only mild febrile illness with rare cases of neurological disease (**Figure 3**) (116). Yet as WNV



Figure 3. Map of WNV distribution worldwide. Map includes both chronological spread (green=prior to 1990s, yellow=post 1990s) and specific strains of interest (stars). Blue stars indicate noneuropathogenic strains of WNV, purple low neuropathogenic strains of WNV, and red highly neuropathogenic strains of WNV.

emerged in Eastern and Western Europe and the Western hemisphere in the 1990s, prevalent strains caused a higher incidence of neurological disease (200, 201). Currently in the US, about 80% of WNV cases are asymptomatic, but severe neurological disease, including WNV-induced acute flaccid paralysis, meningitis, and encephalitis, occurs in ~5% of cases, about 10% of which are lethal (12, 37, 197). Recovery from WNV neurological disease takes several months to years. In some cases patients never fully recover or experience further complications after resolution of the acute infection, including continuing headache and symptoms of encephalitis (145, 146, 189). Although considered an acute disease, recent evidence suggests that WNV can establish a chronic infection as well. WNV-specific antibodies and infectious RNA have been detected in humans in several distal locations (skin, urine, brain) months after the acute infection has been resolved (189, 204). Besides the initial symptoms, some patients and persistently infected rodent models display renal failure several months or years after acute infection. In addition, WNV RNA has been detected in mice for several months after resolution of the acute infection (11, 242, 243). Persistence in the kidneys and CNS of non-human primates has also been documented (208). Active WNV replication has also been reported in a hamster model in CNS and renal tissues for up to 100 days after acute infection (255). The severe pathologies associated with WNV neuroinvasion highlight the importance of research aimed at understanding how host and viral factors contribute to neurological pathology. Currently, no vaccines or specific antiviral

therapies exist for WNV in humans, and developing novel therapeutics to target WNV is of great public health interest.

1.5 WNV dissemination pathway within the mammalian host

WNV enters the body through the bite of a mosquito. While high levels of virus are deposited directly into the epidermal and dermal layers of the skin, studies in mice have demonstrated that low levels of virus are deposited directly into the bloodstream approximately 70% of the time (266). Virus replication within the epidermal and dermal cells attracts immune cells, such as Langerhan dendritic cells, to the site of infection (153). Langerhan dendritic cells are hypothesized to contribute to viral dissemination by trafficking the virus to lymph nodes and the spleen, where a second round of replication occurs (39, 123). High levels of virus in the blood stream then expose distal organs, such as the heart, liver, kidneys, and CNS, to WNV. Although this viral dissemination pathway is generally accepted within the WNV community, several steps of the pathway, such as replication in or uptake of virus by Langerhan cells, have yet to be experimentally confirmed . Additionally, the kinetics of WNV replication in vivo are not always consistent with the current model (266). Further analysis of the kinetics of viral replication within specific cell types may help to clarify the viral dissemination pathway, and aid in the development of new strategies to prevent dissemination to sites that are particularly susceptible, such as the CNS.

1.6 WNV Life Cycle

Although a unique, universal receptor remains to be identified, several known extracellular proteins and ultrastructural motifs mediate WNV attachment, including Dendritic Cell-Specific Intercellular adhesion molecule-3-Grabbing Non-integrin (DC-SIGN), DC-SIGNR, lipid rafts, and $\alpha V\beta 3$ integrin (50, 60, 176). Once attached to the cell surface, WNV particles are internalized by host cells through receptor-mediated endocytosis (**Figure 4**) (49, 97, 98). During transport through the endocytic pathway, endosomal acidification induces a conformational change in the envelope protein, facilitating fusion of the viral particle to the endosomal membrane and release of the viral core into the cytoplasm (8, 137). In the cytoplasm, the viral genome is directly translated into a single polyprotein that is co-translationally cleaved by both viral and cellular proteases into 3 structural and 7 nonstructural proteins (**Figure 5**) (42, 43, 303). The structural proteins capsid or core (C), preMatrix (prM) and envelope (E), together with the viral genome, form the WNV particle. The capsid binds and stabilizes genomic RNA within the viral particle (165). If expressed in trans within the CNS, the capsid itself induces neuropathology (282), although by an unknown mechanism. prM forms a heterodimer with E and is required for the proper folding of the E protein (135, 161). Envelope proteins coat the virion and are cotranslationally inserted into host cellular membranes derived from the ER (194). Located downstream of the structural genes are genes coding for 7 nonstructural proteins: NS1, NS2a, NS2b, NS3, NS4a, NS4b, and NS5

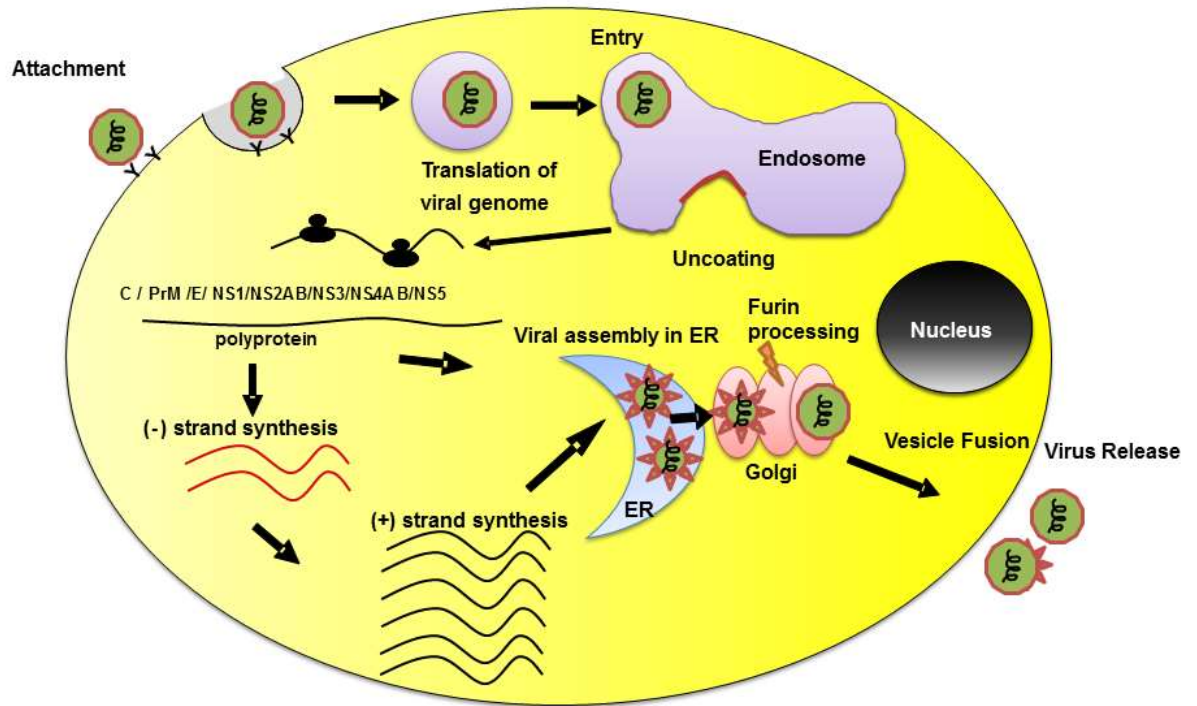


Figure 4. West Nile virus life cycle. WNV enters the cell through receptor mediated endocytosis. Acidification of the endosome triggers fusion of the viral envelope with endosomal membranes and allow for release of the viral core in to the cytoplasm where translation and replication occur. Assembly of WNV particles occurs on ER membranes, and once assembled, viral particles translocate through the exocytic pathways to the trans-Golgi network, where they undergo maturation. Mature viral particles are then released from the cell by fusion of exocytic vesicles with the plasma membrane.

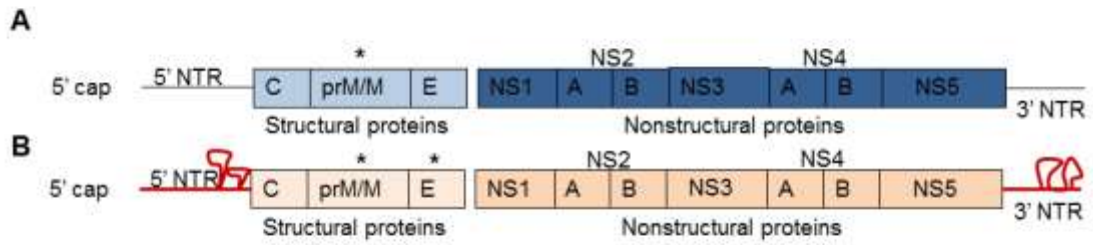


Figure 5. WNV genome. WNV is comprised of 3 structural proteins and 7 nonstructural proteins. (A) WNV-MAD78 contains a single glycosylation site (*) within prM whereas (B) WNV-NY contains glycosylation sites in prM and the envelope protein.

Though few, the nonstructural proteins, along with usurped host proteins, execute all of the functions necessary for successful WNV propagation. NS1 exists in monomeric, dimeric, and multimeric forms, and is present in the cytoplasm, on the surface of infected cells, and secreted in cell culture medium (166, 310, 311). Intracellular NS1 contributes to replication complex assembly, and may be responsible for initiation of negative strand synthesis (128, 154, 155, 190). However, the functions of surface-bound and secreted NS1 remain unclear (168, 306). The NS1 gene also contains a pseudoknot that leads to the synthesis of an additional, truncated protein, NS1' (180). NS1' has been associated with WNV-induced neuropathology, although the mechanism by which NS1' increases neuropathology is currently unknown. NS2a is a transmembrane protein involved in RNA processing and viral assembly. NS2a facilitates immune escape by antagonizing the type-1 interferon (IFN) response, which is known to limit WNV replication and spread within the host (157, 158). NS2B is a cofactor for the ATP-dependent protease and helicase, NS3 (74, 76). In addition to cleaving the viral polyprotein and unwinding dsRNA intermediates, NS3 dephosphorylates viral RNA at the 5' UTR to facilitate cap addition by NS5 (304, 305). NS4a and 4b are both small hydrophobic proteins essential for viral replication and assembly by an unknown mechanism. NS4B is also a type I IFN antagonist (188, 307). The final protein, NS5, is the viral replicase, containing enzymatic activities for both polymerization of RNA as well as the 2'O-methyl capping activity necessary to synthesize the viral 5' RNA cap (78). Along with its necessary replication functions, NS5 also antagonizes type I IFN amplification by blocking

phosphorylation of JAK/STAT receptors (143). The capping function of NS5 also enables WNV to escape the antiviral activity of interferon-stimulated genes, such as interferon-induced protein with tetratricopeptide repeats 1 (Ifit1) (273) .

Following initial viral protein synthesis, replication of the genomic RNA begins. Cleavage of the polyprotein by NS3 and host proteases generates the proteins that assemble into the viral replication complex (VRC), which initiates negative strand synthesis by binding directly to structures within the 3' non-translated region (NTR) of the genome. The 5' and 3' NTRs of the genome contain structures that circularize the viral genome and promote initiation of transcription and translation (69, 103). Following negative strand synthesis, positive strand, genomic RNA is generated from the nascent negative strand template. Several studies of RNA viruses suggest that the ratio of positive strand to negative strands synthesized ranges from 10:1 to 100:1. However, the mechanisms contributing to the switch from negative to positive strand synthesis and the disproportional synthesis of positive strand RNAs remain unknown. Although both the 5' and 3' WNV UTRs are predicted to be highly structured, the strain-dependent differences in the length of the 3' NTR suggests that strains may deviate in the secondary and tertiary structures they form within the 3' NTR, resulting in various efficiencies of viral replication.

After the viral genomic RNA and structural proteins have been successfully synthesized, viral particles assemble in the ER (169). Here, certain motifs in both the prM and envelope proteins are glycosylated before assembling within the ER membrane. Steric hindrance from assembly of the viral particle

within the ER membrane prevents more than one copy of the genome per 180 envelope proteins from being incorporated into each viral particle. Once assembled, the viral particle traffics from the ER to the trans-Golgi to undergo processing. Initial carbohydrates added to proteins in the ER are further modified in the trans-Golgi. Here, the glycosylated portion of the prM protein is cleaved during the processing of prM to the mature form of the protein by the cellular protease furin, causing a conformational change in the envelope protein (111). Conformational changes in the envelope protein result in the rearrangement of the global structure of the virion from a “spike” conformation to a flattened pattern with a 3-2-5 axes of symmetry (**Figure 6**). The cleaved prM, containing the carbohydrate moiety, is released into the extracellular milieu in concert with the mature viral particle. The process of maturation is often inefficient, creating particles with heterogeneous maturation states (207). Although virion maturation was once thought to be required for generation of an infectious viral particle, recent evidence suggests partially mature virions are also infectious. Indeed, the presence of uncleaved prM may enhance binding of virions to attachment factors in some circumstances (60). Recent data suggests that DC-SIGN, a cell-surface protein that binds carbohydrate moieties, acts as an attachment factor and facilitates WNV entry into the cell (60). This suggests that carbohydrate moieties on the envelope protein and prM may play a role for viral attachment and dissemination within the host, depending on levels of attachment factors expressed on specific cell types. Details of maturation mechanisms and implications in neuropathogenesis are currently active fields of WNV research.

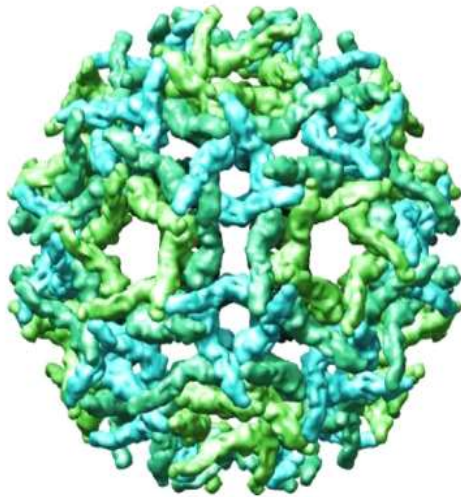
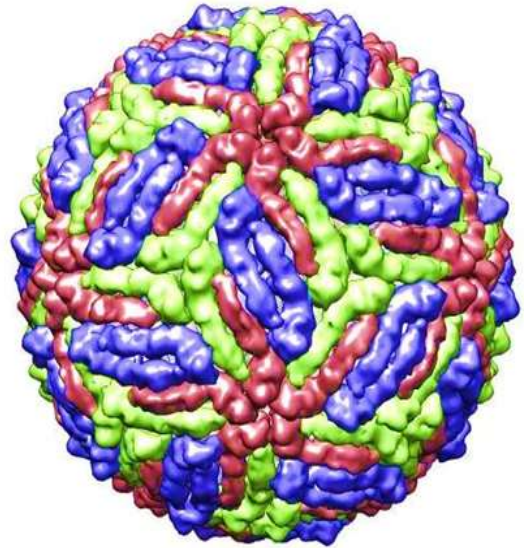
A**B**

Figure 6. WNV particles. Cryo EM images of immature (A) and mature (B) WNV particles. WNV particles are processed in the trans-Golgi network by the host protease, furin. Cleavage of prM by furin induces a conformational change in the structure of the virion from a “spiked” to smooth surface. Images used with permission from protein data bank (PDB) as follows: (A) PDB#2OF6 (322) (B) PDB #3J0B, (321).

1.7 The Blood Brain Barrier (BBB)

The CNS is a highly developed system that regulates all physiological processes, both voluntary and involuntary. As such, entry into the CNS is highly restricted by physical barriers to the brain, including the blood-cerebral-spinal fluid (CSF) barrier and the blood-brain barrier (BBB) (213). The BBB is comprised of two main cell types: endothelial cells, which line the blood vessels, and astrocytes, which are the most populous cell type within the CNS (1, 118, 129) (**Figure 7**). The endothelial cells within the CNS are highly specialized, forming tighter cell-to-cell junctions and exhibiting lower rates of endocytosis and pinocytosis than endothelial cells in the periphery. The endothelial cells are in direct contact with the foot processes of astrocytes that reside within the CNS. Astrocytes maintain the integrity of the endothelial cell layer as well as regulate aberrant neurotransmitter release. In addition to the BBB, the blood-CSF barrier is comprised of highly restrictive epithelial cells that secrete the cerebral spinal fluid that encompasses the brain, and endothelial cells that completely lack cell-cell junctions to allow for free movement of small molecules to contact the specialized epithelial cells that secrete the CSF. The blood-CSF barrier prevents infiltration by maintaining tight cell-to-cell junctions on the epithelial cells and specific ratios of transporters and receptors on the epithelial cell surface to maintain proper balance of nutrients in the CSF while preventing aberrant immune responses (214).

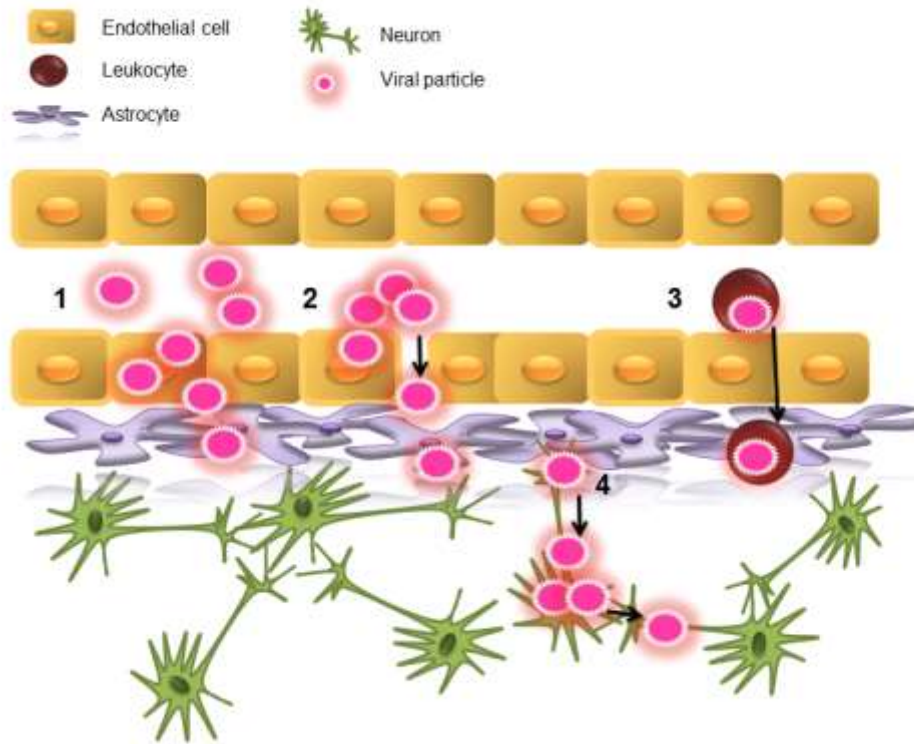


Figure 7. The BBB and mechanisms of neuroinvasion. The blood-brain barrier is comprised of endothelial cells and astrocytes, as indicated. Neurons reside within the CNS, and are the final component of the neurovascular unit. Viral infections traverse the BBB by one of four possible mechanisms, including: 1) replication in and traversal of the endothelial cell layer, 2) disruption of cell-to-cell junctions and paracellular transport of virus across the endothelial cell layer, 3) infected leukocyte attraction and extravasation through the endothelial cell layer, or 4) retrograde transport in neurons from the periphery.

Despite these physical defenses, pathogens across a variety of kingdoms (parasite, bacteria, virus) can successfully infiltrate the CNS. Pathogens enter the CNS through three main routes: retrograde transport from peripheral neurons, trafficking of infected cells into the CNS via a Trojan horse mechanism, or by directly crossing the blood-CSF or BBB (48, 129). Several viruses, such as herpesvirus and rabies virus, enter the CNS through retrograde transport in peripheral neurons (21, 66, 90, 279). After replicating in the epithelium, these viruses initiate replication in neighboring motor and sensory neurons. Within the neurons, the virus hijacks the microtubule transport pathway, attaching to either the kinesin or dynein motors required to move proteins directionally within the neuron (1). After spreading among peripheral neurons through retrograde transport and axonal budding and release, the virus is transmitted to the spinal cord and disseminates throughout the CNS.

The Trojan-horse model for infiltration involves extravasation of virus-infected leukocytes from the blood into the CNS. Several viruses, such as measles virus and human immunodeficiency virus (HIV) actively replicate within leukocytes (29, 196, 240). Another virus, Nipah virus, does not replicate in leukocytes, but attaches to lymphocytes in the periphery (175, 302). For Nipah virus, traversal of lymphocytes with attached virus across the BBB is reported to initiate infection in the CNS. With or without viral replication, traversal of leukocytes from the blood into the brain remains one mechanism of viral neuroinvasion.

Multiple viruses enter the CNS via direct infection of brain endothelial cells (67, 260). Viral replication in the endothelium during influenza virus infection, for example, is responsible for the cytokine storm induced during influenza infections (293), and Venezuelan and eastern equine encephalitis viruses disseminate to the CNS via the hematogenous route (286) . Certain flaviviruses, such as JEV, also enter the CNS via a hematogenous route (156). As the brain is a highly vascularized organ, replication in endothelial cells and traversal of the vascular cells is frequently utilized by viruses to enter into the CNS.

Although the blood-CSF barrier plays a significant role in the stability and maintenance of the CNS, very little has been reported about viral-induced disruption and entry into the CNS via this route. Overall, this mechanism of entry into the CNS appears to be minimal, and has not been found to play a role in WNV infection. While one report documented retrograde transport of WNV within neurons (229), the kinetics of WNV replication in the CNS throughout infection suggests that WNV primarily utilizes a hematogenous route of entry. While WNV can replicate to low levels within leukocytes, infectious virus is detected in the CNS prior to infiltration of infected leukocytes (92, 267), suggesting that the Trojan-horse mechanism is not the initial route of incursion for WNV. Recent evidence demonstrated that WNV replicates in and traverses intact brain endothelial cell monolayers while maintaining the integrity of the monolayer (117, 285), suggesting that infection of brain endothelial cells may play a role in the incursion of WNV into the CNS. Nonetheless, infiltrating leukocytes may contribute to WNV entry and dissemination as the infection

progresses (15, 26). In addition to enhancing viral entry through the infiltration of infected cells, leukocytes secrete matrix-metalloproteinases (MMPs), which actively break down cell-to-cell junctions at the BBB, thereby allowing the unrestricted entry of free virus present in the blood. This suggests that trafficking of leukocytes into the CNS may exacerbate infection in the CNS and actively contribute to disruption of the BBB.

Thus, viral replication within cell types of the BBB and the immune responses in these cell types has implications in CNS disease manifestations. Because this physiological barrier is unique in its ability to modulate immune responses and controls access to the CNS, various therapeutics target responses at the BBB and need to traverse the BBB during CNS infection. Further, therapeutics targeted at modulating immune responses at the BBB during WNV infection may alter neurological pathologies to be less severe early on during infection.

Studies examining immune responses at the BBB comparing nonpathogenic and pathogenic strains of WNV are limited. Modeling the BBB in vitro has provided many insights into CNS physiology and function as well as viral pathogenesis (309). Initial studies performed with pathogenic WNV demonstrated that WNV infects cells of the BBB in an in vitro model system (117, 285). In addition, virus-like particles of a low pathogenic lineage 1 strain of WNV exhibited decreased traversal of an endothelial cell layer compared to a pathogenic strain (108). After crossing the BBB, WNV reaches highly susceptible neurons. Neurological symptoms during WNV infection are a result of neuronal

death caused by either active replication of virus or bystander immune responses. The specific contribution of neurons to the immune response to WNV has been well documented. For example, WNV replication in neurons induces caspase-3 dependent apoptosis (228). Further, infected neurons secrete CXCL10 that attracts CD8⁺ T cells necessary for efficient clearance of WNV from the CNS (131). Mice deficient in IFN β exhibit increased susceptibility to pathogenic WNV infection and increased viral replication in cortical neurons (144). Further, WNV replication is restricted in cortical neurons treated with exogenous IFN β (144). Yet how other cell types contribute to neuropathogenesis is widely unknown.

In addition, viral genetic factors contributing to WNV neuropathogenesis remain elusive. For example, glycosylation on the envelope is associated with increased neuropathogenicity of WNV in mice (13, 24, 237), although the mechanism of increased neuropathogenicity remains unknown. Glycosylation on both prM and envelope proteins improves both entry and assembly (106), and carbohydrate-binding proteins function as attachment factors for WNV entry (60). Thus, glycosylation-dependent cell-to-cell spread within the CNS may contribute to the strain-dependent variation in neuropathology.

1.8 The role of astrocytes in the CNS

Non-neuronal cells, or glial cells, comprise over 90% of the cells in the CNS. This group includes resident tissue macrophages, or microglia, which comprise about 12% of the CNS, oligodendrocytes, which are responsible for

enveloping the axons of neurons and increasing the velocity of action potentials in neurons, and astrocytes, which comprise over 50% of the cells within the CNS (130). Astrocytes are anatomically divided into two main groups based on morphology: fibrous astrocytes (or white matter astrocytes), which directly contact the nodes of Ranvier, and protoplasmic astrocytes (or grey matter astrocytes), which directly contact synapses. Astrocytes of both groups can contact blood vessels within the CNS (130). Once thought to serve merely a structural role, astrocytes are now recognized as cells that aid in development of the CNS, maintain homeostasis within the CNS, regulate blood flow, and resolve infection and trauma within the CNS (259).

Recent studies have elucidated several roles for astrocytes during development of the CNS and maintenance of the CNS thereafter. Astrocytes express receptors for neurotransmitters, and their ability to communicate with and even phagocytose specific synapses at the developmental stage of the CNS provides a unique role in shaping the CNS. Although astrocytes express several ion channels similar to neurons, they lack the ability to initiate an action potential (191, 241). Further, expression of aquaporin and ion channels highlights astrocytes as regulators of the CNS, and at times one astrocyte may contact up to 100,000 neurons (38, 104). Astrocytes also provide nutrients essential for neuronal survival by transporting glucose from blood into the CNS (33). Moreover, astrocytes respond to neuronal cell death by secreting neuronal growth factors, which either stimulate regeneration of axons or dendrites from neighboring neurons, or occupy the space themselves (160). Early in the

developmental process, astrocytes may contribute to the establishment of the formation of the tight junctions of cerebral endothelial cells and therefore contribute to the establishment of the BBB (1, 16). In addition to the development of the BBB, astrocytes are capable of regulating blood flow by expressing soluble molecules, such as nitric oxide, that modulate vasodilation. During viral-induced encephalitis, activated astrocytes regulate infiltration of leukocytes from the blood by gathering around the perivascular space (259, 288). Experimental disruption of astrocytic perivascular cuffing demonstrated an increase in infiltration of lymphocytes, thereby exacerbating inflammation in the CNS.

Astrocytes also play an essential role in initiating the antiviral response within the CNS. Upon stimulation with $\text{IFN}\gamma$, astrocytes express complement receptors (18). In addition, astrocytes can secrete soluble inhibitors to components of the complement cascade, thereby preventing themselves from being opsonized (85). Thus, astrocytes may serve to initiate the opsonization of free viral particles as well as neighboring infected cells, thereby promoting viral clearance, and inhibit their own complement-induced cell death emphasizing their necessity for maintaining homeostasis within the CNS.

Astrocytes express several pattern recognition receptors (PRRs), including TLRs, RLRs, and NLRs. TLR3 plays a central role in both shaping the developing CNS and responding to invading pathogens. In addition, astrocytes secrete several cytokines, chemokines, and growth factors upon stimulation with poly I:C (35, 36). Recognition of viral RNA by RLRs in astrocytes induces an immune response. Knock down of RIGI in virus-infected human astrocyte cell

cultures decreased proinflammatory cytokine expression and decreased neurotoxic factors secreted by virus-infected astrocytes (84). Although astrocyte stimulation triggers the expression of both cytokines and chemokines, astrocytes secrete higher levels of chemokines compared to proinflammatory cytokines, further emphasizing their importance in recruiting leukocytes to the CNS (234). In addition to PRR expression, astrocytes are also capable of expressing MHC I and MHC II molecules, as well as T-cell coreceptors CD40 and SOCS1, suggesting that astrocytes are important antigen presenting cells within the CNS, and may be imperative in modulating cytolytic and regulatory T cell responses (28). In autopsies of patients with WNV-induced encephalitis, viral antigen was present in both neurons and glial cells (282). Further, ex vivo inoculation of rat astrocytes with pathogenic WNV induced neurotoxic factors, suggesting that astrocytes may play a significant role in WNV-induced neuropathologies. In addition, studies in human glial cultures demonstrated that replication of a pathogenic strain of WNV in astrocytes induces expression of monocyte- and T-cell attractant chemokines, suggesting that infected astrocytes may function to initiate or exacerbate immune responses from the periphery (46). Therefore, comparing the replication and innate immune responses initiated by astrocytes infected with pathogenic and nonpathogenic strains of WNV may lead to a more detailed understanding of the progression and underlying mechanisms of WNV-induced neuropathologies.

1.9 Immune response to WNV within the CNS

The immune response within the CNS also plays a significant role in the neuropathogenesis of WNV. The immune system consists of two branches, the innate and the adaptive, that work together to respond to viral infections. While the innate immune system initiates a non-specific response to viral pathogens and activates the adaptive response, the adaptive immune system provides lasting memory and specific action against pathogens.

1.9.1 Cell intrinsic innate antiviral response

Innate immune signaling

The cell intrinsic immune response is established on a cellular level, where pattern recognition receptors (PRRs) recognize pathogen associated molecular patterns (PAMPs) (4, 276), and initiate signaling cascades that result in the transcription of genes required for host defense (**Figure 8**). These genes include secreted factors that amplify the antiviral response as well as factors that directly impede viral infection, thereby limiting spread. There are 4 main groups of PRRs: Toll-like receptors (TLRs), RIG-I like receptors (RLRs), Nod-like receptors (NLRs), and C-type lectin receptors (CLRs). Throughout viral infection, each class of receptor contributes to innate antiviral defense mechanisms.

TLRs are transmembrane receptors expressed either on the surface of the cell or within endosomes. Each TLR contains both an extracellular recognition domain and an intracellular signaling domain (4, 147, 276). The extracellular

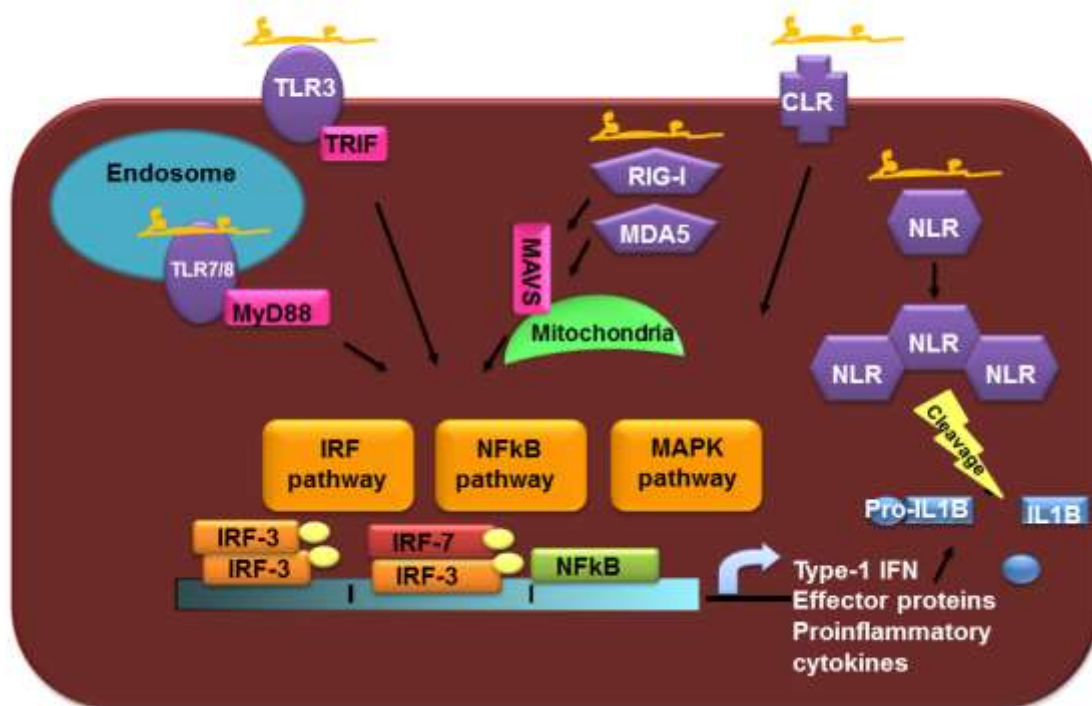


Figure 8. The intracellular innate antiviral response. Pattern recognition receptors (PRRs) recognize pathogen associated molecular patterns (PAMPs) present on virions or produced during the course of viral replication. PRRs then signal through adaptor molecules, such as TRIF, MyD88, and MAVS, to activate signalling pathways, including the IRF, NFκB, and MAPK pathways. These signalling pathways result in the activation of transcription factors essential for promoting antiviral gene synthesis. In addition, NLRs function by activating the inflammasome and cleaving inflammatory cytokines, such as pro-IL1β, to generate active forms of these proteins.

recognition domains contain leucine-rich repeats that recognize conserved non-self moieties, including viral elements such as single-stranded RNA (TLR8, TLR7), double-stranded RNA (TLR3), and DNA (TLR9). Recognition of non-self moieties induces conformational changes within the intracellular domain and results in exposure and autophosphorylation of key residues. This in turn results in the phosphorylation of adaptor molecules, such as myeloid differentiation primary response 88 (MyD88) and TIR-domain-containing adapter-inducing interferon β (TRIF), that contain Toll/Interleukin-1 receptor (TIR) domains (79, 113, 198, 290, 313). In contrast, RLRs detect non-self ss- and ds-DNA and RNA in the cytosol (124, 317). RLRs contain an N-terminal caspase activation and recruitment domain (CARD), an internal ATP-ase driven helicase domain, and a C-terminal repressor domain. Binding of nucleic acid to the C-terminal repressor domain induces a conformational change in the repressor domain, liberating the CARD domain to interact with other CARD-containing proteins, such as the adaptor molecule mitochondrial activating viral sensor (MAVS, also referred to as IPS-1, VISA and CARDIF) (4, 276). Activation of adaptor molecules by either TLRs or RLRs transmits signals through several downstream signaling cascades, including the nuclear factor kappa-light-chain-enhancer of activated B cells (NF κ B) pathway, the interferon regulatory factor (IRF) dependent pathway, and the mitogen-activated kinase (MAPK) pathway (62, 80, 112, 181, 182, 275). Each of these pathways culminates in the activation of transcription factors that bind cognate promoters and mediate transcription of antiviral genes such as type-1 interferon (IFN), innate antiviral effector proteins, and proinflammatory cytokines.

ssRNA and dsRNA from viral infections is also recognized by NLRs in the cytosol (107, 119). NLRs contain a recognition domain as well as several CARD domains that multimerize to form the inflammasome following activation by binding of a viral PAMP (125). Upon multimerization, several highly active proteases cleave either precursory proinflammatory cytokines, such as pro-IL-1 β and pro-IL-18, or caspases, which in turn carry out apoptosis, and are essential for restricting WNV infection in the CNS (212). TLRs, RLRs, and NLRs are essential for the antiviral response to WNV infection within the CNS (54, 82, 212, 280, 297). WNV infection in MAVS^{-/-}, MyD88^{-/-}, IRF3^{-/-}, and IRF7^{-/-} mice results in 100% lethality, with mice exhibiting increased replication in the periphery as well as the CNS (55, 270, 272). TLR3 and TLR7 are also necessary for a productive antiviral response in neurons that leads to viral clearance (54, 280), and deficiencies in the activation of these pathways results in an increase in WNV neuropathology. More recent analyses indicated that NLRs also play a role in regulating the inflammatory response in the CNS after WNV infection and promote resolution of inflammation. Indeed, apoptosis-associated speck-like protein containing CARD (ASC)^{-/-} and IL1 β R^{-/-} mice infected with WNV exhibit increased levels of virus in the CNS as well as increased proinflammatory cytokine expression and increased levels of CD8⁺ T cells late in infection (139, 212). Thus, the contribution of cell intrinsic immune pathways in the CNS is essential for both initiating to and resolving immune responses to WNV infection.

CLRs function at the cell surface or outside the cell, where they bind specific carbohydrate moieties (86). CLR signaling leads to the translocation of

additional transcription factors involved in initiating a proinflammatory cytokine response, thereby amplifying responses initiated by TLRs and RLRs (86). However, CLRs also function as viral attachment factors, which promote viral infection and dissemination within the host (20, 60, 133, 163). The specific contribution of CLR activation to WNV neuropathogenesis has not yet been explored. However, several CLRs have been shown to enhance WNV attachment and entry (60).

1.9.2 Amplification of the antiviral response

The interferon response to WNV

Interferon (IFN) is a class of molecules highly expressed in response to viral infection, and is a product of PRR signaling (120, 121, 224). IFNs are further classified into three subgroups: type I, type II, and type III IFNs. All IFNs are induced during viral infection and act in both an autocrine and paracrine manner by binding to receptors present on host cell membranes, which in turn signal to activate transcription of interferon-stimulated genes (ISGs). Although PRR signaling itself initiates transcription of a subset of ISGs, additional expression of antiviral effector proteins through the action of IFN facilitates amplification of the antiviral state.

The first type of IFN discovered, type-1 IFN, is produced by most nucleated cells. After secretion from the infected cell, type-1 IFNs bind to the type-1 IFN receptor (**Figure 9**). IFN binding to its cognate receptor induces a conformational change that activates the Janus-Kinase (JAK) and Signal

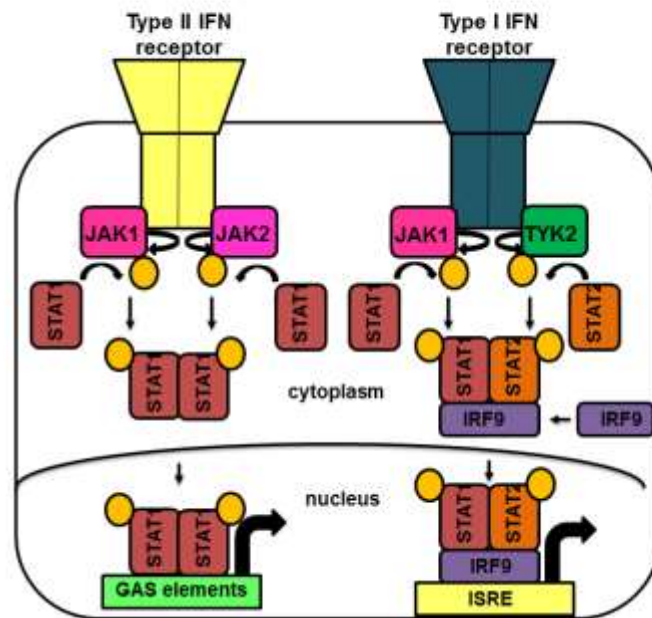


Figure 9. The IFN signal transduction pathway (the JAK/STAT pathway). IFN signalling to neighboring cells begins with binding of IFN to its cognate JAK receptor. Binding of IFN to its receptor triggers activation of the kinase function of receptor associated JAKs, which phosphorylate the IFN receptor. This leads to the recruitment and phosphorylation of signal transducers and activators of transcription (STATs). In the case of type-I IFN, STATs heterodimerize and associate with IRF9 to form the IFN-stimulated gene factor 3 (ISGF3) transcription factor, while STAT homodimers are formed in response to type-II IFN, forming the IFN-gamma activation factor (GAF). These transcription factors translocate to the nucleus, where they bind to either GAS elements (type-2 IFN) or the ISRE (type-1 IFN). These promoters lie upstream of a multitude of genes, and directly lead to the transcription of antiviral genes.

Transducer and Activator of Transcription (STAT) pathway, which mediates transcription of antiviral genes. The type-1 IFN response is essential for survival of WNV infection in mice (127, 144, 226), and mice deficient in either the type-1 IFN receptor or IFN β are unable to clear virus from the CNS. also known as interferon-stimulated genes (ISGs), that function to limit the spread of viral infection.

The wide variety of genes upregulated in response to IFN has been termed the INTERFEROME (225). ISGs carry out a diverse array of functions including regulation of gene transcription and translation, amplification of the IFN response, activation of the adaptive immune response, and initiation of antiviral RNA interference pathways (203), among many others. Although a few of the ISGs have been well described, many mechanisms of ISGs are currently unknown. Some ISGs, such as protein kinase R (PKR), disrupt translation (58, 220, 221, 315). Another ISG that has been well characterized is the 2'-5' oligoadenylate synthetase (OAS). OAS activity is stimulated by dsRNA. Once activated, OAS induces oligamerization of ATP to form 2'-5' linked oligoadnylates (2-5A). 2-5As bind to and activate the cellular endoribonuclease RNaseL, which mediates the degradation of viral and cellular RNAs (52, 171-173). Both PKR and RNase L restrict WNV neuropathogenesis by limiting the spread of WNV from neuron to neuron (230). Moreover, a genetic variant in mice of the *Oas1b* gene that encodes a stop codon is associated with increased susceptibility to flavivirus infection (231, 232) and single nucleotide polymorphisms (SNP) that encode alternate splicing variants of the *OAS1* gene in humans is associated

with increased susceptibility to WNV in humans and horses (150, 216). However, it should be noted that the Oas1b protein in mice is not a functional 2'-5' oligoadenylate synthetase, suggesting that OAS1b may have additional antiviral activities outside of activation of RNaseL. Another ISG, Ifit1, also restricts the spread of WNV specifically in the CNS, although not specifically by limiting replication in neurons or brain endothelial cells. Instead, Ifit1 may play a role in regulating the cellular immune response to WNV infection within the CNS and limiting immune-mediated pathologies (273). Viperin, an ISG that is hypothesized to alter cholesterol levels and membrane formation in the ER, restricts WNV replication in the CNS in both neurons and non-neuronal cells (271).

WNV has evolved several mechanisms to evade the cell intrinsic antiviral response. For example, WNV evades detection by PRRs at early times post-infection, thereby delaying the initiation of the innate immune response (81). Additionally, the NS4B and NS5 proteins of WNV inhibit JAK/STAT activation and thus down regulate the production of ISGs in WNV-infected cells (102, 143, 188). Because of the extensive co-evolution between viruses and the innate immune response, it is essential to further examine immune response modulation during viral infections to better develop therapies to target specific viral escape mechanisms.

WNV infection also induces type-II IFN (59, 224) (also known as IFN γ). Type-II IFN signaling resembles that of type-1 IFNs, although the receptors are structurally and functionally unique to their respective IFN subtype. The type-II IFN receptor is comprised of two subunits that, upon binding type-II IFN, signal

through the JAK-STAT pathway to mediate transcription of Gamma-activated site (GAS) genes. GAS genes promote Th1 T cell development, upregulate binding factors on leukocytes, and upregulate synthesis of proteins required to synthesize reactive oxygen and nitrogen species (14, 206). Type-II IFN is secreted by T cells and natural killer (NK) cells and is essential for activating macrophages, modulating the adaptive response to infection, and clearing viral infection (2). WNV infection in IFN γ ^{-/-} mice and IFN γ R^{-/-} mice results in higher viral load in the lymphoid tissue and earlier incursion of WNV into the CNS (252).

1.9.3 The proinflammatory cytokine response

PRR activation of the innate antiviral pathway also leads to the transcription of several proinflammatory cytokines (6). Proinflammatory cytokines are small proteins synthesized and secreted from the cell via the secretory pathway or secreted upon activation and cleavage by the inflammasome. Following secretion, cytokines bind to neighboring cells that express the cognate cytokine receptor. Receptor binding activates several intracellular pathways and either mediates the amplification of proinflammatory cytokines in a positive feedback mechanism, or increases production of anti-inflammatory cytokines and the repression of the proinflammatory cytokines in a negative feedback mechanism (195).

The proinflammatory cytokine response to infection mobilizes the cellular immune system to the site of infection and modulates physiological responses (**Figure 10**). Since many viruses initially infect peripheral cells (non-myeloid, non-

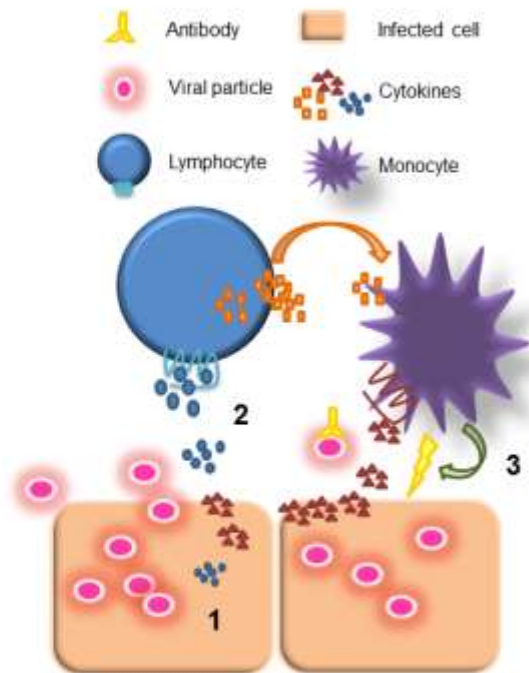


Figure 10. Proinflammatory cytokine synthesis and signalling. 1) Viral infected cells induce PRR-triggered pathways that result in the transcription of proinflammatory cytokines. 2) These cytokines function to activate and mobilize cellular responses, both innate and adaptive, to the site of infection by binding receptors present on leukocytes. Further cytokine expression by leukocytes determines which type of cellular responses to activate. 3) Cellular responses may result in the direct killing of virus by reactive oxygen or nitrogen species within an infected leukocyte, secretion of antibodies to neutralize viral particles, induction of cell death of the infected cell, or resolution of the proinflammatory response by attracting regulatory cells.

lymphoid cells), the ability to clear virus depends on the secretion of proinflammatory cytokines that attract and activate leukocytes to either directly lyse infected cells or aid in viral clearance. Indeed, non-immune cells secrete proinflammatory cytokines at the onset of infection (136). Leukocytes are also primary producers of cytokines. Secretion of cytokines by leukocytes activates the adaptive immune response and controls specific types of antiviral responses. When activated, leukocytes secrete significantly higher levels of cytokines than non-immune cells (**Figure 10**). The effect of the proinflammatory response on viral infection depends on several variables, including the cell types that are recruited and the kinetics of activation (136).

Many cytokines, such as interleukin (IL)-6, tumor necrosis factor α (TNF α), IL-12, and pro-IL-1 β , actively disrupt homeostasis of several physiological systems. For example, once in the blood, these cytokines initiate production of prostaglandins in the hypothalamus, or activate cells of the hypothalamus itself, causing fever (193). Unregulated proinflammatory cytokine responses lead to several harmful consequences, including toxic shock, colitis, and rheumatoid arthritis (134, 136, 184).

Several proinflammatory cytokines play a role in WNV neuropathogenesis. For example, IL23^{-/-} mice exhibit increased mortality during WNV infection due to an inability to attract monocytes to the CNS (280). TNF α expression in the CNS is also essential for attracting CD8⁺ T cells and monocytes to help clear WNV infection in the CNS (253). However, during WNV infection in IL22^{-/-} mice, survival was increased compared to wild type mice due to a decrease in CD45⁺

cell accumulation and a decrease in viral load in the CNS (291). The proinflammatory responses specific to physiological sites of WNV replication, and the kinetics of the innate response at these sites, remains an active area of research.

A subset of chemoattractant cytokines, known as chemokines, functions by forming a gradient to attract cells that express their cognate receptor. While some chemokines bind multiple different receptors, other chemokine:receptor pairs are unique (7). Chemokine receptors are G-protein coupled receptors that signal through several intracellular pathways. Chemokines mobilize and activate leukocytes that express high levels of the receptor on their surface (7). Several chemokines and chemokine receptors play a role in WNV neuropathogenesis. For example, *CCR5*^{-/-} mice are unable to efficiently traffic leukocytes to the CNS, resulting in increased mortality compared to wild type mice (92). In addition, humans who do not express a functional CCR5 are more likely to develop neurological disease from WNV infection (93). Further, mice deficient in CCR2 cannot effectively clear WNV from the CNS and have lower accumulation of leukocytes in the CNS compared to wild type mice (152). Certain chemokines have been shown to play a detrimental role during WNV infection. *CXCR2*^{-/-} and mice depleted of neutrophils after initial WNV infection experience a delay in lethality, and presumably, WNV entry into the CNS (15). The cell types within the CNS that directly contribute to chemokine secretion in response to WNV infection is largely unknown.

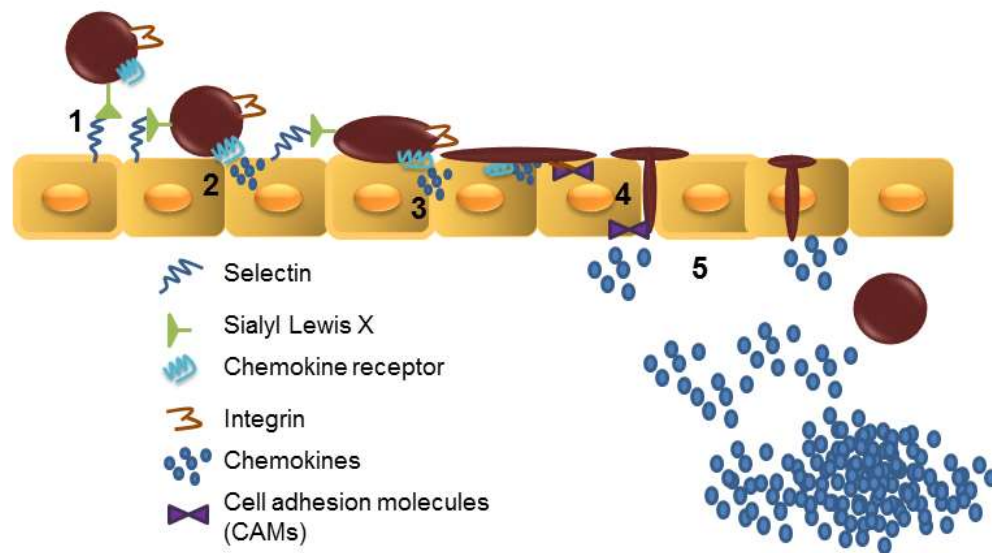


Figure 11. The extravasation process. 1) Activated endothelial cells express increased levels of selectin molecules that bind to glycoproteins on leukocytes, such as sialyl-Lewis-X, facilitating loose attachment. 2) Chemokines secreted by and/or bound to endothelial cells bind to chemokine receptors on leukocytes. 3) Chemokine:receptor binding triggers a conformational change in integrins within leukocytes. 4) Once activated, integrins bind to cellular adhesion molecules either on the endothelium or within cells residing on the basal side of the endothelium. 5) Diapedesis of activated leukocytes is then directed by continuous chemokine gradients throughout the endothelial layer and within infected tissue.

In addition to attracting leukocytes to the site of infection, several proinflammatory cytokines mediate the process of leukocyte extravasation (148) (**Figure 11**). Extravasation involves the traversal of leukocytes across the endothelial barrier and into infected tissue, and is characterized by 3 events: rolling, attachment, and transmigration of leukocytes through the endothelial cell layer (261, 301). Activation of endothelial cells by proinflammatory cytokines results in the increased levels of selectin molecules, which bind carbohydrate moieties, such as sialyl-Lewis X, present on leukocytes during the initial rolling phase of extravasation (126). Firm attachment is then facilitated by chemokines that are secreted or present as immobilized chemokine gradients on the endothelial cell surface. Binding of chemokines to their cognate receptors activates intracellular signaling events within leukocytes that induce conformational changes in integrins present on their surface (142, 210). Activated integrins in turn bind to cellular adhesion molecules (CAMs), such as intercellular adhesion molecule (ICAM) and vascular cellular adhesion molecule (VCAM), present on activated endothelial cells, strengthening the leukocyte:endothelial attachment (40, 41, 318). The process of establishing a chemokine gradient, binding and attaching of leukocytes, and leukocytes transmigrating through the endothelial cell layer, is known as diapedesis (40, 41). Further chemotaxis induced by cells on the basolateral side of the endothelium enhances extravasation events (9, 183, 294). Through this initial cross-talk event between the innate activation of the endothelium and the binding of leukocytes,

the branches of the immune system work together to distribute the appropriate immune cell for clearing the viral infection. If leukocyte extravasation is the mechanism of neuroinvasion for a virus, a decrease in extravasation events may delay neurological pathologies. Indeed, in WNV-infected ICAM^{-/-} mice, viral loads and proinflammatory cytokine expression were decreased compared to wild type mice (57).

Unsurprisingly, several viruses have evolved strategies, such as synthesizing cytokine mimics, to disrupt chemotactic events and thus, cellular response to viral infection (6). Further studies are needed to assess the initial chemokine response to WNV in the CNS, and how to maintain a proper response to prevent neurological injury. Determining how chemokine gradients are induced during WNV infection, including which cells contribute to secretion and binding of chemokines at the site of infection, will further the understanding of WNV disease progression. Additionally, further examination of the proinflammatory response may provide insight into determining whether a chemokine response contributes to neuropathology or viral clearance.

WNV neuropathogenesis as a result of the immune response is a current topic of active research and controversy. Several singular host factors in mice have been shown to either increase or decrease neuropathogenesis in mice (**Table 1**), depending on experimental design. Specifically, the interferon response is required for host survival (127, 144, 226), as well as an active adaptive immune response (63-65). Many components of the IFN, pro- and anti-inflammatory cytokine pathways, such as IL-23, TLRs, IFN γ , TNF α , and IL-1 β ,

are necessary for viral clearance and maintaining a regulated immune response to WNV infection (212, 252, 253, 280, 291, 297). Additionally, several factors contributing to the trafficking of immune cells to the CNS, such as CCR2, CCR5, CXCR3, and CXCL10, are essential for successful viral clearance from the CNS (15, 57, 131, 151, 152).

Table 1. WNV infection in immunodeficient mice after peripheral infection.

Adapted from (227)	Mouse strain ^a	Viral strain (Lineage)	% Lethality	Observed effects on Neuropathogenicity	Ref.
WT	C57/BL6	NY 2000 (I)	30-35	V: LN, S, SPL, CNS, KD I: innate, T, B	(63-65, 131, 177, 178)
	129 Sv/Ev	NY 2000 (I)	60	V: LN, S, SPL, CNS I: innate, T, B	(178, 226)
	C57/BL6x 129 Sv/Ev	NY99/ NY 2000 (I)	50	V: LN, S, SPL, CNS I: B	(177)
	BALB/C (5-6wk)	NY99/ NY 2000 (I)	80	V: S, SPL, CNS, KD, HT I: innate, T, B	(138, 246)
	ICR	WN25 (I)	0	V: none detected	(105)
	Swiss Webster	NY99 (I)	100	No data reported	(314)
	Swiss Webster C3H	MAD78 (II) NY 2000 (I)	0 80	No data reported V: S, SPL, LN, CNS	(127) (34)
Cytokines, chemokines	IL22 ^{-/-}	CT2741 (I)	50	V: ↓ in CNS I: ↓ CD45 ⁺ cells	(291)
	TNFR ^{-/-}	NY 2000 (I)	70	V: ↑ in CNS I: ↓ CD8 ⁺ cells, ↓ CD11b ⁺ , CD45 ⁺ cells	(253)
	IL6 ^{-/-}	CT2741 (I)	40	No Δ in lethality	(280)
	IL12a ^{-/-}	CT2741 (I)	40	No Δ in lethality	(280)
	IL12b ^{-/-}	CT2741 (I)	75	No data reported	(280)
	IL23 ^{-/-}	CT2741 (I)	100	No data reported	(280)
	IL1βR ^{-/-}	TX02 (I)	80	V: ↑ in CNS I: ↑ CD8 ⁺ cells, prolonged IFNβ in CNS	(212)
	CCR5 ^{-/-}	NY 1999 (I)	100	V: ↑ in CNS I: ↓ leukocyte trafficking to CNS	(92)
	CCR2 ^{-/-}	NY 1999 (I)	80	V: ↑ in CNS I: ↓ monocyte	(152)

	CXCL10 ^{-/-}	NY 2000 (I)	90	trafficking from bone marrow into blood V: ↑ in CNS I: ↓ CD8 ⁺ and CD4 ⁺ cells to CNS	(131)
	CCR1 ^{-/-}	NY 1999 (I)	40	No Δ in lethality	(92)
	CX3CR1 ^{-/-}	NY 1999 (I)	40	No Δ in lethality	(92)
	CXCR2 ^{-/-}	CT2741 (I)	90	Delayed lethality	(15)
	IFNβ ^{-/-}	NY 2000 (I)	95	V: ↑ in CNS I: ↓ CD8 ⁺ cells in periphery	(144)
	IFNα/βR ^{-/-}	NY 2000 (I)	100	V: ↑ in all tissues	(226)
	Sema7a ^{-/-}	CT2741 (I)	35	V: ↓ in CNS I: ↓ proinflammatory cytokine expression in CNS	(268)
PRR pathways	TLR3 ^{-/-}	NY 2000 (I)	30	No Δ in lethality, possible signaling in neurons	(54)
	TLR3 ^{-/-}	CT2741 (I)	40	V: ↓ in CNS I: ↓ proinflammatory cytokine expression in CNS	(297)
	TLR7 ^{-/-}	CT2741 (I)	85	V: ↑ in CNS I: ↑ proinflammatory cytokines, ↓ IL12, IL23, ↓ CD11b ⁺ CD45 ⁺ cells in CNS	(280)
	TLR9 ^{-/-}	CT2741 (I)	40	No Δ in lethality	(280)
	IRF7 ^{-/-}	NY 2000 (I)	100	V: ↑ in CNS I: ↑ in IFNα in CNS	(55)
	IRF1 ^{-/-}	NY 2000 (I)	100	V: ↑ in CNS, early CNS entry, ↑ in persistent virus I: ↑ in CD8 ⁺ cells in CNS	(32)
	IRF3 ^{-/-}	NY 2000 (I)	100	V: ↑ in CNS, early CNS entry	(55)
	MyD88 ^{-/-}	NY 2000 (I)	70	V: ↑ in CNS I: ↓ CD45 ⁺ cells in CNS, ↓ chemokine expression in CNS	(272)
	SARM ^{-/-}	NY 2000 (I)	70	V: ↑ in brainstem I: ↓ microglia activation	(274)
	MAVS ^{-/-}	TX02 (I)	100	V: ↑ CNS, early entry I: ↑ activated immune cells	(270)
ISGs	PKR ^{-/-} x RNaseL ^{-/-}	NY 2000 (I)	90	V: early CNS entry	(230)
	Viperin ^{-/-}	NY 2000 (I)	85	V: ↑ in CNS	(271)
Adaptive responses	Perforin ^{-/-}	NY 2000 (I)	78	V: ↑ in CNS, early CNS infection,	(251)

	Perforin ^{-/-} CD8α chain ^{-/-}	Sarafend (II) NY 2000 (I)	18 84	persistent virus in brain No Δ in lethality V: ↑ in CNS, early CNS infection, persistent virus in brain	(300) (249)
	TCR β chain ^{-/-} β2 microglobulin ^{-/-}	CT2741 (I) Sarafend (II)	90 80	V: ↑ in CNS V: ↑ in CNS, early CNS infection	(299) (299)
	MHC-1a ^{-/-} Granzyme A and B ^{-/-}	NY 2000 (I) Sarafend (II)	88 70	V: persistent in CNS V: ↑ in CNS	(249) (300)
	Perforin ^{-/-} x granzyme A and B ^{-/-}	Sarafend (II)	50	V: ↑ in CNS	(300)
	Fas ^{-/-} Gld(FasL ^{-/-})	Sarafend (II) NY 2000 (I)	32 75	No Δ in lethality V: ↑ in CNS I: ↓ CD8 ⁺ in CNS	(300) (247)
	Gld(FasL ^{-/-}) Perforin ^{-/-} x gld MHCII ^{-/-}	Sarafend (II) Sarafend (II) NY 2000 (I)	32 62 100	No Δ in lethality V: ↑ in CNS V: persistent in CNS I: ↑ CD8 ⁺ in CNS	(300) (300) (257)
	CD4 ^{-/-}	NY 2000 (I)	100	V: persistent in CNS I: ↑ CD8 ⁺ in CNS	(257)
	CD40 ^{-/-}	NY 2000 (I)	100	V: ↑ in CNS I: ↓ CD8 ⁺ cells, ↓ CD45 ⁺ cells in CNS	(256)
	TRAIL ^{-/-}	NY 2000 (I)	85	V: ↑ in CNS I: CD8 ⁺ unable to clear virus from CNS	(250)
Inflammasome pathway components	Casp1 ^{-/-}	TX02 (I)	60	No data reported	(212)
	Nlrp3 ^{-/-}	TX02 (I)	60	No data reported	(212)
	Nlrc ^{-/-}	TX02 (I)	30	No data reported	(212)
	ASC ^{-/-}	NY 1999 (I)	95	V: ↑ in CNS I: ↑ cytokine expression in CNS	(139)
BBB molecules	Drak2 ^{-/-}	CT2741 (I)	55	V: ↓ in CNS I: ↓ T cell trafficking into CNS	(295)
	MMP9 ^{-/-}	CT2741 (I)	35	V: ↓ in CNS I: ↓ BBB permeability, ↓ proinflammatory cytokine expression in CNS	(292)
	ICAM ^{-/-}	CT2741 (I)	40	V: ↓ in CNS I: ↓ BBB permeability, ↓ proinflammatory cytokine expression in CNS	(57)
Cellular	Myeloid cells	WN25 (I)	75	V: ↑ in CNS	(26)

depletions					
NK cells	NY 2000 (I)	35	No Δ in lethality	(248)	
CD8 ⁺ T cells	Sarafend (II)	70	V: \uparrow in CNS	(299)	
CD4 ⁺ T cells	NY 2000 (I)	100	V: persistent in CNS	(257)	
Neutrophils prior to infection	CT2741 (I)	100	No data reported	(15)	
Neutrophils after infection	CT2741 (I)	45	No data reported	(15)	
DLN Macrophages	NY 2000 (I)	100	V: \uparrow in CNS	(211)	

^a all knockouts are made in C57/BL6 background unless indicated

However, several studies report contrasting observations; while some studies suggest recruitment of T cells and monocytes to the CNS is beneficial to the host, others suggest that infected leukocytes initiate infection in the CNS (291, 292, 295, 297). Thus, examining neuroinvasion and pathogenesis at a more in-depth, cellular level may provide additional insights into the progression of WNV neuropathogenesis.

1.9.4 Adaptive immune response to WNV in the CNS

The cellular immune response is comprised of all leukocyte subtypes, both innate and adaptive. Trafficking of innate immune cells to the site of infection, including macrophages, monocytes, dendritic cells and neutrophils, serves two main purposes: the direct killing of viruses by production of reactive oxygen or nitrogen species (ROS or RNS), and presentation of antigen to adaptive immune cells, such as B and T cells, that mature in the lymphoid tissues. The innate immune response also promotes trafficking of lymphoid cells, such as cytotoxic cells (T-cells), T-helper cells, and antibody-producing cells (B-cells), into infected tissues to both kill infected cells and neutralize viral particles (287). Importantly, the T- and B-cell responses to viral infection are specific and lead to lasting immunity to viral infection. T cells recognize infected cells upon binding of their T-cell receptor to major histocompatibility complex (MHC) molecules containing viral antigen on an infected cell (202, 215) (**Figure 12**). T cell activation also requires binding of cytokines and additional ligands synthesized by an infected cell to corresponding receptors present on the lymphoid cell (238). During viral

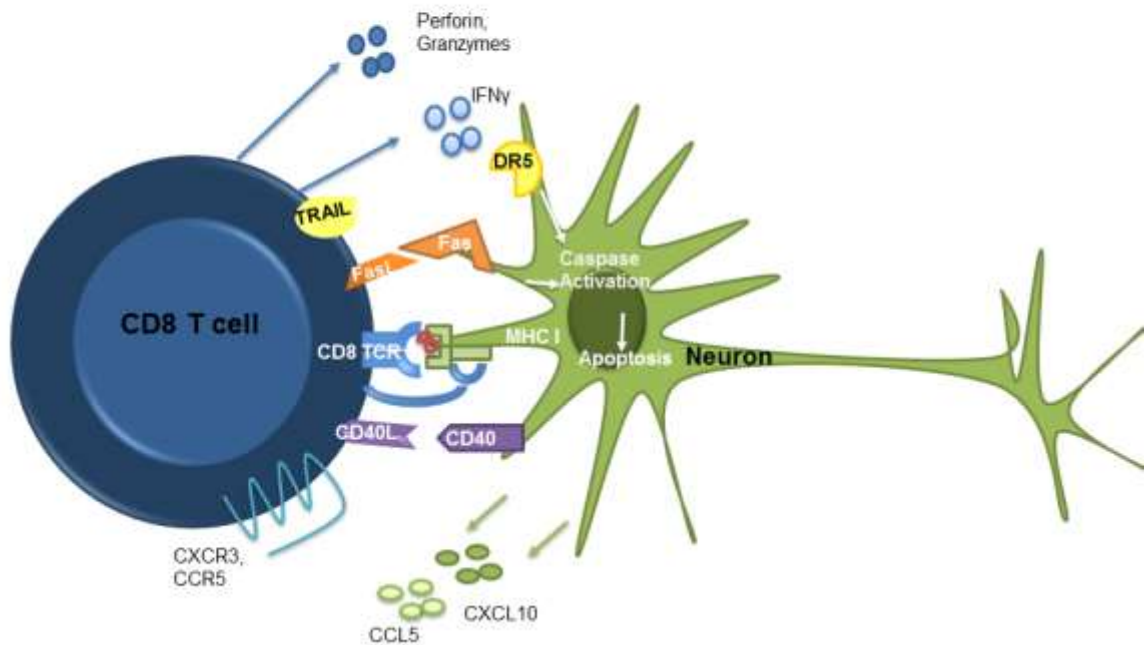


Figure 12- Recognition of a WNV-infected neuron by a CD8⁺ T cell. WNV-infected neurons present antigen via MHC I to CD8⁺ T cells and express increased levels of Fas, CD40 and DR5. In addition, WNV-infected neurons secrete CCL5 and CXCL10 to recruit CD8⁺ T cells to the CNS. Upon recognition of antigen, CD8⁺ T cells secrete IFN γ and release granules containing perforin and granzymes. FasL and TRAIL expressed on the surface of CD8⁺ T cells binds to Fas and DR5, respectively, on neurons, and induce caspase-3 dependent apoptosis in the infected neuron.

infection, antigen presentation and recognition by activated T cells is essential for complete viral clearance, resolving immune responses, and maintenance of the immune system through long term immunity. In contrast, B cells recognize exogenous antigens directly. Recognition of antigen by B cells is also essential for generating and maintaining an active antibody response to neutralize viral particles and maintain immune recognition of infection. In order to escape the effects of the adaptive immune response, many viruses have co-evolved strategies to escape T or B cell activation within permissive hosts (316).

T-cells are classified into several subgroups according to the type of T cell receptor they express. All T cell subtypes respond to WNV infection and play a role in viral clearance and maintenance of a regulated adaptive immune response (247, 248, 250, 251, 256, 257, 296, 298, 299). CD8-bearing T cells are cytolytic, whereas CD4-bearing T cells either regulate immune responses (Tregs) or activate B cells to produce antibodies. The class of MHC molecule presented by an infected cell will determine whether a CD4⁺ or CD8⁺ T-cell response will be initiated. After engagement of the MHC molecule and costimulation by additional cell surface receptors, T cells carry out their distinctive functions. Activated CD8⁺T cells express high levels of Fas Ligand, which upon engaging Fas receptors on infected cells leads to apoptosis in the infected cell. CD8⁺ T cells also secrete perforin, a pore-forming molecule, and granzymes, which are serine proteases, that enter into and induce apoptosis in infected cells. Depending on the cytokine environment they encounter after maturation, activated CD4⁺ cells further develop into subsets of helper T cells, which stimulate B cells, repress the

innate immune system, or regulate the immune response during viral clearance. Thus, both CD4⁺ and CD8⁺T cell responses are essential components of the immune response to viral infections (233), and necessary for successful viral clearance. Indeed, a productive adaptive immune response to WNV infection is essential for host survival. Although evidence suggests certain T-cell activities have both pathogenic and protective roles during WNV infection (248) (298), it is clear that productive and regulated T- and B-cell-specific responses to WNV infection are essential for host survival (64). Early B cell activation during WNV infection is dependent on IFN signaling and essential for survival (211), and the production of WNV-specific antibodies is necessary for lasting immunity to WNV. However, the production of antibody to immature viral particles may contribute to antibody-dependent enhancement of WNV (192). Antibody-dependent enhancement is a process where antibodies with lower affinities to the viral antigen do not neutralize the viral particle, and instead facilitate viral entry into cells expressing Fc receptors. Since the particle is not neutralized, it remains infectious, entering cells via an indirect method. This phenomenon is primarily responsible for the increasing severity of subsequent dengue virus infections of different strains, and has also been observed in WNV infections in mice (192). Thus, instead of being anti-viral in nature, lower affinity antibodies permit viral particles to enter cells that may not express the cognate receptor for the virus.

The T-cell response to WNV infection in the CNS occurs in three stages: attraction to the site of infection, recognition of infected cells, and killing of infected cells. T cell infiltration into the CNS of WNV-infected mice is dependent

on inflammatory cytokines produced by infected cells of the CNS. For example, once infected, neurons secrete CXCL10, which binds to the cognate receptor on T cells, CXCR3. Expression of this chemokine:receptor pair is necessary for an effective T cell response and clearance of virus from neurons during WNV infection (131). Additionally, WNV upregulates expression of CCL3, 4 and 5 in the CNS, all of which bind to the cognate CCR5 receptor (92). Deletion of CCR5 is associated with decreased trafficking of T cells to the CNS, leading to increased morbidity (92). In addition, the trafficking of T-cells into the CNS and transmigration across the BBB is dependent on CD40-CD40L and TNF α -TNF α R interactions (253, 256).

After infiltrating the CNS, CD8⁺ T cells recognize infected cells by the upregulation of MHC I on neurons (47). Upon recognition, activated CD8⁺ T cells secrete chemokines to promote viral clearance, such as IFN γ , which are necessary for controlling WNV infection (87). Besides MHC molecules, WNV-infected neurons express increased levels of death receptor 5 (DR5) and Fas, which bind Tumor necrosis factor-related apoptosis-inducing ligand (TRAIL) and Fas ligand (FasL) on T cells respectively (247, 250). Binding of both DR5 and Fas to their receptors induces a conformational change in their cytoplasmic regions, and leads to induction of apoptosis within the infected neuron. Finally, increased viral loads in the CNS of perforin^{-/-} mice suggest that perforin leads to CD8⁺-induced viral clearance during WNV infection (251).

Although T-cell development is essential for clearance and preventing persistence in the CNS, an overreactive response can contribute to

pathogenesis. Depletion of CD8⁺ T-cells in mice and rag^{-/-} mice exhibited increased survival when inoculated with attenuated strains of WNV (298, 299). This suggests that, as with several other aspects of WNV infection, the adaptive immune response can be either harmful or helpful depending on the context. Further research into how different strains of WNV initiate adaptive responses and the kinetics of the adaptive response will help to determine how a regulated, protective response to WNV infection is initiated and sustained.

1.10 Significance of PhD Dissertation Research

Neuroinvasive viruses are a severe public health threat. Many arboviral vectors, including mosquitoes and ticks, that spread neuroinvasive viruses continue to increase in population and global distribution. Likewise, climate change facilitates overwintering of infected arboviral vectors, potentially prolonging the life cycles of vectors and increasing encounters with hosts. Moreover, many viral infections, including WNV, once considered acute infections, may be persistent in the CNS and cause downstream neurological complications (186, 263). Neuropathology is also observed in many latent viral infections, such as HIV (10). Prevention and treatment of CNS pathologies must consider both viral and host factors. Examining contributions from both the kinetics of the host immune response and the viral replication kinetics at specific sites within the CNS is necessary for developing appropriate preventative treatments and therapies for multiple stages of infection. The CNS is increasingly recognized as a distinct immunological system, with unique responses to

infections (213). The consequences of disturbing the regulation of the immune system in the CNS are not completely understood. In several models of both acute and chronic disease, CNS disease pathologies resulted from aberrant or unregulated immune responses in the CNS (92, 94, 95). Thus, understanding how this unique and significant system is regulated is necessary for combating neuroinvasive disease.

Animal models have provided information linking ultimate neurological pathology to certain unique host and viral factors (See table 1). However, the contributions of the kinetics of the immune response in the CNS and viral replication in the various cell types within the CNS to neuropathology remain unclear. To address these questions, I examined, *in vitro*, various cell types at the interface of the BBB to assess cell-type specific antiviral responses to WNV, and host and viral responses within interacting cell types in the neurovascular unit (NVU). Along with a distinctive BBB model, I used WNV strains of both high pathogenicity (WNV-NY) and low pathogenicity (WNV-MAD78) to identify host antiviral responses and strain-specific factors that may contribute to their naturally occurring differential abilities to induce neuropathogenicity (23).

Initially, replication kinetics and spread were examined for each strain in each cell type of the NVU. Replication of WNV-NY and WNV-MAD78 was equivalent in both neurons and endothelial cells. Additionally, both strains exhibited a similar capacity to traverse an endothelial cell layer grown in a suspended transwell, and an equivalent number of astrocytes were initially infected when they were added to the bottom well of the transwell model system.

However, in astrocytes, WNV-MAD78 replication was delayed compared to WNV-NY. Additionally, in astrocytes WNV-MAD78 was restricted in cell-to-cell spread compared to WNV-NY, and this restriction was independent of type-1 IFN. Together, these data suggest that astrocytes are a potential site for regulation of WNV neuropathology.

Because I demonstrated that astrocytes play a role in limiting nonneuropathogenic WNV replication, a more critical analysis on both cellular factors in astrocytes and potential genetic virulence factors was undertaken. While a differential expression of secreted antiviral molecules did not account for the restriction in WNV-MAD78 spread in astrocytes, furin activity and expression was increased in astrocytes compared to other cell types. In addition, the infectivity of WNV-MAD78 particles derived in astrocytes was restricted compared to the infectivity of WNV-NY particles derived in astrocytes. Therefore, novel viral chimeras were constructed and infectious particle production and viral replication in astrocytes were examined. The restriction of WNV infectious particle production in astrocytes was highly attributed to the composition of structural genes. These data provide support of a novel mechanism for restricting infectious particle production within astrocytes independent of the innate antiviral response

The innate immune responses in the cell types of the BBB were also examined individually and in concert in vitro. WNV-MAD78-infected endothelial cells exhibited increased chemokine expression and distribution across an endothelial cell layer compared to WNV-NY-infected endothelial cells. However,

WNV-NY-infected astrocytes displayed increased chemokine expression compared to WNV-MAD78-infected astrocytes. Moreover, when astrocytes were added to the bottom layer of a transwell containing endothelial cells, the distribution of chemokines within the endothelial layer was disrupted. Additionally, WNV-NY-infected astrocytes secreted higher levels of chemokines compared to WNV-MAD78-infected astrocytes. The addition of astrocytes to the BBB model displayed that the immune response to WNV in the CNS is a dynamic process that is modified as infection progresses through the BBB.

To provide additional insight into the physiological relevance of the in vitro studies undertaken, preliminary animal experiments were performed. Initial experiments demonstrated that there is an additional restriction for WNV-MAD78 entry into the CNS compared to WNV-NY. Viral RNA and neutralizing antibodies were detected in the serum and spleen prior to initiation of a proinflammatory antiviral response at any of these sites. A lack of cytokine and chemokine response in the serum, spleen and brain at early times post infection suggests that chemokine responses are a result of WNV infection in the brain, and do not precede viral incursion into the CNS. Together with the in vitro data, these data led to a more complete model for the differences in replication and the immune responses at the BBB between neuropathogenic and nonneuropathogenic strains of WNV.

Chapter 2- Materials and Methods

Cells and viruses. Previously characterized human brain microvascular endothelial cells (HBMECs) were obtained from K.S. Kim (Baltimore, MD) (312). HBMECs were isolated from individuals with seizure disorders and transformed by stably transfecting cells with the SV-40 large T antigen. HBMECs were grown in RPMI 1640 supplemented with 10% FBS, antibiotic/antimycotic, nonessential amino acids, MEM vitamins, 5 U/mL Heparin, NuSerum (10%), 2mM L-glutamine, 1 mM sodium pyruvate, and 150 µg/ml endothelial growth supplement. All HBMEC experiments were performed with cells passaged no more than 12 times. Donor matched primary human brain cortical astrocytes (HBCAs) (ABRI371) and human brain microvascular endothelial cells (HBMVECs) (ABRI401) derived from normal human tissue were purchased from CellSystems (Kirkland, WA). Both cell types were maintained according to the manufacturer's instructions. All experiments with HBMVECs and HBCAs were performed on cells passaged no more than 14 times. Primary cortical neurons were prepared from day 15 C57BL/6 mouse embryos as previously described (131). Cortical neuron experiments were performed using neurons that were cultured for 3 to 4 days in neurobasal medium containing B27 and L-Glutamine (Invitrogen). Neuro2A and Vero cells were maintained in DMEM supplemented with 10% FBS, 2 mM L-glutamine, 1 mM sodium pyruvate, antibiotic/antimycotic solution and non-essential amino acids (complete DMEM). Neuro2A cells were differentiated 3 days prior to infection by reducing the FBS concentration to 0.5%

and were maintained in differentiation media throughout the course of the experiment.

Working stocks of WNV-NY strain 3356 were generated from an infectious clone pFL-WNV (245). Briefly, infectious particles were recovered as previously described (245), passaged once in 293 cells at a low multiplicity of infection (MOI), and subsequently passaged in Vero cells. WNV-MAD78 was obtained from the World Reference Center of Emerging Viruses and Arboviruses (Galveston, TX). Lyophilized virus was resuspended in complete DMEM supplemented with 20% FBS, amplified once in Vero cells and plaque purified. Viral stocks were amplified once in 293 cells at a low MOI and working stocks were generated by passaging once in Vero cells. All viral stocks were aliquotted and stored at -80°C .

Growth curves. Cell cultures were infected with WNV-NY or WNV-MAD78 at the indicated MOI for 1 hour at 37°C . Unless otherwise stated, the amount of virus added to cultures to achieve the indicated MOI was calculated using the titer of the viral stock on the respective cell line. The inoculum was removed and complete media was added. Culture supernatants were recovered at the indicated times and clarified by low speed centrifugation for 5 minutes. Supernatants were transferred to new tubes and stored at -80°C . Viral titers were determined by plaque assay on Vero cells.

Virus titration by plaque assay. Monolayers of Vero cells in 6 well plates were washed once with PBS prior to the addition of serial dilutions of viral samples. The cells were incubated in a 5% CO_2 incubator for 1 hour at 37°C with

rocking, the inocula removed and complete DMEM solution with 0.9% low melt agarose (Fisher) was overlaid. VSV plaques were counted 24 hours post-infection. For WNV titration, cell monolayers were incubated for 48 hours and a second overlay of agarose-containing complete DMEM supplemented with 0.003% neutral red (Sigma) was added. The plates were incubated for an additional 48 (WNV-NY) to 96 hours (WNV-MAD78) prior to counting plaques. All titers were performed in duplicate.

Viral translocation assay. HBMECs or HBMVEs (4×10^4 cells) were plated on the luminal side of a fibronectin-coated cell culture insert with a pore size of 3 μm pores (BD Biosciences) and incubated for 5 days at 37°C in a 5% CO_2 incubator. The widely accepted methods of transendothelial electrical resistance (TEER) and translocation of FITC-labeled dextran were used to assess the integrity of the endothelial monolayers (264) (285). As previously reported, monolayers reaching TEER values between 250 to 300 ohms/cm^2 were largely impermeable to FITC-labeled dextran (285). Therefore, monolayers were considered confluent once a minimum TEER value of 250 ohms/cm^2 was achieved. Confluent cultures were infected at an MOI of 0.1 by adding virus to the upper, luminal chamber. Inoculum was removed after incubating for 1 hour at 37°C and 500 μl of appropriate complete medium was added to both chambers. Medium was collected from both the chambers at indicated times and the level of infectious virus was determined by plaque assay.

In vitro BBB model. HBMECs (4×10^4 cells) and HBCAs (7.5×10^3 cells) were plated on the transewell insert and bottom chamber, respectively. The

transendothelial electrical resistance (TEER) of the HBMEC monolayer was measured 5 days after plating using a Millicell ERS. Cultures were considered confluent when a resistance of 250 to 300 ohms/cm² was recorded. The HBMEC monolayer was infected at an MOI of 0.1 by adding virus to the luminal chamber. Inoculum was removed after incubating for 1 hour at 37°C and 500 µl of appropriate complete medium was added to both chambers. Medium was collected from both the chambers at indicated times and the level of infectious virus determined by plaque assay.

Indirect immunofluorescence analysis (IFA). At the indicated times post-infection, the HBCA or HBMEC monolayer was washed with PBS and fixed with 3% paraformaldehyde. Cell monolayers were permeabilized with a solution of PBS/0.2% Triton X100, blocked with PBS containing 10% normal goat serum, and incubated with the indicated primary antibodies from the following: WNV hyperimmune ascitic fluid (1:1000, World Reference Center of Emerging Viruses and Arboviruses), rabbit anti-NFκB (1:500, Santa Cruz ab7151), followed by corresponding secondary antibodies as follows: goat anti-mouse IgG Dylight 549nm-conjugated (1:800, Jackson ImmunoLaboratories) or goat anti-rabbit IgG Alexafluor 488nm-conjugated (1:500, Jackson ImmunoLaboratories). All monolayers included a nuclear Hoescht stain (0.1µg/mL). Cells were visualized with an Olympus IX51 microscope equipped with a digital camera.

Flow cytometry. HBCA monolayers infected with WNV-NY or WNV-MAD78 (MOI of 0.01) were removed from plates by trypsinization, washed 2 times with PBS and fixed in 3% paraformaldehyde. Cells were permeabilized with

PBS/0.2% Triton X-100, blocked in PBS containing 0.5% heat-inactivated FBS and probed with WNV hyperimmune ascitic fluid (1:1000, World Reference Center of Emerging Viruses and Arboviruses) followed by goat anti-mouse IgG 633nm Dylight conjugated antibody. For flow cytometry analysis, 100,000 single cell events were collected using a FACS Canto (BD Biosciences).

Type-I Interferon Bioassay. A549s (7×10^4 cells) in 24-well plates were treated with 2-fold serial dilutions of human leukocyte IFN α (BEI Biosciences) or cell-free, UV-inactivated supernatants recovered from WNV-infected HBCAs. Pretreated cells were infected with VSV (MOI of 1) and supernatants collected at 24 hours post-infection. Viral titers were determined by plaque assay on Vero cells as described above. IFN concentrations were determined based on a standard curve generated from the titers recovered from samples treated with IFN α .

Neutralization of type-I IFN. The antibody concentration necessary to neutralize the IFN present in supernatants recovered from WNV-infected HBCAs was determined by pretreating A549 cells for 24 hours with 160 IU/mL of IFN α or β in the presence of 10-fold dilutions of the antibodies to IFN α (BEI) or IFN β (BEI). Control wells consisted of cells treated with IFN only, no IFN or isotype matched antisera to IFN α or IFN β . Pretreated cells were infected with VSV (MOI of 1) and supernatants collected at 24 hours post-infection. Viral titers were determined by plaque assay on Vero cells. For neutralization experiments, HBCAs were inoculated with WNV (MOI of 0.01) for 1 hour at 37°C. The inoculum was replaced with complete DMEM containing 2 times the amount of

antibody necessary to neutralize 160 IU/ml IFN α and/or IFN β or the appropriate control sera.

Quantitative Real-time PCR (qRT-PCR) Total RNA was extracted from HBCAs infected with WNV-MAD78 or WNV-NY (MOI=0.01) or from HBMECs mock-infected or infected with WNV-NY or WNV-MAD78 (MOI=0.1) using Trizol (Invitrogen Life Technologies, Inc.) and treated with TurboDNase (Applied Biosystems). Spleen and brains were harvested from mice and homogenized in 1mL TRIZOL-LS treated with TurboDNase (Applied Biosystems). Where applicable, RNA was extracted from supernatants (Qiagen). Total viral RNA levels were determined by quantitative real-time PCR analysis on a Roche LC480 using Veriquest One-Step SYBR green MasterMix (Affymetrix Biosystems) with 50 ng of RNA, or One-Step SYBR green from Quanta Biosciences with 50 ng of RNA. Primer efficiencies were determined and the fold change relative to mock-infected cells at 1 h post infection was calculated using the Paffl method. Primers used for qPCR are indicated in table 1. Two-step qPCR was used to determine strand-specific viral RNA levels. cDNA was generated from 500 ng of RNA using Moloney murine leukemia reverse transcriptase (NEB Biosciences) and gene-specific primers. The resulting cDNA was used as template for qPCR with SYBR green 2x Veriquest MasterMix (Affymetrix). Primers used for 2-step qPCR were the primers for WNV-NY and WNV-MAD78 (fwd) and (rev) in the table below.

Table 2. Primers used for qPCR and qRT-PCR.

Primer name	Sequence
WNV-NY E (fwd)	5'- GGA CCT TGT AAA GTT CCT ATC TCG-3'
WNV-NY E (rev)	5'-AGG GTT GAC AGT GAC CAA TC-3'
WNV-MAD78 E (fwd)	5'-CTG TAA GGT GCC CAT TTC C-3'
WNV-MAD78 E (rev)	5'-CCT CTT CCC ACC ACA ATG TAG-3'
hGAPDH (fwd)	5'- CCA CTC CTC CAC CTT TGA C-3'
hGAPDH (rev)	5'- ACC CTG TTG CTG TAG CCA-3'
hCCL2 (fwd)	5'-TCT CTG CCG CCC TTC TGT G-3'
hCCL2 (rev)	5'-GCT TCT TTG GGA CAC TTG CTG CTG-3
hCCL5 (fwd)	5'-CTC TGT GAC CAG GAA GGA AGT-3'
hCCL5 (rev)	5'-GGG TTG AGA CGG CGG AAG-3'
mGAPDH (fwd)	5'-AAG GTC GGT GTG AAC GGA TTT-3'
mGAPDH (rev)	5'-ATT TGC CGT GAG TGG AGT CAT AC-3'
mCCL2 (fwd)	5'-G CAC CAG CAC CAG CCA AC-3'
mCCL2 (rev)	5'-CCA GAA GCA TGA CAG GGA CC-3'
mCCL5 (fwd)	5'-CGC CAA GTG TGT GCC AAC-3'
mCCL5 (rev)	5'-ACC GAG TGG GAG TAG GGG A-3'
mCXCL2 (fwd)	5'-CCA CTC TCA AGG GCG GTC-3'
mCXCL2 (rev)	5'-TCA GGT ACG ATC CAG GCT TC-3'

ELISAs. The concentration of hCCL2 and hCCL5 in the supernatants of mock and WNV-infected cells was determined by ELISA according to the manufacturers' instructions (BD Biosciences and R&D systems, respectively). The concentration of TNF α , IL-12p40, and IL-6 in the serum of mock and WNV-infected mice was determined by ELISA according to manufacturers' instructions (BD Biosciences and R&D systems).

Permeability assays. FITC-dextran (100 μ l of 100 μ M, Sigma, 4kda) was added to the luminal chamber of a transwell plate and incubated for 1 h at 37 $^{\circ}$ C in the dark. Media was recovered from the abluminal chamber and diluted 1:2 in 2% Triton lysis buffer to inactivate virus. Fluorescence levels were quantitated using a FLUOstar Omega fluorescence microtiter plate reader (BMG LabTech). For positive control, monolayers were incubated in 5mM EDTA in PBS for 1 h prior to the addition of FITC-dextran.

Confocal Microscopy. HBMEC monolayers grown on transwell inserts with or without HBCAs plated in the bottom chamber were infected as described above. The luminal and abluminal sides of the transwell insert were washed with PBS at 48 (HBMEC alone) or 72 (coculture) hours post-infection, fixed with 4% paraformaldehyde, and permeabilized in 0.2% Triton-X100/PBS. Cells were blocked with 10% Normal goat serum/PBS and incubated for 1 h in the presence of rabbit anti-CCL2 (1:10, Abcam), goat anti-CCL5 (1:15, R&D systems), and WNV hyperimmune ascitic fluid (1:1000, Arbovirus resource center). Cells were washed three times with PBS containing 0.5% Tween-20 and incubated with Dylight488 anti-rabbit IgG (1:100, JacksonImmunoLabs) Dylight549 anti-mouse

IgG (1:800, JacksonImmunoLabs), Alexafluoro633 anti-goat IgG (1:200, Invitrogen) and Hoechst stain (0.1ug/mL). The inserts were mounted on slides using Mowiol media (Calbiochem). Imaging and Z-stacks were captured using a Zeiss LSM 710 Microscope at 40x objective. All quantification analysis was performed using ImageJ software (239).

Type-1 IFN and TNF α treatments. HBMEC monolayers were either pretreated 24h before inoculation with either TNF α (5ng/mL Invivogen), Human leukocyte IFN α (BEI Resources), or recombinant human IFN β (BEI Resources) or post-treated after inoculation with either WNV-NY or WNV-MAD78 (MOI=1). Monolayers that were pretreated were also post-treated with the same cytokine. At 24 and 48 h post inoculation, culture supernatants and cell lysates were collected for plaque assays and Western blot analysis, respectively.

Western Blotting. Cell monolayers were washed twice with modified DPBS (Hyclone), and lysed with Ripa buffer (10 mM Tris pH 7.4, 150 mM NaCl, 0.02% NaN₃, 1% sodium deoxycholate, 1% Triton X-100, 0.1% sodium dodecyl sulfate [SDS], and 1X protease inhibitors [Sigma]). Lysates were subjected to SDS-polyacrylamide gel electrophoresis (PAGE) and transferred to nitrocellulose membranes. Nitrocellulose membranes were then blocked in 5% NFD milk diluted in Western wash buffer (PBS+0.1% Tritoxn-X) and incubated with the following primary antibodies: polyclonal rabbit anti-GAPDH (1:5000, Abcam; ab36845), polyclonal mouse anti-WNV (1:1000, Arbovirus Resource Center; T35570), rabbit anti-ISG15 (1:2500, gift from the Haas lab), rabbit anti-ISG56 (1:2500, gift from Ganes Sen), mouse anti-VCAM (1:50, Santa Cruz ab 13160),

mouse anti-ICAM (1:50, Santa Cruz ab 18853). Following primary antibody incubation, anti-mouse or anti-rabbit antibodies conjugated to HRP were incubated with membranes and blots were visualized using ECL (GE Healthcare).

Adhesion assay. HBMECs were either mock-infected, infected with either WNV-NY, WNV-MAD78 (MOI=0.1) for 48h, or treated with 100ng TNF α for 24h as a positive control. THP-1 cells were labeled using CellTracker™ Green CMFDA (2 μ M, Invitrogen) and 2 x 10⁶ labeled cells in 500 μ l complete THP-1 media were added to each well after removal of supernatant. Plates were rocked for 30 minutes at 37 degrees Celcius, 5% CO₂ and washed vigorously 3 x with PBS to remove nonadherent cells. Cells were fixed using 3% paraformaldehyde and visualized on an Olympus microscope model IX51.

Transmigration Assay. Cells were plated and inoculated as described above for the *in vitro* BBB. At 72h postinfection, THP-1 cells were labeled using CellTracker™ Green CMFDA (2 μ M, Invitrogen) and 2 x 10⁶ labeled cells in 500 μ l complete THP-1 media were added to each well after removal of supernatant. Cultures were then incubated at 37°C for 6 hours to allow for transmigration of labeled THP-1 cells through the endothelial monolayer. After incubation the total components in the abluminal chamber were lysed directly by adding 500 μ L 2x Triton-X lysis buffer (2% Triton-X 100,) directly to the 500 μ l of culture media. Lysed samples were removed and places into light-sensitive tubes prior to reading fluorescence of 150 μ l each sample in triplicate on an Omega FLUOstar (Absorbance 485nm, emission 520nm).

Ethics statement. All procedures with mice were done in accordance with the recommendations in the Guide for the Care and Use of Laboratory Animals of the National Institutes of Health. The protocol was approved by the University of Maryland Institutional Animal Care and Use Committee (permit #: R0969).

Animal Experiments. Four week old Swiss-webster female mice were purchased from Harlan Laboratories. Animals were inoculated intravenously by injecting 100 μ l containing 10^4 pfu of WNV-NY, WNV-MAD78 or PBS directly into the tail vein. Animals were weighed and monitored for signs of morbidity daily. Viral stocks for animal experiments were generated by passaging WNV-NY and WNV-MAD78 one time in Vero cells. Blood was collected at 8, 24, 48, 96 and 120 hours post inoculation via orbital bleed and serum separated via centrifugation (1000xg, 20 mins) and subjected to plaque assays. Spleen and brain were harvested at the same time points as blood after transcardial perfusion with 20mL PBS. Each organ was divided and subjected to either RNA extraction in TRIZOL or homogenized in 1mL PBS. Quantification of virus at these three sites within mice was performed using plaque assay, nested PCR, and/or integrated PCR.

Nested PCR. RNA was extracted using TRIZOL reagent as described by manufacturers instructions. RNA was resuspended in 15 μ l water, and 2 μ l was used as template in the RT-PCR reaction, consisting of SYBR Mastermix (Quanta biosciences), and external WNV primers (sense- 5'-TCC TTG ATT GGA CTG AAG -3', antisense 5'-TGA GTG GCT CCA ACC TG -3'). Products were then buffer exchanged (Promega) and eluted in 40ul water. The following round

of PCR consisted of 1 ul of the eluted template and utilized internal WNV-NY primers (sense 5'- CAG ACA CAC GGA GAA ACG AC-3', antisense 5'- TGA GTG GCT CCA ACC TG -3') or WNV-MAD78 primers (sense 5'-CAT GGA CGT GGG ATA CCT CTG -3', antisense 5'- TGA GTG GCT CCA ACC TG -3'). All reactions were run on 2% agarose gels and visualized using ethidium bromide.

Integrated PCR. Supernatants of homogenized infected mouse organs were inoculated onto HBMEC monolayers. After 1 hour of inoculation, complete HBMEC media was added to the flasks. At 72 and 96 hours post inoculation, supernatants were collected and subjected to plaque assays. At 96 hours post inoculation, cells were washed 3x with PBS and lysed in 1mL Trizol. RNA extraction was subjected to RT-PCR with MMLV (NEB Biosciences) using 7µg of and random hexamers (10µM). PCR was carried out using primers for the E gene of either WNV-NY or WNV-MAD78 (See above table for primer) and Taq polymerase (NEB biosciences).

Plaque Reduction Neutralization Test (PRNT). Serum collected from animal experiments was heat inactivated at 56°C previous to incubation with appropriate parent virus (WNV-NY or WNV-MAD78, 1:1 ratios) for 30 minutes, and plaque assays performed on Vero cells as described above. Values are graphed as an inverse of the dilution where >50% of plaques were inhibited compared to control plaque assays. Serum for mock-infected animals were utilized as a negative control, and serum from animals from timepoints at 48, 96, and 120hpi were assessed.

RT- PCR amplification of products for synthesis of infectious clone.

WNV-MAD78 RNA was isolated from infections in Vero cells using TRIzol (Life Technologies). After extraction, 2-7µg of RNA was used for reverse transcription with murine leukemia reverse transcriptase (MMLV- RT, NEB) with either random hexamers or sequence-specific primers. To amplify all WNV-MAD78 products, 5µl cDNA and a combination of the following Taq polymerase enzymes with their complementary buffers were utilized: Deep Vent Polymerase (NEB), Vent Polymerase (NEB), Phusion Polymerase (Finnzymes). Primers used to amplify specific fragments are described in the table below. PCR products were ligated into cloning vector pVL-blunt to amplify and confirm sequence.

Table 3- Infectious clone primer sets

Virus synthesized	PCR amplification fragment	Sequence of primer pairs	Tm	Enzyme
WNV-MAD78 infectious clone	5'UTR/KpnI→SphI	Mlu/T7/5'UTR: 5'-CAT ACG CGT TAA TAC GAC TCA CTA TAG AGT AGT TCG CCT GTG TGA GCT GA-3' Fwd:5'-GGT ACC AGT AGT TCG CCT GTG TGA GCT GAC-3' Rev: 5'-CCA TGG TTG GGC ATG CGG CTC	60	Vent

		TTG TTG-3'		
	XhoI (SphI)→ClaI	Fwd: 5'-GCT CGA GTG ATG GAA GCA G-3' Rev: 5'-ATC GCA GGC CGC AAA TTC CTT CC- 3'	72	Phusion
	ClaI→BamHI	Fwd: 5'-CAA GAA CTC CGC TGT GGG AGT GGA G-3' Rev: 5'-GTT CTC TTG GTT GGT CCA TCT CGC C-3'		Phusion
	BamHI→KpnI	Fwd:5'-GTT CGC TGA GGC GAA CTC GG-3' Rev: 5'-TTT GGT ACC GGA TAG GAA GTC CTC TC-3'	72	Phusion
	KpnI→(XmnI)XhoI	Fwd: 5'-CCG GTA CCA AAC CTC CGC-3' Rev: 5'-ATC CTC AGA AAG CCC AAT TTG TGA GCG TT-3'	68	Phusion
	BamHI	Fwd: 5'-GGG ATC CGA	50	Vent

	(Nhe)→(Xmnl)Xbal	GTG TAC TCA GAC C-3' Rev: 5'-TTC TAG ACT GTT GTT GCG TTC C-3'		
	Xmnl→Xbal	Fwd: 5'-CGG TGA GAA CTG TCA GGG AAG-3' Rev: 5'-CCT GAC TTT TGG TCC TTT CCC TTT CC-3'	69, 72	Phusion
	Xbal→NotI	Fwd: 5'-CGG GTA CAT CCT GAA GTC GGT TGG GGT GAG G-3' Rev: 5'-AGC GGC CGC AGA TCC TGT GTT CTT GCA CCA C-3'	70.3	Phusion
WNV-MAD78 P156S	1102(s)→1426 mutation	Fwd: 5'-AGA TGA TGA AGA TGG AAG CAG C- 3' Rev: 5'-CAA CCT GCG TGG AGT AGT TAC CAT GGG A-3'	46, 52	DeepVent
	1426 mutaiton→BamHI	Fwd: 5'-GGT AAC TAC TCC ACG CAG GTT	44, 56	DeepVent

			GGAG-3' Rev: 5'-GTT CTC TTG GTT GGT CCA TCT CGC C-3'		
WNV-NY S156P	BamHlt7→ 1426 mutation	1426	Fwd: 5'-caa agg atc cta ata cga ctc act ata gAG TAG TTC GCC TGT GTG AGC TGA-3' Rev: 5'-AAC CTG TGT AGG GTA GTT TCC GTG CGA C-3'	54, 55	DeepVent
	1426 mutation→4087 (as)		Fwd: 5'-CGG AAA CTA CCC TAC ACA GGT TGG AGC CAC-3' Rev:5'-CTC TAG ACA CTC CTC TTC TCC CT- 3'	47, 52	

Assembly of infectious clones and in vitro transcription. After the sequence of each individual fragment was confirmed, WNV fragments were subcloned into

medium-copy vectors (peGFP, pBKSM), and further subcloned into low-copy vectors (pWSK29, pWSK129) as described in **Figure 13**. In addition, the BssHI site in the vector of pWSK29 was mutated for ligation of 5'-Mlu/T7/5'UTR of WNV-MAD78. For in vitro transcription, full-length constructs were sequenced prior to digestion with NotI (WNV-MAD 78) or XbaI (WNV-NY) (NEB). Digestions were treated with Proteinase K (5mg/mL), purified with phenol:chloroform extraction and ethanol precipitation, and 1µg of DNA was used for in vitro transcription (T7 Ampliscribe Max Cap kit Epicentre). RNA was purified as per manufacturer's instructions and visualized on a non-denaturing agarose gel prior to electroporation.

Glycosylation mutants and structural/nonstructural chimeras were synthesized using Gibson Assembly MasterMix as described in **Figure 13**. The two-plasmid system established takes advantage of a naturally occurring NgoMIV site within the 5' end of WNV-NY NS1, and an engineered, silent mutation made in the same location of the WNV-MAD78 NS1. Thus, plasmid 1 contains 5' UTR→E of either WNV-NY or WNV-MAD78, whereas plasmid 2 contains NS1→3' UTR, effectively separating the genome into structural and nonstructural proteins. The strategy utilized was similar to published clones of WNV-TX02/ WNV-MAD chimeras (269). Briefly, PCR fragments were generated utilizing the full length infectious clones as template, and primers containing any desired mutations. In addition, the vector plasmid for the Gibson reaction (i.e. p1 of WNV-MAD78 for the two-plasmid system) was linearized using naturally occurring restriction sites that allowed for 20-100 bp of DNA homologous to

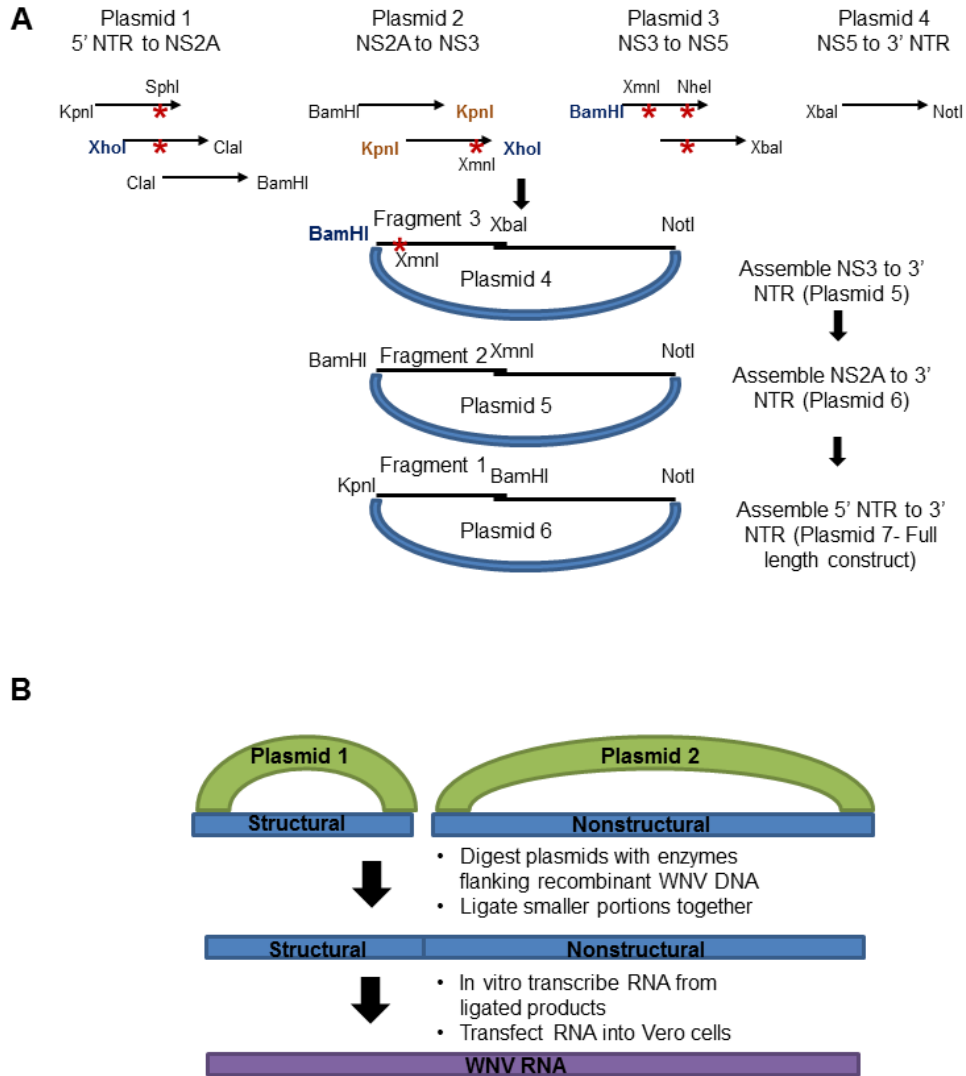


Figure 13. Assembly of infectious clones. (A) Assembly of WNV-MAD78. RNA was isolated from infections in A549 cells and RT-PCR performed with the primers described in Table 3. Prior to assembly in medium copy vectors, each fragment was cloned in a high copy vector and the sequence verified. After cloning in medium copy vectors, fragments were combined in low copy vector pWSK29. (B) Assembly of chimeric viruses. Gibson assembly was performed in order to introduce mutations desired (89). After assembly into 2 separate plasmids, an in vitro ligation was performed and in vitro transcription carried out.

either end of the PCR products generated. The PCR product/s and the digested vector plasmid generated were then added at a 1:2 vector: PCR product ratio to a recombinase, ligase, and polymerase mastermix (NEB) and incubated for 60 minutes at 50 °C. The reaction was directly transformed into MDS42 E. coli, and single colonies were screened and sequenced prior to preparation. To generate template for in vitro transcription using the two-plasmid system, p1 of either virus was digested with BamHI (WNV-NY) or MluI (WNV-MAD78) and NgoMIV, and p2 with NgoMIV and XbaI. DNA fragments were isolated and purified, and p1 and p2 genomic fragments were combined in a 1:1 molar ratio (p1:p2) up to 10µg of total DNA. The combined DNA was then ethanol precipitated, resuspended, and ligated using T4 DNA ligase (NEB) overnight at 16°C. The ligation was then treated with Proteinase K (5mg/mL), purified through phenol:chloroform extraction and ethanol precipitation, and 1µg of DNA was used for in vitro transcription (T7 Ampliscribe Max Cap kit Epicentre). RNA was purified as per manufacturer's instructions and visualized on a non-denaturing agarose gel prior to electroporation.

Electroporation and amplification of virus. Viral RNA (10-12µg) was electroporated (Neon-Invitrogen) into Vero cells (1×10^6) and cultured in DMEM (CellTech) supplemented with 10% FBS (Hyclone) for 7 days. Viral stocks were further amplified once in Vero cells and stored at -80 °C. RNA was extracted using 1mL TRIzol (Life technologies) for each virus synthesized and RT-PCR performed to confirm viral mutations throughout amplification.

Furin activity assay. Cells were lysed in assay buffer (Triton-X100 0.5%, 0.5mM CaCl₂, 100mM HEPES pH 7.0), and a fluorogenic substrate (pERTKR-AMC, R&D systems, 100µM) was added to equivalent amounts of HBMEC or HBCA cell lysates. Fluorescence was immediately read over a 10 minute period with readings taken every 20 seconds (excitation, 380nm; emission, 460nm). As a control, recombinant furin (R&D systems, 0.2µg/mL), was assayed.

Inhibition of furin in HBCAs. In order to determine the necessary amount of inhibitor to use to inhibit furin activity in HBCAs, furin inhibitor (Dec-RVKR-CMK diluted in PBS, 5mM stock concentration) was added at increasing concentrations to a set number HBCAs over a 48h period. After incubation with inhibitor for 48h, HBCA cell lysates were collected as described above and furin activity assays were performed. It was found that 50µM Dec-RVKR-CMK effectively inhibited the furin in HBCAs, and a second dosing at 24h was necessary to maintain the inhibition of furin. During infection, HBCAs were inoculated (MOI=0.01) with either WNV-NY or WNV-MAD78 and either PBS or furin inhibitor was added to media after inoculation (final concentration=50µM). At 24h, an additional dose of furin inhibitor (final concentration=50µM) or PBS was added. Cell supernatants were clarified by low-speed centrifugation at 48h post infection and plaque assays performed in Vero cells as described above.

Focus forming assay of HBCA supernatants on HBCAs. Prior to inoculation, supernatants from WNV-infected HBCAs were either treated with control antisera or antibodies to type-1 IFN (both α and β) at concentrations determined above (see type-1 IFN Bioassay and treatments) for 1h at 37°C.

Antibody-treated supernatants or supernatants that were left untreated were then serially diluted and added to HBCA monolayers. Inoculum was then removed after 1h, complete media was added and HBCAs were incubated for 16h at 37°C, 5% CO₂. At 16h, media was removed, cells washed 2x with PBS, and fixed in 3% paraformaldehyde. Cells were stained as described in indirect immunofluorescence assay section above with antisera to WNV and Hoescht nuclear stain. Individually stained cells were counted. The ratio of the titer found in HBCAs using the focus-forming assay was compared to that of the titer of the same supernatants using plaque assays in Vero cells.

Secreted factor assays. HBCAs were either mock-infected or infected with WNV-NY or WNV-MAD78 (MOI=0.01). At 48hpi, culture supernatant was clarified and subjected to type-1 IFN bioassays. Supernatants were UV-inactivated and diluted 1:1 in 2xDMEM supplemented with 20% FBS. Supernatants were either treated with control antisera to IFN α and IFN β , or antisera to IFN α and IFN β for 1h at 37°C. After incubation, treated or untreated supernatants were added to HBCA monolayers and incubated for 6h at 37°C, 5% CO₂. HBCAs were then washed 1x with serum free DMEM and inoculated with either WNV-NY or WNV-MAD78 (MOI=0.01). During inoculation, fresh supernatant was prepared as described above. After 1h, inoculum was removed and the corresponding supernatants were added to HBCAs. Infected monolayers were incubated for 24h. Culture supernatants were removed, clarified by low speed centrifugation, and subjected to plaque assays in Vero cells.

Statistical Analysis. Graphpad Prism 5 was used to generate all statistical analyses. Standard error and significance were determined using either one-way Anova with Bonferroni post-test correction or a two-tailed paired or unpaired student t-test.

Chapter 3-Differential replication for Pathogenic and Nonpathogenic strains of WNV within Astrocytes

Abstract

The severity of West Nile virus (WNV) infection in immunocompetent animals is highly strain dependent, ranging from avirulent to highly neuropathogenic. Here, we investigate the nature of this strain-specific restriction by comparing the replication of avirulent (WNV-MAD78) and highly virulent (WNV-NY) strains in neurons, astrocytes, and microvascular endothelial cells, which comprise the neurovascular unit within the central nervous system (CNS). We demonstrate that WNV-MAD78 replicated in and traversed brain microvascular endothelial cells as efficiently as WNV-NY. Likewise, similar levels of replication were detected in neurons. Thus, WNV-MAD78's non-neuropathogenic phenotype is not due to an intrinsic inability to replicate in key target cells within the CNS. In contrast, replication of WNV-MAD78 was delayed and reduced compared to that of WNV-NY in astrocytes. The reduced susceptibility of astrocytes to WNV-MAD78 was due to a delay in viral genome replication and an interferon-independent reduction in cell-to-cell spread. Together, our data suggest that astrocytes may regulate WNV spread within the CNS, and therefore may be an attractive target for ameliorating WNV-induced neuropathology.

Introduction

The *Flaviviridae* includes several globally important emerging arthropod-borne viruses, such as yellow fever virus, dengue virus, Japanese encephalitis virus and West Nile virus (WNV). WNV has re-emerged as a pathogen that causes severe neurological disease. Prior to the 1990s, most WNV infections were asymptomatic or associated with a mild febrile illness known as West Nile fever. Since its introduction into the United States in 1999, annual outbreaks of WNV have resulted in ~16,000 reported cases with neurological complications, including meningitis, encephalitis, and acute flaccid paralysis. These cases have resulted in greater than 1,500 deaths, making WNV the leading cause of mosquito-borne neuroinvasive disease in the United States (<http://www.cdc.gov/ncidod/dvbid/westnile/index.htm>). In addition, outbreaks have occurred in other parts of the world, including Eastern and Western Europe (199, 200). Nevertheless, the factors responsible for the increase in pathogenicity of WNV remain poorly understood.

Many neuroinvasive viruses, including WNV, preferentially enter the CNS via the hematogenous route by crossing the blood-brain barrier (BBB). The BBB is comprised of specialized endothelial cells, which line the cerebral microvasculature, and the foot processes of astrocytes, which envelop >99% of the endothelium. Under normal physiological conditions, the BBB tightly regulates transport of molecules into and out of the CNS. The restrictive nature of the BBB is a consequence of the formation of complex cell-to-cell tight junctions and lower basal levels of pinocytosis and endocytosis (1, 129). Although

astrocytes were once thought to serve a structural role in the BBB, it is now clear that they play an important role in maintaining its functional integrity. *In vitro*, co-cultures of brain endothelial cells and astrocytes establish a tighter barrier than endothelial cells alone, and secretion and activation of matrix metalloproteases (MMPs) by astrocytes result in disruption of the BBB during disease (101, 284). Astrocytes also modulate neuronal health and activity through the uptake of excess neurotransmitters and secretion of nutrients (96, 109, 217, 218). Thus, astrocytes serve as a structural and functional bridge between endothelial cells and neurons. Together, these three cell types form the neurovascular unit (NVU), which functions to regulate blood flow, the integrity of the BBB, and neuronal activity in response to environmental changes (118). Understanding how viruses replicate within the NVU may facilitate novel strategies for treating viral infection of the CNS.

The neuroinvasive potential of WNV is strain dependent. While most, if not all, strains of WNV are neurovirulent when mice are inoculated intracranially, only a subset of strains are neuroinvasive when inoculated via a peripheral route (23). The mechanistic basis for the increased neuroinvasiveness of some strains of WNV remains poorly understood. However, the observation that exogenous disruption of the BBB enables a non-neuropathogenic strain of WNV to enter the CNS (164) suggests that the capacity to traverse the BBB is a determining factor for neuropathogenicity. Here, we investigated the nature of the restriction at the BBB by comparing the ability of an avirulent lineage 2 African isolate, WNV-MAD78 (258), and a highly virulent lineage 1 North American strain isolated in

2000, West Nile virus New York (WNV-NY), (23, 127, 253) to replicate in various cell types comprising the NVU. While both strains replicated efficiently in brain microvascular endothelial cells and neurons, WNV-MAD78 replication was restricted within astrocytes compared to WNV-NY. WNV-MAD78 exhibited both a delay in viral genome synthesis and reduced cell-to-cell spread in astrocytes compared to WNV-NY. Moreover, the restriction of WNV-MAD78 replication and spread in astrocytes was independent of type-I interferon (IFN). Together, our findings suggest that astrocytes may play an important role in controlling WNV dissemination within the CNS.

Results

WNV-NY and WNV-MAD78 replicate to similar levels in neuronal cells. Because neurons constitute a primary target of WNV infection *in vivo* (73), we compared WNV-MAD78 and WNV-NY replication in primary cortical neurons derived from wild type C57BL/6 mice and the mouse neuroblastoma cell line Neuro2A (**Figure 14 A and B**) at a multiplicity of infection (MOI) of 0.01 and 0.1, respectively. WNV-NY and WNV-MAD78 reached similar peak titers in both cell types, although the kinetics of WNV-MAD78 replication were slightly delayed at 24 hours in cortical neurons (9.2-fold, $P = 0.03$). Despite the slight growth delay, neuronal cells were highly permissive for WNV-MAD78 replication, suggesting that the non-neuropathogenic phenotype documented in mice (23, 127) is not due to a reduced capacity to infect and replicate in neurons.

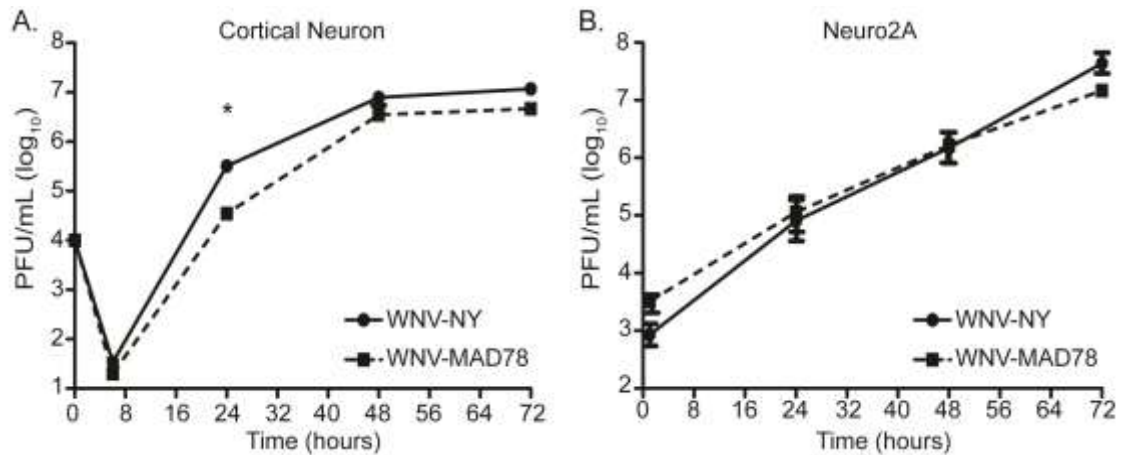


Figure 14. WNV-NY and WNV-MAD78 replication in neuronal cells.

Cortical neurons isolated from C57BL/6 mice (MOI of 0.01) (**A**) and differentiated Neuro2A cells (MOI of 0.1) (**B**) were infected with WNV-NY or WNV-MAD78. The MOI was calculated using the titer of the viral stocks on Vero cells. Culture supernatants were recovered at the indicated times and titers determined by plaque assay on Vero cells. Values represent the average number of plaque forming units (PFU) per mL (+/- standard error) of supernatant and are from at least two separate experiments. A student's unpaired t-test was performed to determine statistical significance. Asterisks indicate differences that are statistically significant (* $p < 0.05$).

WNV-MAD78 efficiently infects and traverses human brain endothelial cells.

Although many viruses achieve high levels of viremia, under normal conditions the BBB is highly effective at protecting the brain from circulating virus in the blood stream. However, neuroinvasive viruses have evolved a variety of mechanisms to breach the BBB and gain access to the CNS (129). Because replication in brain endothelial cells is sufficient for transport of neuroinvasive strains of WNV across brain microvascular endothelial cells (285), we hypothesized that the decreased neuropathogenicity of WNV-MAD78 was due in part to a deficiency in replication in brain endothelial cells. Therefore, we monitored replication of WNV-NY and WNV-MAD78 in an established human brain microvascular endothelial cell line (HBMEC) that has been widely used as a model to study bacterial and parasitic neuroinvasion (100, 115, 264, 265, 312) and primary brain microvascular endothelial cells (HBMVECs) derived from normal brain cortex tissue (45, 285). WNV-NY and WNV-MAD78 replicated at similar rates and to equivalent levels in both cell types, reaching peak titers between 32 and 48 hours post-infection (**Figure 15 A & B**) without induction of CPE (data not shown). However, we did observe a statistically insignificant, decrease in WNV-MAD78 titers very late in infection. These data suggest that replication in endothelial cells is not responsible for the decreased neuropathogenicity of WNV-MAD78.

It was recently reported that non-replicating virus-like particles (VLPs) generated from a lower virulence lineage 1 strain of WNV exhibited reduced transcellular migration across human umbilical vein endothelial cell monolayers

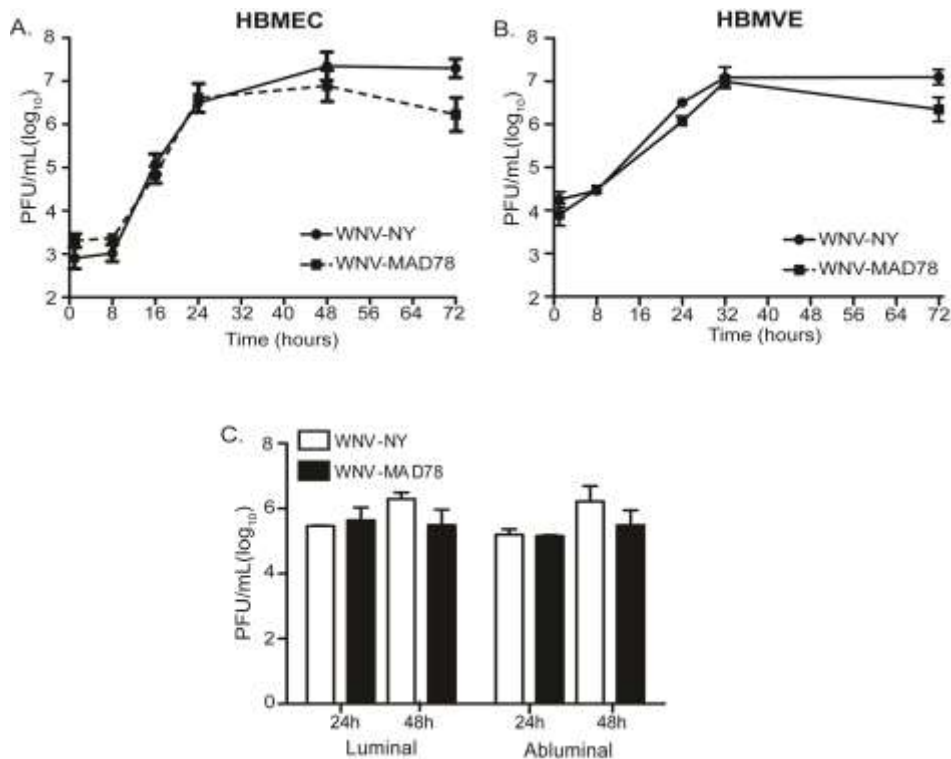


Figure 15. WNV-NY and WNV-MAD78 replication in human brain microvascular endothelial cells. Immortalized HBMECs (**A**) or primary HBMVECs (**B**) were infected with WNV-NY or WNV-MAD78 (MOI of 0.1). Culture supernatants were recovered at the indicated times and titers determined by plaque assay on Vero cells. Values represent the average number of plaque forming units (PFU) per mL (+/- standard error) of supernatant from at least two separate experiments. (**C**) Traversal of HBMVEC by WNV-NY and WNV-MAD78. Confluent monolayers of HBMVECs were cultured on transwell inserts and infected with WNV-NY or WNV-MAD78 (MOI of 0.1). Culture supernatants were collected from the luminal and abuminal chambers at the indicated times and titers determined by plaque assay on Vero cells. Values represent the average number of plaque forming units (PFU) per mL (+/- standard error) of supernatant from two separate experiments.

compared to those generated from a highly virulent strain (108). Thus, non-neuropathogenic strains, such as WNV-MAD78, may have a reduced capacity to traverse the BBB despite replicating efficiently in brain microvascular endothelial cells. To test this, we infected HBMEC or HBMVEC monolayers grown on transwell supports and measured virus yields in both luminal (upper) and abluminal (lower) chambers. Equivalent levels of infectious particles were present in the luminal and abluminal chambers of WNV-NY- and WNV-MAD78-infected HBMECs (data not shown) and HBMVECs (**Figure 15C**) at 24 and 48 hours post-infection, demonstrating that both strains are capable of traversing the BBB at similar rates and levels. Therefore, the non-neuropathogenic phenotype of WNV-MAD78 does not correspond to a reduced capacity to replicate in or traverse brain microvascular endothelial cells.

WNV-MAD78 replication is restricted in co-cultures of HBMECs and HBCAs. We next tested whether astrocytes, which constitute the periparenchymal layer of the BBB, differentially limit WNV-MAD78 replication using an *in vitro* BBB model comprised of HBMECs cultured on transwell supports with primary human brain astrocytes derived from the cerebral cortex (HBCAs) in the bottom chamber. As previously observed, both strains of WNV were detected in medium recovered from the abluminal chamber 24 hours after infection of the HBMEC monolayer (**Figure 16A**). However, viral protein expression was not detected in the HBCAs until approximately 48 hours after infection (**Figure 16B**, panels iii & iv). At this time, equivalent numbers of infected cells were present in

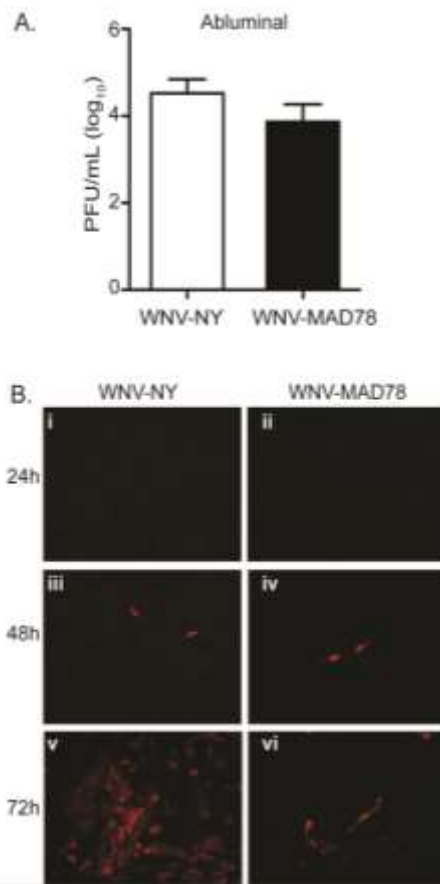


Figure 16. WNV replication in an *in vitro* model of the BBB. (A and B)

HBMECs cultured on transwell inserts with HBCAs plated in the abluminal chamber were infected with WNV-NY or WNV-MAD78 (MOI of 0.1). **(A)** Culture supernatants were recovered from the abluminal chamber of the transwell at 24 hours post inoculation and viral titers determined by plaque assays on Vero cells. Values represent the average number of plaque forming units (PFU) per mL (+/- standard error) of supernatant from at least three separate experiments. **(B)** Viral replication in the HBCA layer of an *in vitro* BBB model. HBCAs were fixed with 3% PFA at the indicated times and probed with WNV hyperimmune ascitic fluid and goat anti-mouse IgG 549nm-Dylight conjugated secondary antibody. Images are representative of at least three independent experiments.

WNV-NY- and WNV-MAD78-infected cultures (144 ± 61 , 109 ± 63 WNV⁺ cells, respectively), suggesting that WNV-NY and WNV-MAD78 had similar capacities to establish an initial infection within the astrocyte monolayer. However, by 72 hours post-infection, substantially more WNV-positive HBCAs were detected in WNV-NY-infected cultures compared to WNV-MAD78-infected cultures (**Figure 16B** compare panels v & vi). Thus, WNV-MAD78 spread within the *in vitro* BBB model was constrained compared to that of WNV-NY.

WNV-MAD78 replication within astrocytes is restricted at multiple steps in the virus life cycle. To further investigate the contribution of astrocytes in restricting WNV-MAD78 replication within the *in vitro* BBB, we examined WNV replication in HBCAs alone. In contrast to the donor matched HBMVECs utilized in Figure 2B and C, WNV-MAD78 infectious particle production in HBCAs was lower than that observed for WNV-NY throughout the course of infection (**Figure 17A**). At the point of peak viral production, WNV-MAD78 titers were reduced approximately 45-fold ($P < 0.005$) compared to WNV-NY. Moreover, the latent period prior to the detection of extracellular infectious particles in WNV-MAD78-infected cultures was prolonged compared to WNV-NY-infected cultures, suggesting that WNV-MAD78 replication is delayed in HBCAs. A similar delay and reduction in WNV-MAD78 infectious particle production was observed when cultures were infected at an MOI of 2, which established a near synchronous infection of the monolayer (data not shown).

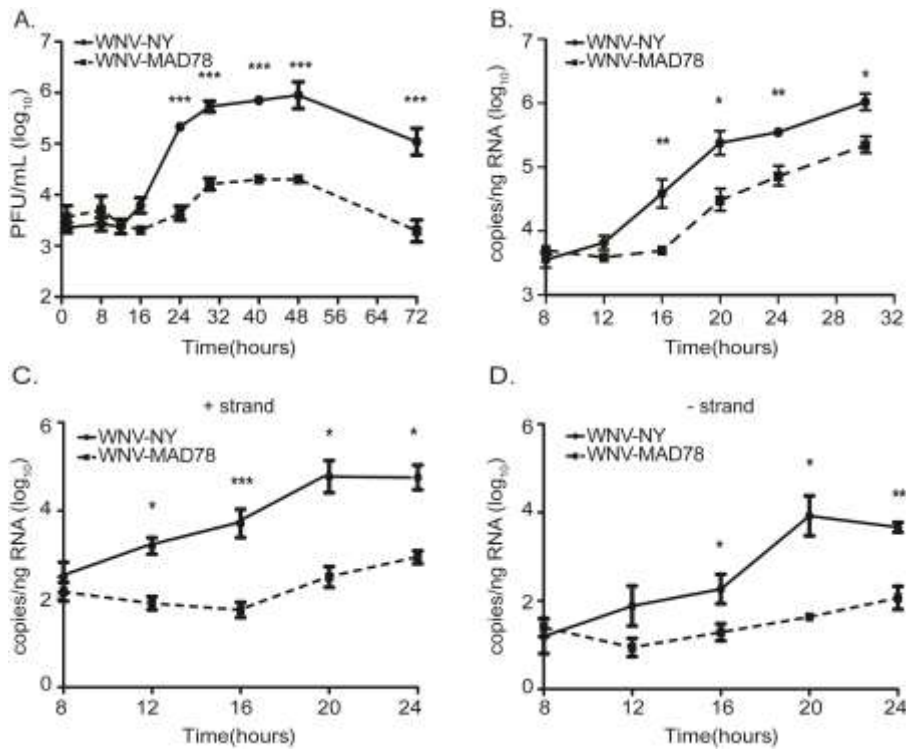


Figure 17. WNV replication in HBCAs. HBCAs were infected with WNV-NY or WNV-MAD78 (MOI of 0.01). **(A)** WNV-NY and WNV-MAD78 infectious particle production in HBCAs. Culture supernatants were removed at the indicated times and titers determined by plaque assay on Vero cells. Values represent the average number PFU per mL (+/- standard error) of supernatant from at least three separate experiments. Asterisks indicate differences that are statistically significant (** $p < 0.005$). **(B-D)** RNA synthesis of WNV-NY and WNV-MAD78 in HBCAs. Total RNA was recovered from HBCAs infected as in **(A)**. Total **(B)** and strand-specific **(C, positive; D, negative)** viral RNA levels were determined by qRT-PCR. Values represent the average (+/- standard error) of at least three independent experiments. A student's unpaired t-test was performed to determine significance. Asterisks indicate differences that are statistically significant (* $p < 0.05$, ** $p < 0.01$, *** $p < 0.005$).

Accumulation of intracellular viral RNA also was delayed in WNV-MAD78-infected HBCAs compared to WNV-NY-infected HBCAs (**Figure 17B**). Thus, the prolonged lag period prior to infectious particle production in the supernatants of WNV-MAD78-infected HBCAs may be due to a delay in viral RNA replication rather than assembly of virus particles. To better define the nature of the delay in WNV-MAD78 replication, we assessed the rate of accumulation of both positive and negative strand RNA at early times post-infection. Synthesis of both positive and negative strand WNV-MAD78 RNA was delayed compared to that of WNV-NY (**Figure 17C and D**), suggesting that WNV-MAD78 replication in astrocytes is restricted at an early step in the virus life cycle.

The delay in synthesis of WNV-MAD78 viral RNA corresponded with a decrease in the number of extracellular infectious particles produced per infected cell compared to WNV-NY-infected cells at 24 hours post-infection (**Figure 18A**). However, by 48 hours post-infection, WNV-NY- and WNV-MAD78-infected HBCAs produced similar levels of infectious particles per cell. In spite of this, the level of total infectious particles detected in WNV-MAD78-infected cultures remained substantially reduced compared to WNV-NY throughout the course of infection (see **Figure 17A**), suggesting that factors independent of viral RNA synthesis also are involved in restricting WNV-MAD78 replication within astrocytes. Indeed, visualization of WNV-infected astrocytes in the BBB co-culture system indicated that WNV-MAD78 is also limited in cell-to-cell spread compared to WNV-NY (**Figure 16B**, compare panels v & vi). To confirm these results, we quantitated the number of infected HBCAs over the course of

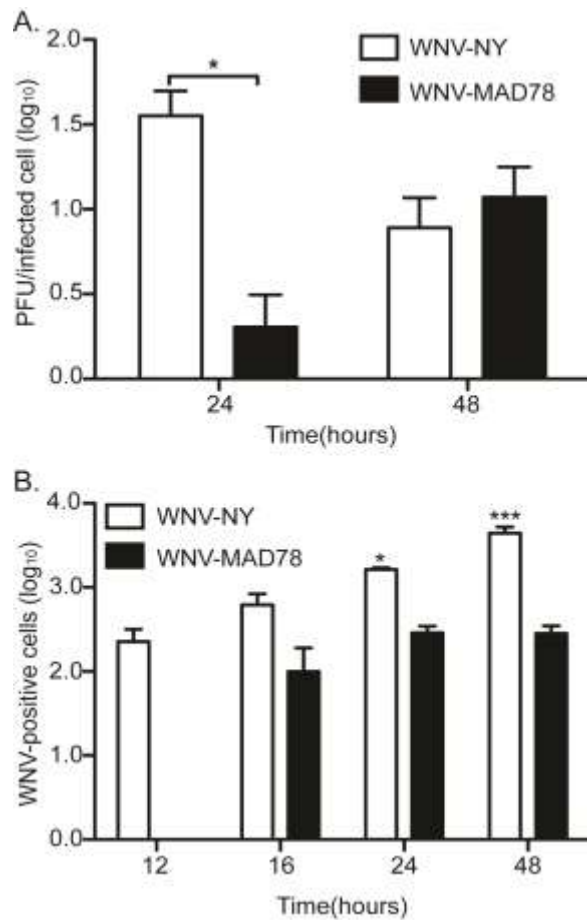


Figure 18. Infectious virions released per cell and cell-to-cell spread in HBCAs. HBCAs were infected with WNV-NY or WNV-MAD78 (MOI of 0.01). Culture medium was removed at the indicated times and titers determined by plaque assay on Vero cells. The number of infected cells within the monolayer was determined by flow cytometry. Cells were removed from the plate by trypsinization, fixed with 3% PFA, probed with WNV hyperimmune serum followed by goat anti-mouse IgG 633nm Dylight conjugated antibody and subjected to flow cytometry. **(A)** Infectious particle production per infected cell. The number of infectious extracellular particles was determined by dividing viral titers by the number of infected cells. Values represent the averages from three independent experiments. A student's unpaired t-test was performed to

determine significance. Asterisks indicate differences that are statistically significant (* $p < 0.05$) **(B)** WNV-positive cells per 10^5 cells from three independent experiments. Values represent the averages from three independent experiments. A student's unpaired t-test was performed to determine significance. Asterisks indicate differences that are statistically significant compared to the WNV-NY 12 hour time point (* $p < 0.05$, *** $p < 0.005$).

infection using flow cytometry (**Figure 18B**). Low levels of WNV-positive cells were detected at 12 hours post-infection in WNV-NY infected cultures. However, antigen-positive cells were not detected in WNV-MAD78-infected cultures until 16 hours post-infection, which is consistent with the delay in viral replication. Importantly, the baseline number of WNV-NY-infected HBCAs at 12 hours post-infection was comparable to the number of WNV-MAD78-infected HBCAs detected at 16 hours post-infection, confirming that both strains are capable of establishing an initial infection within the astrocyte monolayer. While the number of WNV-NY-positive cells continued to increase throughout the course of infection, the number of WNV-MAD78-positive cells remained unchanged. By 48 hours post-infection, there was a 15-fold ($P < 0.01$) increase in antigen-positive cells detected in WNV-NY-infected HBCAs compared to WNV-MAD78-infected HBCAs. Overall, our data suggest that WNV-MAD78 is both delayed in initiation of viral synthesis in HBCAs and impaired in its ability to spread to neighboring cells compared to WNV-NY.

The reduced susceptibility of HBCAs to WNV-MAD78 is independent of type-I interferon (IFN). The restriction to WNV-MAD78 spread within astrocytes was suggestive of the paracrine protection of type-I IFNs (120, 121, 205). Therefore, we examined supernatants recovered from WNV-infected HBCAs for the presence of type-I IFNs using a bioassay. Measureable levels of IFN were first detected at 30 and 40 hours post-infection in supernatants recovered from WNV-NY and WNV-MAD78-infected HBCAs, respectively

(Figure 19A). Furthermore, infection of HBCAs with WNV-NY induced significantly higher levels of IFN compared to WNV-MAD78 at all time points examined. Therefore, the kinetics and amplitude of induction of secreted IFN did not correlate with WNV-MAD78's diminished capacity to spread from cell to cell early in infection. However, WNV-MAD78 is more sensitive to IFN treatment than pathogenic strains of WNV in other cell types (127) . Thus, local levels of type-I IFNs surrounding the WNV-MAD78-infected cells may be sufficient to inhibit viral spread. To assess this possibility, we examined viral spread and infectious particle production in HBCAs infected with WNV-NY or WNV-MAD78 in the presence or absence of neutralizing antibodies to IFN- α and β (**Figure 19B-D**). We consistently observed a significant increase in the number of WNV-NY-infected cells in the presence of neutralizing antibodies to IFN- α (Figure 19B). Additionally, neutralizing antibodies to IFN- α or IFN- β enhanced infectious particle production in WNV-NY-infected HBCAs (**Figure 19C & D**). In contrast, neutralizing antibodies to IFN α and/or β did not enhance viral spread or infectious particle production in WNV-MAD78-infected cells (**Figure 19B-D**). This data suggests that IFN- α plays a role in restricting WNV-NY, but not WNV-MAD78, replication and spread in HBCAs.

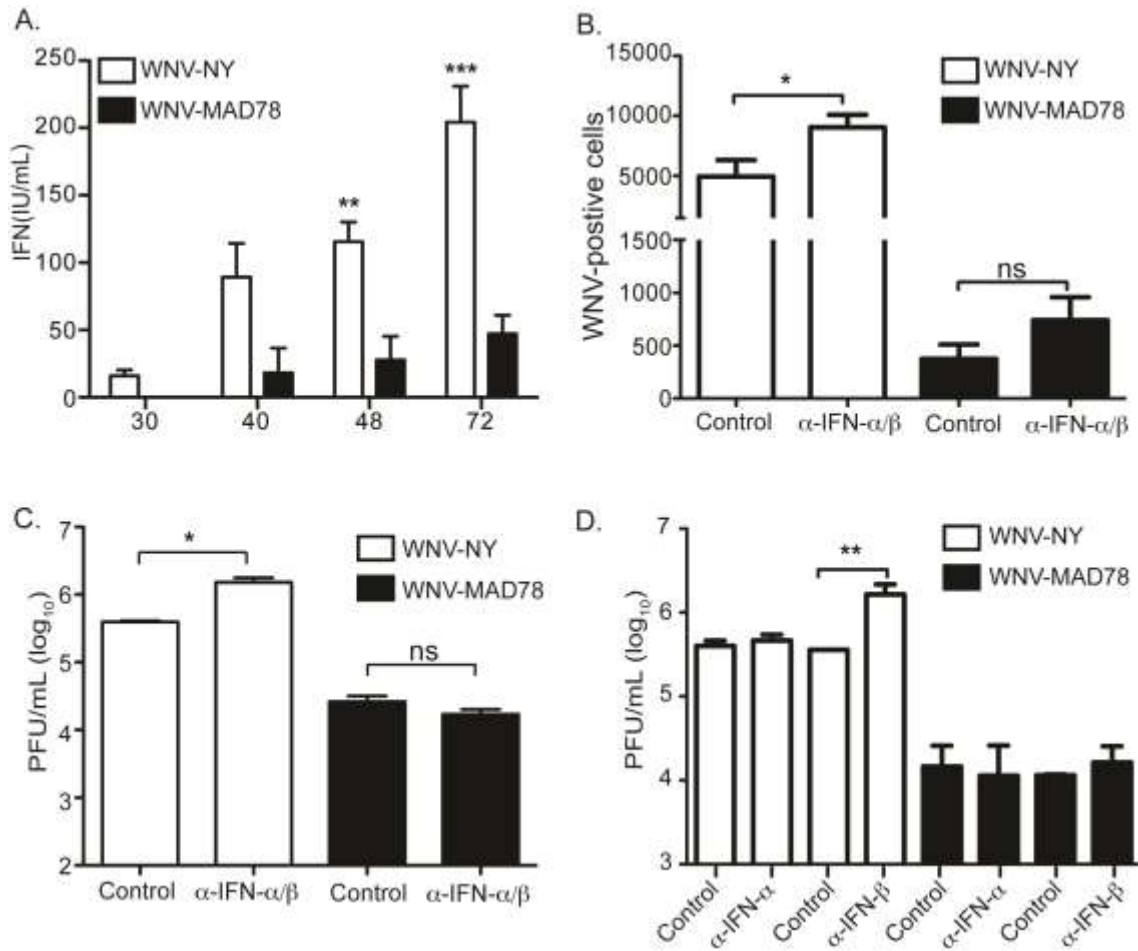


Figure 19. Role of type-I IFN in limited WNV replication and spread in HBCAs. (A) Level of secreted type-I IFN secretion in supernatants recovered from WNV-infected HBCAs. Culture supernatants were removed from HBCAs infected with WNV-NY or WNV-MAD78 (MOI of 0.01) at the indicated times post-infection. IFN levels were determined using a VSV-based bioassay. Values represent the level of type-I IFN (IU/mL) (+/- standard error) from a minimum of 2 independent experiments. A student's unpaired t-test was performed to determine significance. Asterisks indicate differences that are statistically significant (** $p < 0.01$, *** $p < 0.005$). (B-D) The effect of neutralization of type-I IFN on WNV spread and replication in HBCAs. HBCAs were infected with WNV-NY

or WNV-MAD78 (MOI of 0.01) and the inoculum replaced with culture media containing control antisera or neutralizing antibodies to IFN- α and - β combined **(B & C)** or individually **(D)**. **(B)** Cells were fixed at 48 hours post-infection with 3-4% PFA, permeabilized, probed with WNV hyperimmune serum followed by goat anti-mouse IgG 633nm Dylight conjugated antibody and subjected to flow cytometry. Values represent the average number of WNV-positive cells per 10^5 cells (+/- standard error) from at least two independent experiments. A student's unpaired t-test was performed to determine significance. Asterisks indicate differences that are statistically significant (* $p < 0.05$). **(C & D)** Culture supernatants were recovered at 48 hours post-infection and viral titers determined by plaque assay on Vero cells. Values represent the average number PFU per mL (+/- standard error) of supernatant from at least two separate experiments. A student's unpaired t-test was performed to determine significance. Asterisks indicate differences that are statistically significant (* $p < 0.05$, ** $p < 0.01$).

Discussion

The naturally occurring diversity in virulence among WNV strains provides an excellent model system to define the viral and host factors involved in pathogenesis. To better understand the mechanistic basis for the differential neuropathogenicity between WNV strains, we compared the replication of pathogenic and nonpathogenic strains of WNV within the various cell types of the NVU. Consistent with reports that WNV-MAD78 is neurovirulent when mice are infected via intracranial inoculation (253), we observed that WNV-NY and WNV-MAD78 replicate to equivalent levels in neuronal cells. This suggests that WNV-MAD78's non-neuropathogenic phenotype is due to an inability to access highly susceptible neurons under peripheral infection conditions. Indeed, the non-neuropathogenic phenotype of some strains of WNV has been attributed to an inability to invade the CNS (23, 108, 164). Increasing evidence suggests that WNV entry into the CNS is a multistep process that can occur through one of several routes (15, 229, 285, 291, 297, 308). WNV entry into the CNS has been shown to precede disruption of the BBB and leukocyte infiltration (15, 88, 185, 291), suggesting that WNV utilizes a direct mechanism to initially invade the CNS, such as basolateral secretion of virus particles from infected brain endothelial cells or transcytosis. Thus, the brain endothelium likely constitutes a primary barrier to WNV neuroinvasion. Using an established endothelial cell line that exhibits the physiological characteristics of the brain endothelium (99, 115, 264, 265, 283, 312) and primary brain endothelial cells, we have demonstrated

that WNV-MAD78 can replicate in and traverse the brain endothelium as efficiently as WNV-NY. Our findings are consistent with reports that high and low neuropathogenic strains of Semliki Forest virus replicate to equivalent levels in endothelial cells (77, 260), suggesting that the capacity to cross the BBB is not always the determining factor for neuropathogenicity.

The initial invasion of WNV into the CNS brings the virus into close proximity with the second component of the BBB, astrocytes. Indeed, infected astrocytes have been detected in some fatal human cases of WNV encephalitis, suggesting that these cells are also targeted by WNV *in vivo* (282). We observed both a delay in the kinetics of WNV-MAD78 replication and a reduction in peak infectious particle production in astrocytes compared to WNV-NY. Since the astrocyte and primary brain endothelial cells lines used in this study were recovered from the same donor, it is unlikely that the constrained replication of WNV-MAD78 in HBCAs was due to a donor-specific restriction. Further comparison of the growth characteristics of WNV-NY and WNV-MAD78 in HBCAs indicated that both strains were capable of establishing an initial infection within this cell type. However, accumulation of viral protein and RNA was delayed in WNV-MAD78-infected HBCAs compared to WNV-NY. Analysis of kinetics of accumulation of viral positive and negative strand RNA indicated that the delay in WNV-MAD78 replication was at, or prior to, the initiation of negative strand synthesis. However, it is unlikely that a delay in viral replication alone would result in the significant reduction in peak viral titers observed in WNV-

MAD78-infected HBCAs, suggesting that an additional factor(s) is involved in restricting WNV-MAD78 accumulation in astrocytes.

The host innate antiviral response plays a pivotal role in controlling WNV replication in many cell types (56, 82, 127, 144, 230, 270). This response consists of a direct IRF-3-dependent and an indirect IFN-dependent mechanism, which function to constrain viral replication within the infected cell and prevent viral spread to neighboring cells, respectively. Measureable levels of type-I IFN were detected in supernatants recovered from both WNV-NY- and WNV-MAD78-infected HBCAs. However, significantly higher levels of IFN were detected in WNV-NY-infected HBCAs, which corresponded with the increased replication and spread of this strain within the monolayer. Moreover, the high levels of IFN induced by WNV-NY, specifically IFN- α , suppressed viral spread and replication in astrocytes. In contrast, the low levels of IFN induced by WNV-MAD78 late in infection did not substantially restrict replication or spread within astrocytes.

In addition, the observation that WNV-NY- and WNV-MAD78-infected HBCAs produced equivalent levels of infectious particles per cell at 48 hours post-infection suggests that the IRF-3-dependent arm of the host antiviral response does not differentially restrict WNV-NY and WNV-MAD78 replication within infected cells. Furthermore, induction of the direct IRF-3 target proteins ISG15 and ISG56 in HBCAs corresponded with the rate of WNV-NY and WNV-MAD78 replication (data not shown), indicating that WNV-MAD78 does not preferentially induce antiviral programs within the infected cell. Combined, these data suggest that the restriction to WNV-MAD78 replication and spread in

astrocytes occurs prior to the induction of the host antiviral response. Therefore, the host antiviral response appears to play a minimal role in the reduced susceptibility of astrocytes to WNV-MAD78.

Determining both the viral and host cell factors involved in constraining WNV-MAD78 replication in astrocytes will be necessary to fully elucidate the nature of the restriction of WNV-MAD78. One possible viral factor is the presence of specific N-linked glycans on the envelope protein, which correlates with the ability to invade the CNS (23, 24, 31). WNV-MAD78 lacks this glycosylation site; thus, our data suggest that glycosylation is not a determining factor in the initial infection of brain endothelial cells or subsequent replication in neurons. Consistent with this, WNV-MAD78 replicates efficiently in neurons when introduced directly into the brain by an intracranial route (253). Experiments are currently underway to determine whether glycosylation contributes to WNV replication and/or spread in astrocytes.

We hypothesize that the constrained replication of WNV-MAD78 in astrocytes has several effects on WNV-mediated neuropathology. First, the restricted replication of WNV-MAD78 in astrocytes may minimize the initial amplification of virus and reduce the rate of spread within the CNS, thus allowing more time for the host innate and adaptive immune responses to clear the virus prior to widespread infection of highly susceptible neurons. Second, as with other disease states, WNV infection induces astrocytes to release neurotoxic factors that exacerbate neuropathology (282). Therefore, suppression of viral replication within astrocytes may reduce the extent of bystander cell death of

uninfected neurons. The combined effects of reduced replication in astrocytes and decreased production of neurotoxic molecules is consistent with reports that mortality is delayed and reduced in mice infected with WNV-MAD78 via intracranial inoculation (253).

Studies with *Icam1*^{-/-}, *Mmp9*^{-/-} or *Drak2*^{-/-} mice suggest that WNV undergoes a second round of entry and dissemination within the CNS as a result of recruitment of infected leukocytes and/or perturbation of the BBB (57, 292, 295). There is circumstantial evidence that astrocytes contribute to the second wave of WNV neuroinvasion through the upregulation of MMPs, which disrupt the BBB, and proinflammatory cytokines, which recruit infected leukocytes (282, 284). Indeed, propagation within astrocytes, neurons, and glial cells prior to the breakdown of the BBB is believed to be a common strategy of neuroinvasive viruses, including tick-borne encephalitis virus and HIV, to enhance dissemination within the CNS (75, 223). Therefore, the inability of WNV-MAD78 to replicate in astrocytes may limit the capacity of the virus to undergo a second round of entry into the CNS (15, 291). Thus, astrocytes may play a central role in both the initial dissemination of WNV to the CNS as well as secondary waves of spread, which are likely to exacerbate WNV-mediated neuropathology.

Overall, our data suggest that WNV-MAD78 is capable of invading the CNS. However, the inability to amplify and spread within astrocytes may block WNV-MAD78 dissemination to neurons. Furthermore, our findings suggest that astrocytes play an essential role in initiating and regulating WNV infection in the CNS, and may act as a critical determinant of differential WNV neuropathology.

Determining which astrocyte factors limit WNV infection may ultimately promote the development of therapies that regulate neuronal injury after the onset of WNV infection.

Chapter 4-Role of glycosylation and cellular processing in WNV infection in astrocytes

Abstract

Maturation of flaviviral particles is the final step prior to release from the cell. However, complete maturation of the viral particle does not need to occur for flaviviral particles to be infectious. Previously, we observed that a nonneuropathogenic strain of WNV, WNV-MAD78, was restricted in cell-to-cell spread in astrocytes compared to a neuropathogenic strain, WNV-NY. After determining that the restriction in infectious particle production for WNV-MAD78 in astrocytes was not a result of a differentially-induced host factor, we investigated the role of maturation of WNV in astrocytes. When furin inhibitor was added during WNV-MAD78 infections in astrocytes to block viral particle maturation, an increase in infectious particles was observed. To examine the contribution of viral factors that contribute to the state of the mature virion, we constructed recombinant viruses containing the structural proteins from WNV-MAD78 and nonstructural proteins from WNV-NY. Indeed, we observed a restriction in infectious particle production in astrocytes similar to that of WNV-MAD78. Recombinant viruses constructed with the structural proteins from WNV-NY and nonstructural proteins from WNV-MAD78 replicated to levels similar to that of WNV-NY in astrocytes. Thus, processing of the virion in astrocytes restricts infectious particle production for WNV-MAD78, and may play a role in the limitation for WNV-MAD78 in inducing neurological pathologies.

Introduction

West Nile virus (WNV) is a positive sense, RNA virus in the Flaviviridae family. All members of the Flaviviridae undergo viral particle modification and processing in the ER and trans-Golgi. Both prM and the envelope are glycosylated in the ER, and these carbohydrate moieties are further modified in the trans-Golgi. Final cleavage of prM by the cellular protease furin induces a conformational change in the envelope proteins and the global structure of the virion (262). While mature viral particles are considered more infectious than immature viral particles, processing of the virion in many cases is incomplete. Partially mature particles are capable of initiating infection (53, 192). Yet how cell-specific expression of enzymes that contribute to particle processing within permissive cells contributes to limiting cell-to-cell spread remains unknown.

Since its introduction into the Western hemisphere in 1999, WNV has been the causative agent of over 15,000 cases of neurological disease {webpage, #7067}. Neurological symptoms include meningitis, encephalitis, and poliomyelitis; all of these symptoms are caused by the death of neurons within the CNS. During WNV infection, neuronal cell death may be due to viral replication and/or bystander death due to the production of neurotoxic factors by other cells within the CNS. How some strains of WNV cause severe neuropathology and others do not is not fully understood.

WNV primarily enters the CNS via the hematogenous route by crossing the blood-brain barrier (BBB) (117, 285). The BBB is a highly restrictive barrier

that protects the CNS from aberrant immune responses and pathogens in the periphery. It is comprised of endothelial cells that line the cerebral vasculature and astrocytes in direct contact with endothelial cells within the CNS. Endothelial cells in the CNS contain cell-to-cell junctions that are tighter than their peripheral counterparts, while astrocytes act as physical supports for endothelial cells (1). In addition, astrocytes help to maintain homeostasis in the CNS by regulating the permeability of the BBB and by taking up excess neurotransmitters (118). Beyond the BBB lie sensitive neuronal cells that are responsible for controlling all physiological systems within the body.

Responses to viral infection within astrocytes have been given much recent attention. Further, viral replication in astrocytes may have implications in physiological outcomes during viral infection of the CNS (5, 209). Previously, we demonstrated that both a neuropathogenic strain, WNV-NY, and a nonneuropathogenic strain, WNV-MAD78, of WNV are capable of establishing a productive infection within astrocytes. However, WNV-MAD78 exhibited a delay in viral replication and an IFN-independent restriction in cell-to-cell spread within astrocytes.

Here we explore the cellular and viral factors involved in restricting WNV-MAD78 replication within astrocytes. Examination of the intrinsic immune response indicated that these classical antiviral pathways were not responsible for the differential replication of WNV-NY and WNV-MAD78 within astrocytes. An examination of WNV particles indicated that WNV-NY particles were significantly more infectious than WNV-MAD78 particles derived from astrocytes, suggesting

that the decreased viral spread in astrocytes may be due to the increased production of defective particles by WNV-MAD78. Examination of endogenous furin expression and activity in astrocytes indicated that this cell type expressed higher levels of furin than cell types where WNV-NY and WNV-MAD78 replicate to equivalent levels, suggesting that a decrease in viral maturation is not responsible for the reduced infectivity of WNV-MAD78.

In order to identify the viral factors responsible for the cell type-specific restriction of WNV-MAD78, we assessed the replication of a series of recombinant viruses in astrocytes. While neither glycosylation of the envelope protein nor the entire nonstructural region were sufficient to reduce spread, replacement of the structural genes of WNV-NY with those of WNV-MAD78 was sufficient to restrict infectious particle production in astrocytes. The following study identifies novel mechanisms, both host and viral, by which nonneuropathogenic strains may be restricted in infectious particle production in astrocytes and, therefore, restricted in neuropathogenesis.

Results

WNV-MAD78 replication in astrocytes is not restricted by a secreted host factor

Since WNV-MAD78 replication and spread is delayed in astrocytes compared to WNV-NY, and the spread is type-1 IFN independent (117), we hypothesized that an additional host factor may restrict WNV-MAD78 replication and spread. Several secreted factors, including chemokines, cytokines, and

reactive nitrogen and oxygen species (RNS and ROS), as well as astrocyte-specific activation, have previously been identified as host factors that restrict viral replication (179, 209). To further examine all secreted factors during WNV infection in astrocytes, astrocytes were pre- and post-treated with supernatants from previous infections at 48h, and infectious particle production was examined (**Figure 20 A and B**). Because type-1 IFN is secreted and restricts WNV-NY cell-to-cell spread in astrocytes (117), antibodies to type-1 IFN were added to the supernatants with which the cells were treated to negate the effect of type-1 IFN. Still, no decrease in infectious particle production was observed for WNV-MAD78-infected astrocytes, suggesting that the restriction to WNV-MAD78 infectious particle production in astrocytes is not due to a preferentially induced antiviral state compared to WNV-NY-infected astrocytes.

Astrocyte-derived WNV-MAD78 particles are less infectious than WNV-NY particles

Because the restriction for the infectious particle production of WNV-MAD78 in astrocytes was not due to a preferentially induced antiviral state compared to WNV-NY-infected astrocytes, we examined infectivity of viral particles produced during infection in astrocytes. When the amount of viral RNA present in the supernatant (genome equivalent) was compared to the infectious particle production (plaque forming units) during WNV infection of astrocytes, WNV-NY had a significantly lower GE/PFU ratio compared to WNV-MAD78 (**Figure 21A**). The lower ratio for WNV-NY suggests that the particles produced

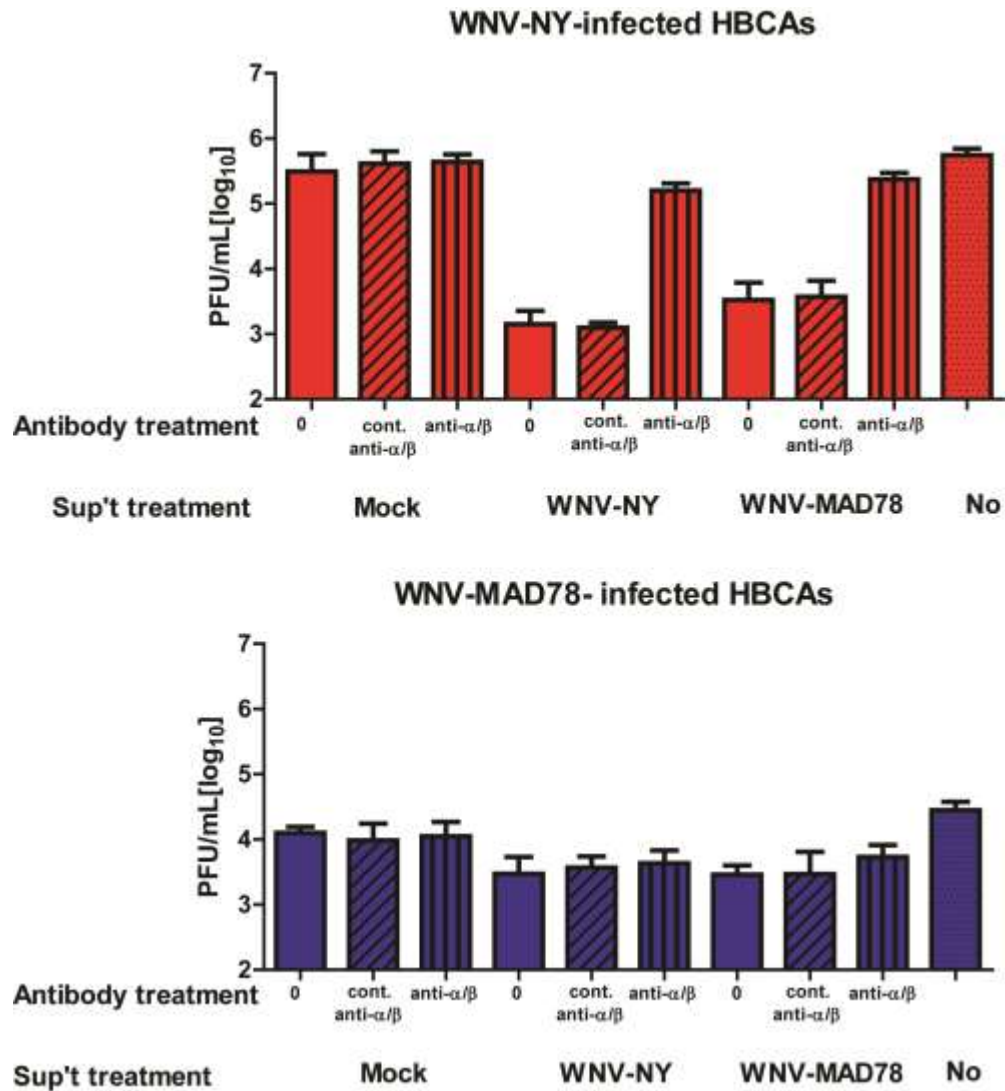


Figure 20. WNV-MAD78 replication in astrocytes is not restricted via canonical pathways. HBCAs were pretreated (6h) with supernatants from a previous infection in HBCAs (+/- antibodies to type-1 IFN) and infected with either (A) WNV-NY or (B) WNV-MAD78 (MOI=0.01). After inoculum was removed, cells were post-treated with supernatants (+/- antibodies to type-1 IFN) as described in materials and methods and 24hpi supernatants were collected and plaque assays were performed in Vero cells. Data presented is an average (+/- standard error) of 3 independent experiments.

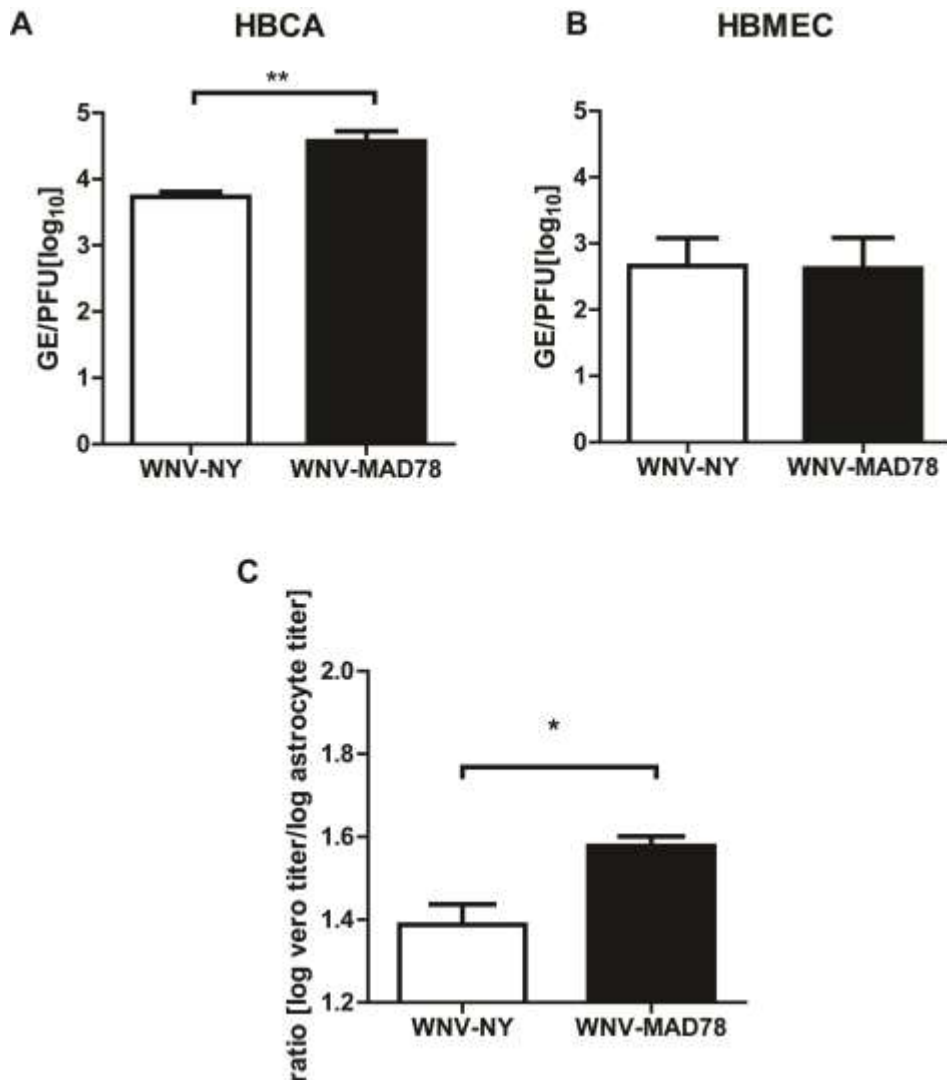


Figure 21. WNV-MAD78 particles derived from astrocytes are less infectious than WNV-NY particles derived in astrocytes. (A) HBCAs were inoculated with WNV-NY or WNV-MAD78 (MOI=0.01) and at 24 and 48hpi, supernatants were collected. Similarly, (B) HBMECs were inoculated with WNV-NY or WNV-MAD78 (MOI=0.1) and at 24hpi and 48hpi, supernatants were collected. For both cell types, plaque assays were performed in Vero cells to determine infectious viral particle production (PFUs). RNA was isolated from the supernatant and subjected to qRT-PCR with primers specific for each virus (genomic equivalent, GE). The ratio of viral RNA present in the supernatant to

infectious viral particle is displayed. Data presented is an average (+/- standard error) of at least 3 independent experiments. (C) HBCAs were inoculated (MOI=0.01). At 48hpi, supernatants were collected, and the viral titer was determined in the supernatants both by plaque assay in Vero cells and focus forming assays in HBCAs. Data presented is the ratio of the viral titer on Vero cells to the viral titer on HBCAs, and is the average (+/- standard error) of 3 independent experiments. ** p<0.01

in WNV-NY-infected astrocytes are more infectious and therefore more likely to infect neighboring cells than the particles produced in WNV-MAD78-infected astrocytes.

Previously we demonstrated that WNV infection of endothelial cells was equivalent for both neuropathogenic and nonneuropathogenic strains of WNV (117). To further assess the infectivity of WNV particles produced during astrocyte infection, we compared the infectivity (GE/PFU) of astrocyte and endothelial cell derived virus particles (**Figure 21B**). WNV-NY- and WNV-MAD78-infected endothelial cells produced particles that were equivalently infectious. Further, particles produced in endothelial cells were more infectious than those produced during infection in astrocytes (Compare GE/PFU ratio on 21A vs B), which may account for the lower overall peak viral titers in astrocytes compared to endothelial cells for both strains.

To further examine WNV-MAD78 particles derived in astrocytes, focus-forming assays were performed on astrocytes to assess the ability of astrocyte-derived virus to infect astrocytes. Because these supernatants are from a late time during infection (48h), the particles are exclusively derived from astrocytes. The viral titer of these supernatants on astrocytes was then compared to the viral titer of the supernatant on Vero cells, thus examining the cell-specific infectivity in astrocytes (**Figure 21C**). When the Vero titer:astrocyte titer ratio of WNV-MAD78 particles was compared to WNV-NY particles treated in the same manner, we observed that WNV-MAD78 viral particles did not infect HBCAs as efficiently as

WNV-NY particles. Together with the particle:PFU ratio, these data suggest that WNV-MAD78 viral particles are less infectious in astrocytes compared to WNV-NY particles, and may contribute to their inability to spread from cell to cell.

WNV-MAD78 infectious particle production is partially limited by furin activity in astrocytes

Infectivity of viral particles is thought to be a function of viral maturation; immature viral particles are still infectious, but to a lesser degree than completely mature particles (53). Since there was a significant difference in the infectivity of the astrocyte-derived particles compared to endothelial cell-derived WNV particles, we hypothesized that there were cell-type dependent differences in the processing of WNV particles. Since furin is involved in maturation of the WNV particle, we examined the activity of furin in both endothelial cells and astrocytes (**Figure 22A**). Furin activity was greater in astrocytes compared to endothelial cells, suggesting that WNV maturation may be more efficient in astrocytes compared to endothelial cells. Surprisingly, inhibition of furin in astrocytes led to increased infectious particle production for WNV-MAD78-infected astrocytes (**Figure 22B**), suggesting that higher levels of particle maturation in astrocytes may be detrimental to WNV-MAD78.

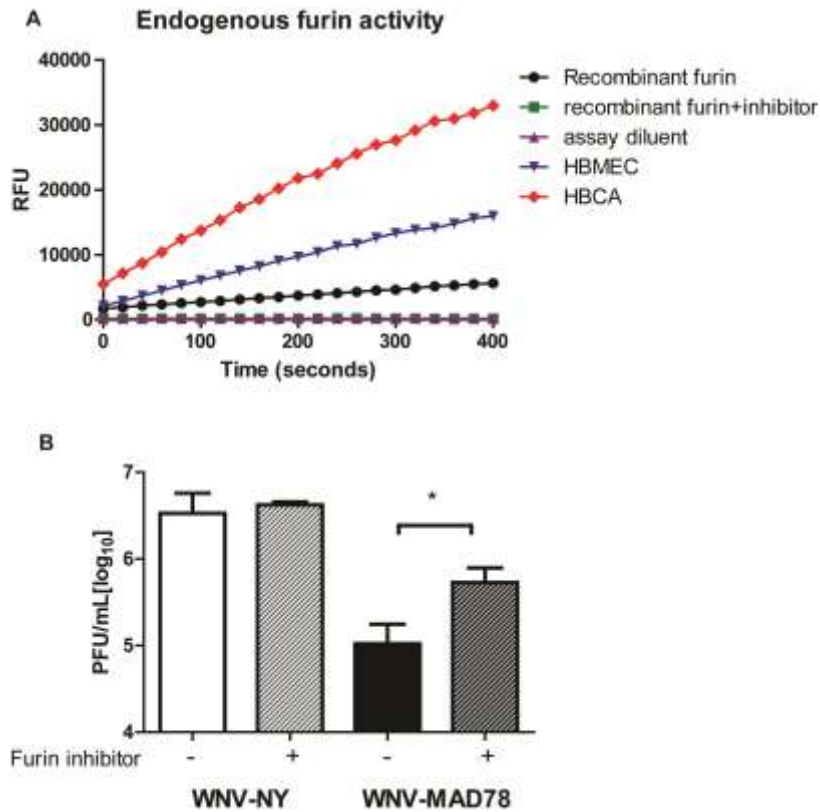


Figure 22. Furin activity in astrocytes is greater than that in endothelial cells and plays a role in inhibiting WNV-MAD78 infectious particle production. (A) The same number of HBCAs and HBMECs were lysed in lysis buffer (Triton-X100 0.5%, 0.5mM CaCl₂, 100mM HEPES pH 7.0) and along with recombinant furin, recombinant furin with inhibitor (5mM), or assay diluent alone, assayed for furin activity according to the process described in the materials and methods. Data is representative of activity assays performed at least twice. (B) HBCAs were inoculated with either WNV-NY or WNV-MAD78 and after inoculation, media with or without furin inhibitor (Dec-RVKR-CMK diluted in PBS, 5mM). For detailed materials and methods on inhibition of furin in astrocytes, please see materials and methods. At 48hpi, supernatants were collected and

subjected to plaque assays performed on Vero cells. Data presented is an average (+/- standard error) of at least 3 independent experiments. * $p < 0.05$

WNV structural proteins contribute to infectious particle production in astrocytes

One of the consequences of maturation of WNV particles is cleavage and release of prM. Several identified cellular attachment factors for WNV, such as Dendritic Cell-Specific Intercellular adhesion molecule-3-Grabbing Non-integrin (DC-SIGN) and DC-SIGNR, specifically bind carbohydrate moieties (60). WNV-MAD78 contains only one glycosylation site, in prM, while WNV-NY contains this same site and an additional glycosylation site in the envelope protein. However, the prM glycosylation site is cleaved off during maturation of the viral particle. Therefore, WNV-MAD78 particles in astrocytes may contain fewer carbohydrate moieties within the virion, and may be unable to bind attachment factors on neighboring cells. We hypothesized that glycosylation of the envelope contributes to WNV spread within astrocytes, and therefore increased neurological disease associated with pathogenic strains of WNV. Recombinant viruses were generated that introduced the glycosylation site into the envelope protein for WNV-MAD78 and removed the site from WNV-NY (**Figure 23A**). Modifications to the glycosylation site did not increase WNV-MAD78 replication nor decrease WNV-NY replication in astrocytes. Next, we examined recombinant viruses comprised of either WNV-MAD78 structural proteins and WNV-NY nonstructural proteins (WNV-MAD78 S/WNV-NY NS) or WNV-NY structural proteins and WNV-MAD78 nonstructural proteins (WNV-NY S/WNV-MAD78 NS) and compared viral replication to that of the parental viruses in

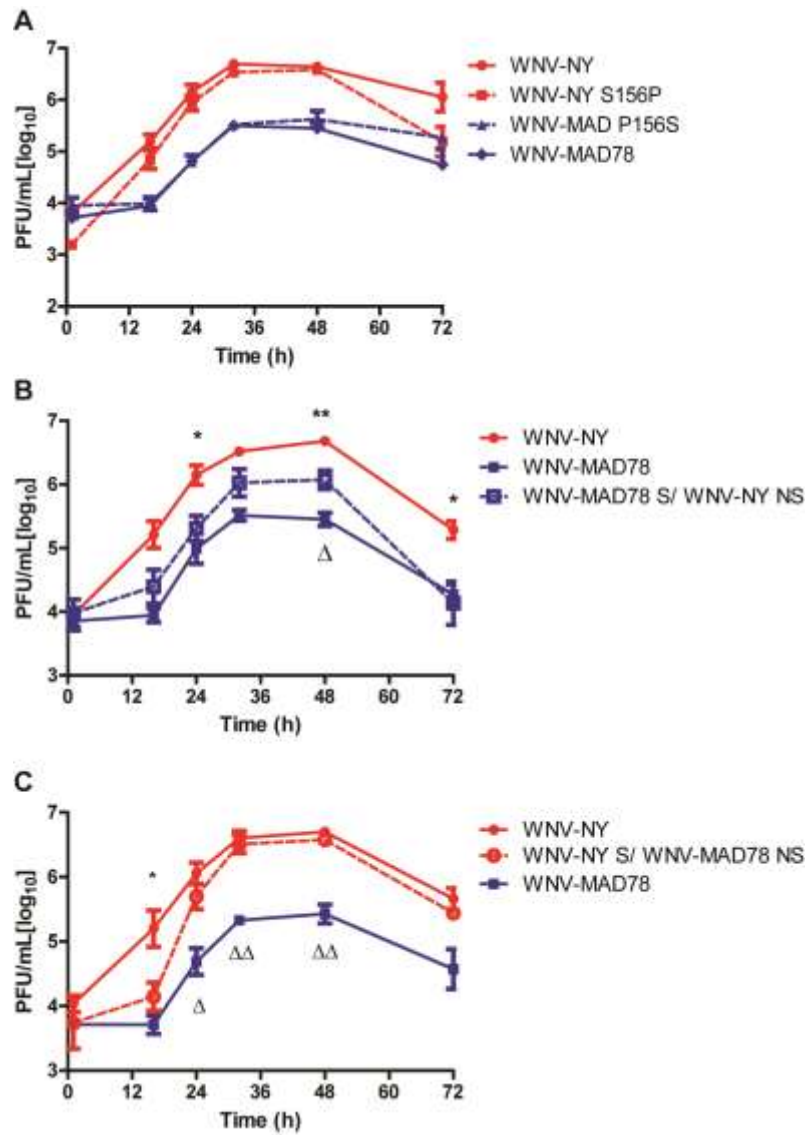


Figure 23. Structural proteins of WNV contribute to infectious particle production in astrocytes. HBCAs were infected with either WNV-NY, WNV-MAD78 (displayed in all figures), WNV-NY S156P, WNV-MAD78P156S (A), WNV-MAD78/UTR NY (B), WNV-MAD S/WNV-NY NS, or WNV-NY S/WNV-MAD78 NS (C) at an MOI=0.01. At the times indicated, viral supernatants were collected and plaque assays done in Vero cells. Data presented is an average (+/- standard error) of at least 3 independent experiments. The (*) represents

data significantly different from WNV-NY, while the (Δ) represents data significantly different from WNV-MAD78. */ Δ $p < 0.05$, **/ $\Delta\Delta$ $p < 0.01$

astrocytes (**Figure 23 B**). The production of infectious viral particles was delayed for both recombinant viruses. However, WNV-NY S/WNV-MAD78 NS infectious particle production reached levels similar to WNV-NY at 24 hours post infection. In contrast, WNV-MAD78 S/WNV-NY NS remained restricted in infectious particle production compared to WNV-NY, although viral titers were higher than WNV-MAD78 at 48 hours post-infection. Together, these data suggest that the structural proteins contribute to the restriction in infectious particle production of WNV-MAD78 in astrocytes. In addition, these data support our hypothesis that viral particle processing and the components of the virion in astrocytes plays a role in the ability for pathogenic strains to spread from cell to cell.

Discussion

The mechanistic basis for the differential neuropathology induced by various strains of WNV remains unknown. Our studies examine astrocyte-specific host responses to strains of WNV that vary in their abilities to induce neuropathogenicity. We have previously shown that the restriction in cell-to-cell spread for WNV-MAD78 was independent of type 1 IFN (117). Although WNV-MAD78 has been shown to be more sensitive to type-1 IFN than WNV-NY in vivo (127). However, WNV-MAD78 cell-to-cell spread in astrocytes is restricted prior to the activation of the antiviral response, suggesting that although type-1 IFN may restrict WNV-MAD78 replication in other cell types, WNV-MAD78 cell to cell spread in astrocytes is not efficient enough where type-1 IFN plays a role. In addition to type 1 IFN, other host immune responses, such as glial fibrillary acidic

protein (GFAP) activation and nitrous oxide production, were examined in astrocytes to assess if they were differentially regulated during WNV-MAD78 infection in astrocytes (data not shown). GFAP expression is a classical indicator of highly responsive astrocytes (72), and increased expression of GFAP has been shown in astrocytes infected at a high MOI with a highly pathogenic strain of WNV (284). However, we failed to detect increased GFAP expression for WNV-infected cells. Further, WNV infection did not upregulate GFAP expression in astrocytes, suggesting that astrocyte activation does not play a role in restricting nonneuropathogenic WNV infection in astrocytes. Junin virus replication in astrocytes is restricted by reactive nitrogen species produced during infection (209). However, inhibition of inducible nitric oxide synthetase (iNOS) did not lead to increased cell-to-cell spread for WNV-MAD78 (data not shown). Further, restricted infectious particle production of WNV-MAD78 was independent of any secreted factor. These data did not address the delay in initiation of replication for WNV-MAD78 compared to WNV-NY in astrocytes, where astrocytes may contribute a cell-specific component. It is very likely that astrocyte-specific intracellular components promote replication and contribute to the delay in initiating replication in WNV-MAD78-infected astrocytes compared to WNV-NY-infected astrocytes. More extensive studies can assess these factors and the delay for WNV-MAD78 in initiating replication in astrocytes. Together, these data demonstrate that the restriction in cell-to-cell spread for WNV-MAD78 compared to WNV-NY is likely independent of a differentially expressed host factor in astrocytes.

Since host responses to WNV infection in astrocytes did not appear to contribute to the restriction in cell-to-cell spread for WNV-MAD78 in astrocytes, we examined the contribution of the viral particles produced during astrocyte infection and the ability to infect neighboring astrocytes. To assess whether there were deficiencies in astrocyte-derived viral particles, we examined both the particle:PFU ratio and compared the infectivity of astrocyte-derived particles on astrocytes and Vero cells. Both of these assays demonstrated that WNV-MAD78 particles derived in astrocytes are less infectious compared to WNV-NY particles. Thus, the host response may not be restrictive to WNV-MAD78, but rather, the viral particle itself is less infectious. WNV processing in cells occurs in the ER and involves several glycosidases that glycosylate specific moieties on both prM and, in some cases, the envelope protein. In the trans-Golgi, these carbohydrates are further modified and the cellular protease furin, which cleaves off the glycosylated moiety in prM to be released in the extracellular milieu during maturation of the particle. Only pathogenic strains of WNV are glycosylated at this envelope residue (13, 24, 237), leading us to hypothesize that it may play a role in restricting cell-to-cell spread in astrocytes. Previous data suggests that mature particles are more infectious than immature particles (53). Surprisingly, furin activity in astrocytes was higher compared to activity in other cell types, such as endothelial cells, where there is no difference in infectious particle production between WNV-NY and WNV-MAD78 (117). When furin was inhibited throughout infection in astrocytes, we observed an increase in the number of infectious viral particles produced for WNV-MAD78 compared to infections

without inhibitor. However, WNV-NY titers were not affected. These data further suggested that enhanced viral processing may be detrimental to WNV-MAD78 replication in astrocytes and may contribute to the inability for WNV-MAD78 to spread from cell to cell.

While viral egress and release is an important step in WNV infection, subsequent binding to neighboring cells and entry into a naïve cell is necessary for perpetuation. Several viral attachment factors have been suggested to play a role in WNV entry (50, 60, 176). In particular, DC-SIGNR and DC-SIGN are capable of promoting WNV infection in some cell types. However, we did not find an increased expression of either of these two molecules in astrocytes compared to highly permissive cells (data not shown). Since these receptors bind carbohydrate moieties, we hypothesized that the glycosylation, and therefore maturation, state of the viral particle may play an important role in cell-to-cell spread in astrocytes. Glycosylation of the envelope during WNV infections has been found to improve viral assembly and egress, and contributes to increased neuropathogenesis in mouse models (106). However, equivalent total particle production was detected for WNV-NY and WNV-MAD78 in astrocytes, suggesting that the restricted cell-to-cell spread of WNV-MAD78 was due to the production of defective particles rather than a decrease in particle production. Since glycosylation of other types of viral particles, such as HIV (320), has been shown to affect viral entry and cell-to-cell spread, we constructed recombinant viruses that exchanged residues in the glycosylation motif between WNV-NY and WNV-MAD78. However, these recombinant viruses replicated similar to their

parental counterparts, and glycosylation did not alone account for the reduction in infectious particle production during infection of astrocytes. Yet at 72hpi, infectious particle production of the WNV-NY S156P recombinant virus decreased to levels similar to WNV-MAD78. Thus, while glycosylation may not play a role in cell-to-cell spread in astrocytes, it may contribute to the stability of the viral particle. In contrast, recombinant viruses containing the structural proteins from WNV-MAD78 and the nonstructural proteins from WNV-NY replicated similar to WNV-MAD78, suggesting that the structural components alone were sufficient to restrict infectious particle production in astrocytes. How the structural genes contribute to the restriction in spread is still left to be uncovered. It is likely that factors other than glycosylation on the envelope protein within the virion are able to bind to subsequent astrocytes, and therefore contribute to the restriction in cell-to-cell spread for WNV-MAD78. Further experiments are necessary to assess the contribution of individual proteins within the particle and specific residues contribute to the restriction of cell-to-cell spread for WNV-MAD78 in astrocytes.

While the structural proteins appear to play a role in the restriction of cell-to-cell spread in astrocytes, viral replication and capability to cause neuropathogenesis in vivo has yet to be described. Although preliminary studies have been done in mice with recombinant viruses similar to the ones synthesized in these studies (269), these studies did not examine neuropathology. Further studies in vivo will also clarify the contribution for viral replication in astrocytes in promoting or restricting WNV neuropathology. In addition, the host responses

elicited to the viral chimeras that may contribute to neuropathology also needs to be assessed. The recombinant viruses synthesized could be used as a tool to further assess viral factors that contribute to the astrocyte-specific delay in initiation in viral replication for WNV-MAD78. These recombinant viruses may aid in identifying the astrocyte-specific factors that inhibit viral replication compared to other cell types. Astrocyte-specific factors may therefore serve as novel therapeutic targets in limiting severe CNS neuropathologies.

This study examined both host and viral determinants contributing to the restriction in WNV-MAD78 replication and spread within astrocytes. Previously, we hypothesized that all strains of WNV may be able to enter into the CNS. However, in astrocytes, WNV replication is restricted for nonneuropathogenic strains of WNV both at the level of initiating replication as well as cell-to-cell spread. Since differential host responses did not contribute to the restriction in infectious particle production for WNV-MAD78-infected astrocytes, we hypothesized a novel role for cellular processing specific to nonneuropathogenic viruses and in restricting cell-to-cell spread. Indeed, we observed that cellular processing by furin was sufficient to inhibit infectious viral particle production in astrocytes for nonneuropathogenic WNV, and when furin was inhibited, nonneuropathogenic strains produced increased amounts of infectious viral particles. In examining which viral components contributed to the restriction in infectious particle production, we observed that the strain that the structural genes are derived from determines the amount of infectious particles produced in astrocytes, suggesting that structure and processing of the virion may play a role

in inducing WNV neuropathogenesis. These novel insights provide both targets for development in therapeutics as well as possible candidate vaccines. Further research into what types of immune responses occur during infection in astrocytes with the recombinant viruses and how they likewise contribute to spread in other cell types of the CNS will expand the in vitro model for WNV infection of the CNS.

Acknowledgement

We would like to thank Rianna Vandergaast Zielstra for helping with the construction of viral chimeras used in this chapter.

Chapter 5- Observations on WNV-induced neuroinflammation

Abstract

The neuroinflammatory response to West Nile virus (WNV) infection can be either protective or pathological depending on the context. Though several studies have examined chemokine profiles within brains of WNV-infected mice, little is known about how various cell types within the central nervous system (CNS) contribute to chemokine expression. Here, we assessed innate immune responses in cell types in brain microvascular endothelial cells and astrocytes, which comprise the major components of the blood-brain barrier (BBB), in response to avirulent (WNV-MAD78) and highly virulent (WNV-NY) strains of WNV. Intrinsic innate immune responses to both strains of WNV were activated with similar kinetics in both endothelial cells and astrocytes. While WNV-MAD78-infected endothelial cells established a more pronounced chemokine gradient compared to WNV-NY-infected endothelial monolayers, the chemokine profile was disrupted when endothelial cells were co-cultured in the presence of astrocytes. WNV-NY-infected astrocytes also expressed higher levels of chemokines compared to WNV-MAD78-infected astrocytes. Chemokine expression was functional in both endothelial cell monolayers alone or cocultured with astrocytes, as increased monocyte adhesion was observed in WNV-MAD78-infected endothelial cell layers, but WNV-NY infected cocultures exhibited increased transmigration of monocytes through the coculture model. Combined

these data suggest that cells comprising the BBB contribute to a dynamic proinflammatory response that evolves as WNV infection progresses.

Introduction

West Nile virus (WNV) is a positive-strand, RNA virus in the family Flaviviridae. Initially identified in sub-Saharan Africa in 1937, WNV infection typically resulted in a mild febrile disease, though rare neurological complications were reported. In contrast, the emergence of WNV in the Western hemisphere in the 1990s has been associated with an increased rate of meningitis, encephalitis, and acute flaccid paralysis (<http://www.cdc.gov/ncidod/dvbid/westnile/index.htm>), making WNV the leading cause of mosquito-borne neuroinvasive disease in the United States. Recent outbreaks have also occurred in other parts of the world, including Eastern and Western Europe (199, 200), suggesting that WNV continues to impact global health. Nevertheless, no WNV-specific antiviral therapies or vaccines exist for humans. A greater understanding of the mechanistic basis for the differential neuropathogenicity among WNV strains may provide insights into the development of new therapies for the treatment of WNV neuroinvasive disease. In addition, assessment of the kinetics of the immune response to WNV strains that vary in pathogenicity within various cell types of the CNS may reveal additional mechanisms that contribute to neuropathology.

Recognition of viral moieties by pattern recognition receptors (PRRs) induces several signaling cascades that lead to the direct transcription of antiviral genes, proinflammatory cytokines and chemokines (4). Antiviral gene products

function in several ways, including directly cleavage of viral RNA, inhibition of protein synthesis, and amplification of the antiviral response. However, TLR3^{-/-} mice may experience decreased levels of WNV replication in the CNS compared to wild type mice, suggesting that not all antiviral responses to WNV infection are beneficial to the host (297). How viral infections initiate an innate immune response within the CNS is just beginning to be uncovered.

Recently it has been demonstrated that CNS immune responses differ from immune responses in the periphery (254). Under normal homeostatic conditions, the CNS is an immune specialized compartment with limited leukocyte infiltration. This is due in large part to the restrictive nature of the blood-brain barrier (BBB). The BBB is comprised of specialized endothelial cells, which line the cerebral microvasculature, and the foot processes of astrocytes, which envelop >99% of the endothelium. The complex intercellular tight junctions between endothelial cells at the BBB form 50-100x tighter seals compared to their peripheral counterparts, severely restricting paracellular movement of solutes and circulating immune cells (1).

In addition to the innate intracellular immune response within cells of the BBB preventing spread of viral infection, cell types of the BBB are involved in mobilizing the cellular immune response. Proinflammatory cytokines mobilize the cellular immune response to the site of infection. The cellular response either leads to clearance of infected cells and free virus and serves as a perpetuator of long term-immunity. One specific class of antiviral cytokines, type-1 IFNs, amplify the antiviral response by acting in both an autocrine and paracrine fashion to

prevent viral cell-to-cell spread (120, 121). The innate intracellular antiviral response to WNV infection has been characterized in several cell types in vitro and in vivo (127, 144, 226, 230, 271). For example, IFNAR^{-/-} mice experience higher levels of replication of WNV in all tissues and have markedly decreased survival during WNV infection with either pathogenic or nonpathogenic strains compared to wild type mice. As with many neuroinvasive pathogens, WNV induces expression of additional proinflammatory cytokines within the CNS (15, 92, 131, 152, 246). Chemokines are another specialized class of cytokines that function by forming gradients to attract circulating leukocytes to the site of infection. WNV infection in the CNS induces chemokine expression (92). Moreover, chemokine expression was higher in the brains of mice inoculated with a neuropathogenic strain of WNV compared to mice inoculated with a nonneuropathogenic strain of WNV at late times during infection (246). Thus, chemokine expression leading to leukocyte infiltration may contribute to WNV-mediated neuropathologies.

Despite the restriction to pathogens and immune responses at the BBB, one of the hallmarks of WNV encephalitis is the infiltration of inflammatory leukocytes into the central nervous system (CNS) (197). The process of leukocyte infiltration into infected tissue is a highly regulated, multistep process mediated by a family of chemoattractant cytokines known as chemokines (40, 183). Recruitment of leukocytes to the site of infection can be divided into two phases: the initial attraction and movement of immune cells across the endothelial layer and the subsequent migration within the infected tissue. The

first step in the recruitment of leukocytes, crossing the endothelial layer, is mediated by solid phase gradients formed by chemokines binding to anchored sugar residues or scavenger receptors on endothelial cell surfaces (183). Immobilized chemokines expressed on endothelial cells attract leukocytes, which initially undergo selectin-dependent tethering and rolling. Binding of immobilized chemokines to their cognate receptors on leukocytes activates integrins on the surface of leukocytes. Integrins bind to cell adhesion molecules present either on endothelial cells or cells directly in contact with the endothelium in the basolateral surface, thereby promoting firm attachment to the endothelial cell layer. Chemokine gradients established within endothelial cells also direct migration of leukocytes across the endothelial monolayer (diapedesis) (40, 183). While entry of circulating leukocytes into infected tissues or organs is critical for controlling an invading pathogen, aberrant or unregulated entry can have pathological consequences.

Determining which cell types in the CNS initiate chemokine production in response to pathogenic and nonpathogenic strains of WNV may facilitate development of therapies to modulate the process of neuroinflammation. Therefore, we examined the antiviral response within cell types of the BBB, including induction of ISGs, cytokines, and chemokines that may modulate the cellular response to WNV infection in the CNS. Two strains of WNV that vary in their capacity to induce neuropathology, WNV-NY, a neuropathogenic strain, and WNV-MAD78, a nonneuropathogenic strain, were utilized to determine strain-specific contributions to neuroinflammation. Treatment of human brain

microvascular endothelial cells (HBMECs), with TNF α during or prior to infection had no effect on WNV replication. In contrast, WNV replication was delayed in HBMECs treated with type-1 IFN. Post treatment of type-1 IFN was less restrictive to viral replication for WNV-NY compared to WNV-MAD78 in HBMECs. When the innate intracellular antiviral response to WNV infection in astrocytes was compared to that in endothelial cells, astrocytes displayed a more robust innate antiviral response. We also assessed the chemokine response of WNV-infected HBMECs and human brain cortical astrocytes (HBCAs). WNV-MAD78-infected endothelial cell monolayers expressed higher levels of CCL5 compared to WNV-NY-infected monolayers. In contrast, the chemokine profile observed when endothelial cells were co-cultured in a transwell system in the presence of astrocytes was less pronounced for both strains of WNV. Under these conditions, WNV-induced chemokine secretion and gradient formation did not affect the integrity of the endothelial cell monolayer, suggesting that the initial entry of leukocytes into the CNS in response to WNV is an active process. Additionally, we observed increased expression of cellular adhesion molecules (CAMs) in WNV-infected astrocytes compared to mock treated astrocytes. In contrast, no upregulation in expression of CAMs was observed in WNV-infected HBMECs. When fluorescently labeled monocytes were added to infected HBMEC monolayers, increased levels of monocytes attached to WNV-MAD78-infected cells compared to WNV-NY infected cells. However, when monocyte traversal was examined in a coculture model, increased levels of monocytes traversed cocultures inoculated with WNV-NY compared to cocultures inoculated with

WNV-MAD78. Combined this data suggests that, as with other neurotropic viruses (75, 162, 187), the cells comprising the BBB contribute to the proinflammatory response to WNV.

Results

Treatment with type-1 IFN but not TNF α inhibits WNV replication in HBMECs

Neither TNF α nor type-1 IFNs are induced at detectable levels during WNV infection of HBMECs (data not shown), suggesting that effects in vivo from these cytokines at the BBB may be from cytokines produced in another cell type. In addition, treatment of HBMEC monolayers with exogenous TNF α did not increase the permeability of the monolayer (data not shown). However, studies in mice indicate that high levels of virus are detected in the blood prior to high levels in the CNS. In addition, replication in the periphery induces the secretion of several proinflammatory cytokines, such as TNF α and type-1 IFNs (226, 253). An initial study examining WNV neuroinvasion suggest that the incursion of WNV into the CNS is a result of the breakdown of the BBB from TLR-dependent induction of proinflammatory cytokines, such as TNF α (297). To examine the effects of proinflammatory cytokines on WNV replication in cells that comprise the BBB, human brain microvascular endothelial cells (HBMECs) were either mock-infected or infected with WNV-NY or WNV-MAD78 and either left untreated, pre- and post-treated, or post-treated with either type-1 IFN or TNF α . Although treatment of HBMECs with TNF α (**Figure 24**) did not alter WNV

replication in HBMECs, treatment with high levels of type-1 IFN reduced peak viral titers for both WNV-NY- and WNV-MAD78-infected HBMECs. Consistent with previous studies performed in other cell types (127), WNV-MAD78 replication was more sensitive to type-1 IFN treatment compared to WNV-NY replication in HBMECs. Further, in HBMECs treated with TNF α , NF κ B translocated to the nucleus, demonstrating that HBMECs are not deficient in these signal transduction pathways (**Figure 25 A**). In addition, HBMECs treated with exogenous type-1 IFN, expressed low levels of ISGs (**Figure 25 B**), suggesting that HBMECs can respond to exogenous treatment of both TNF α and type-1 IFNs. Together, these data suggest that endogenous expression of TNF α and type-1 IFN at the BBB are not induced by WNV. Moreover, exposure to exogenous TNF α does not affect WNV replication in HBMECs. However, exogenous type-1 IFN treatment reduces WNV replication in HBMECs, possibly limiting the initial infection of HBMECs in vivo.

WNV-MAD78 and WNV-NY initiate similar activation kinetics of the innate intracellular antiviral responses in HBMECs and HBCAs.

High levels of WNV can traverse endothelial monolayers and reach astrocytes at equivalent levels, and type-1 IFN is secreted during WNV infection in astrocytes (117). Thus, one additional restriction to WNV replication in astrocytes may be the initiation of the innate intracellular response. Therefore, we compared the innate antiviral response to WNV-NY and WNV-MAD78 in HBMECs and HBCAs. To monitor the innate antiviral response in HBMECs, we

examined the steady state levels of the intracellular antiviral effector proteins ISG56, ISG20, Viperin, and ISG15, which have been previously shown to be induced in response to WNV-NY infection in other cell lines (83, 127, 236, 271). Expression of ISG56, ISG20 and Cig5 was not detected by western blot analysis in either mock- or WNV-infected HBMECs (data not shown). In contrast, ISG15 was constitutively expressed in both mock and WNV-infected cultures (**Figure 26**) at equivalent levels. ISG15 differs from other antiviral proteins; it must be conjugated to intracellular proteins, a process referred to as ISGylation, in order to mediate its antiviral activity (159, 323). However, low levels of ISGylation were only observed in WNV-MAD78-infected cells at 48 hours post-infection. This suggests that despite constitutive ISG15 expression in this cell line, it is not functionally activated in response to WNV until very late in infection. The lack of induction of antiviral effector protein in response to WNV infection was not due to the disruption of the Jak/Stat signaling, as ISG56 expression and ISG15ylation was induced by treatment with exogenous type I IFN (**Figure 25B**, data not shown).

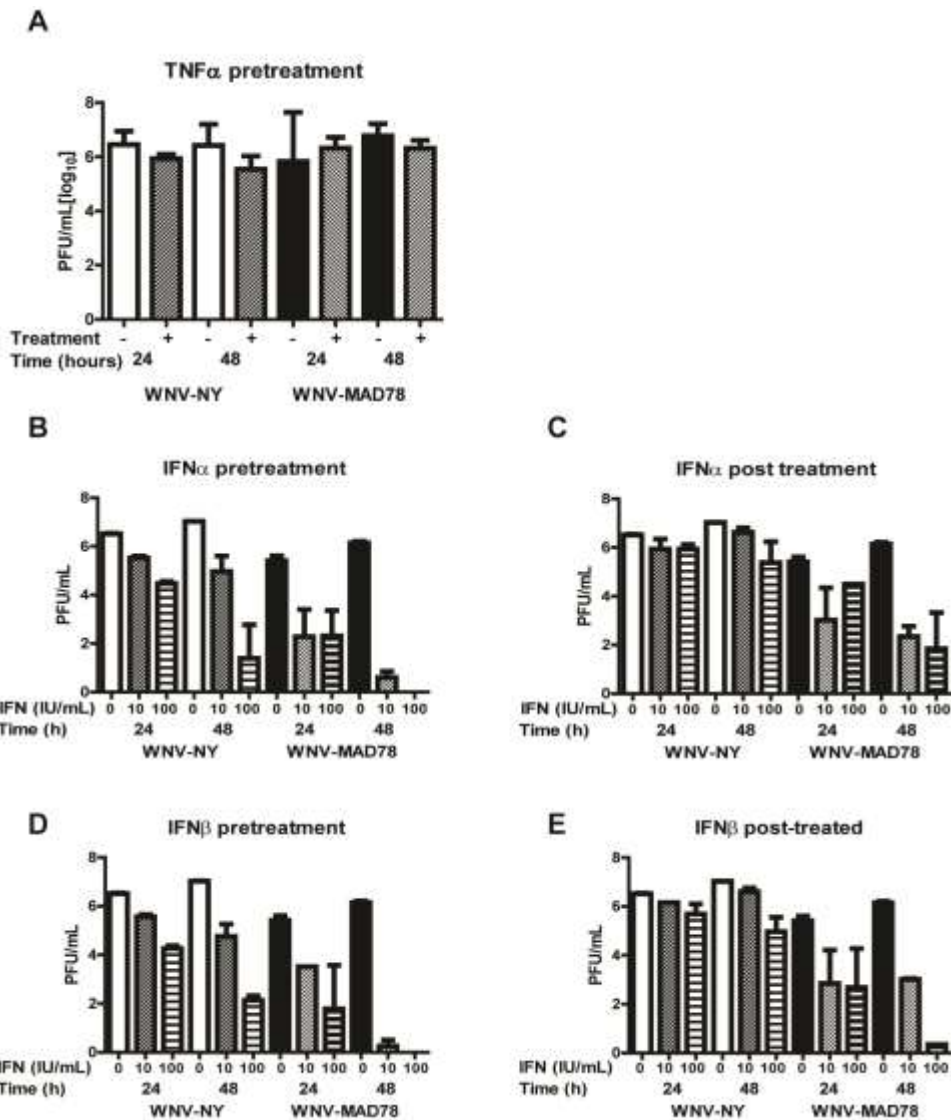


Figure 24. Treatment of endothelial cells with proinflammatory cytokines. HBMEC monolayers were either left untreated, (A) pretreated with TNF α (5ng/mL) or pre- or post-treated with either (B and C) IFN α or (D and E) IFN β and infected (MOI=1) with either WNV-NY or WNV-MAD78. Plaque assays were performed on supernatants collected at the indicated timepoints. Values presented are an average (+/- standard error) of 2 independent experiments.

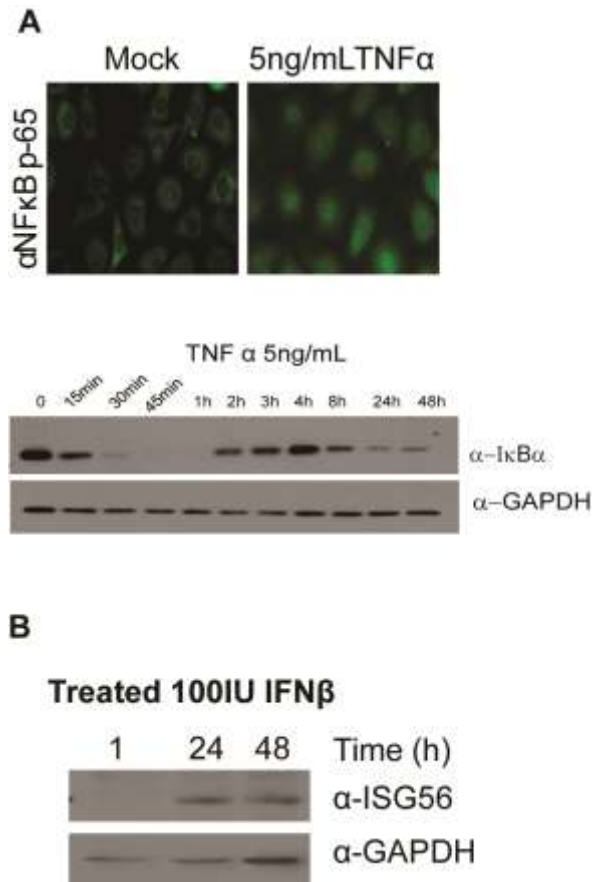


Figure 25. HBMECs respond to exogenous proinflammatory cytokine expression. (A) HBMECs were treated with TNF α (5ng/mL) for 1 hour and fixed in 3% PFA. Cells were then probed using an anti-NF κ B antibody. HBMEC monolayers were treated with TNF α (5ng/mL) and cell lysates were collected at the indicated timepoints. SDS-PAGE gels were run before probing with indicated antibodies. Data presented are representative of at least 2 independent experiments. (B) HBMECs treated with 100IU IFN β were lysed at times indicated. Lysates were run on SDS PAGE gels and transferred onto nitrocellulose as described in the materials and methods. Membranes were probed with antibodies to GAPDH and ISG56. Data presented is representative of at least 2 individual experiments.

Combined this data suggests that the antiviral response to WNV infection in HBMECs is extremely muted. Yet, it is possible that the muted antiviral response in HBMECs, a transformed cell line, is suppressed by expression of the large T antigen (3). Therefore, we examined human brain microvascular endothelial cells (HBMVEs) that are not transformed and donor matched to the astrocyte cell line used. In HBMVEs, the intrinsic innate immune response is initiated at similar timepoints for both WNV-NY and WNV-MAD78 (**Figure 26 B**). This further suggests that despite initiation of the antiviral response, both neuropathogenic and nonneuropathogenic strains replicate to high levels in the brain endothelium (117). Thus, the intrinsic innate immune response does not differentially limit infectious particle production for nonneuropathogenic strains of WNV in brain endothelial cells.

However, HBCAs mounted an antiviral response. The antiviral effector proteins ISG56 and ISG15 were up regulated in response to WNV-NY and WNV-MAD78 infection (**Figure 26 C**) as well as other effector proteins including Viperin and ISG20 (data not shown). However, the initiation of the innate intracellular antiviral response in HBCAs in response to both WNV-NY and WNV-MAD78 was similar in both kinetics and amplitude. Together, these data suggest that the restriction of WNV-MAD78 cell-to-cell spread in astrocytes is not due to a differentially activated intrinsic innate immune response. Further, despite the innate antiviral response in HBMECs and HBMVEs in response to WNV infection, replication occurs to high levels in endothelial cells for both WNV-NY and WNV-MAD78.

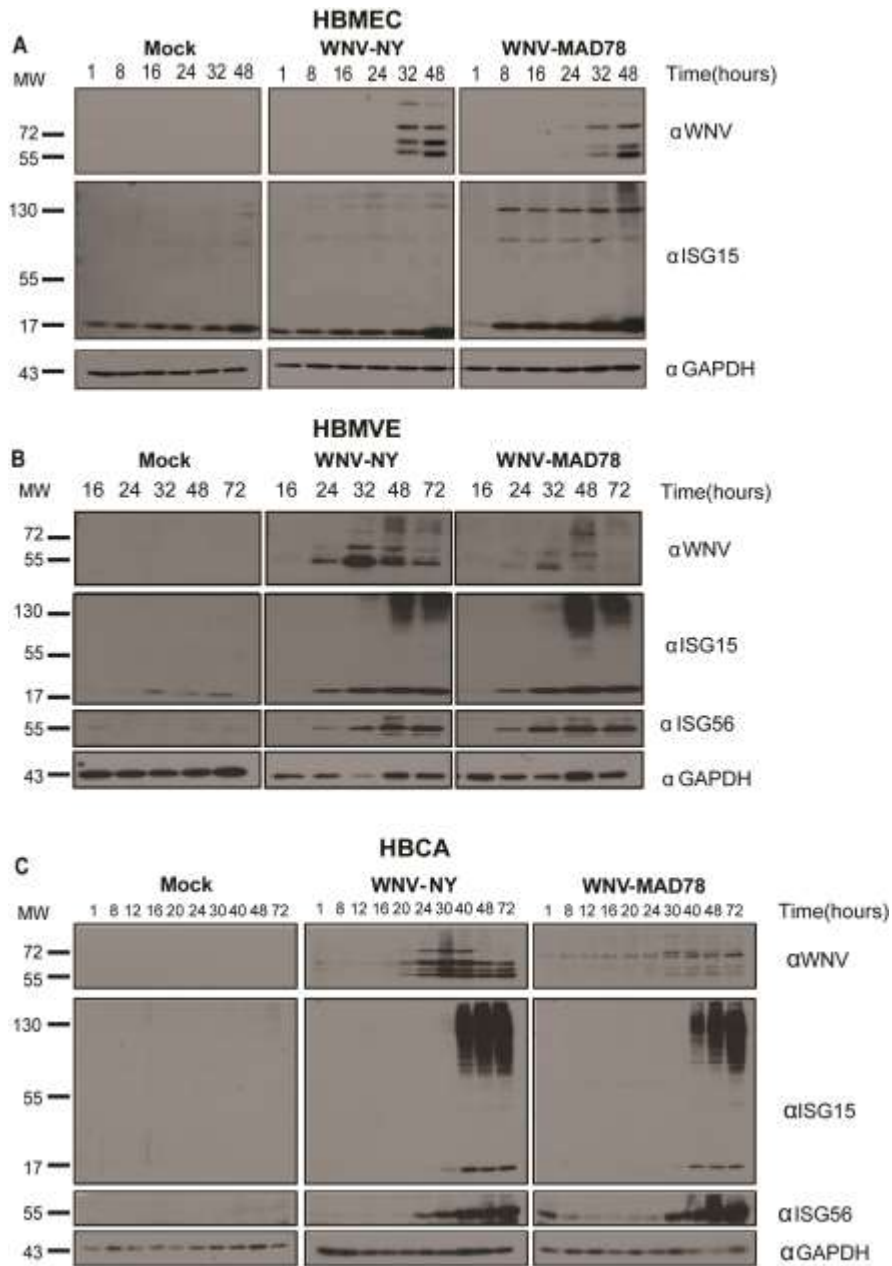


Figure 26- Innate intracellular antiviral responses in HBMECs and HBCAs. (A) HBMECs were mock treated or inoculated (MOI=0.1) with either WNV-NY or WNV-MAD78. Cell lysates were collected at the time indicated, lysates run on denaturing SDS-PAGE gels, and blots probed with the indicated antibodies. Blots presented are representative of at least 2 independent experiments. (B) HBMVEs were mock treated or inoculated (MOI=0.1) with either

WNV-NY or WNV-MAD78. Cell lysates were collected at the time indicated, lysates run on denaturing SDS-PAGE gels, and blots probed with the indicated antibodies. Blots presented are representative of at least 2 independent experiments. (C) HBCAs were mock treated or inoculated (MOI=0.01) with either WNV-NY, or WNV-MAD78. Cell lysates were collected at the time indicated, lysates run on denaturing SDS-PAGE gels, and blots probed with the indicated antibodies. Blots presented are representative of at least 2 independent experiments.

CCL2 and CCL5 expression and localization in WNV-infected HBMECs. Previous studies propose that WNV replication in brain microvascular endothelial cells facilitates WNV entry into the CNS (117, 284, 285). Thus, to determine if brain microvascular endothelial cells play an integral role in the early neuroinflammatory response to WNV, we examined the expression of CCL2 and CCL5, two chemokines highly upregulated in the brains of WNV-infected mice (92, 152, 246), in human brain microvascular endothelial cells (HBMECs) infected with WNV-NY or WNV-MAD78. Consistent with a previous report (51), CCL2 was expressed in mock-infected HBMECs (**Figure 27A & B**). Moreover, WNV infection did not significantly alter CCL2 mRNA or protein levels in HBMECs ($P > 0.05$), despite the fact that this cell line is equally permissive to both strains of WNV (117). Because stimulation of endothelial cells induces the redistribution of constitutively expressed CCL2 to the cell surface (51), we also used a transwell model system to examine the localization of CCL2 throughout the endothelial cell layer during WNV infection. Examination of the cellular distribution of CCL2 by confocal microscopy revealed several differences in CCL2 staining patterns between mock-, WNV-NY- and WNV-MAD78-infected HBMECs (**Figure 28 A & B**). Notably, CCL2 expression shifted from a diffuse staining pattern in mock-infected cells to a punctate staining pattern in WNV-infected cells. Thus, during WNV infection in endothelial cells, CCL2 chemokine gradients are established by the redistribution of CCL2 instead of upregulation of mRNA or secretion.

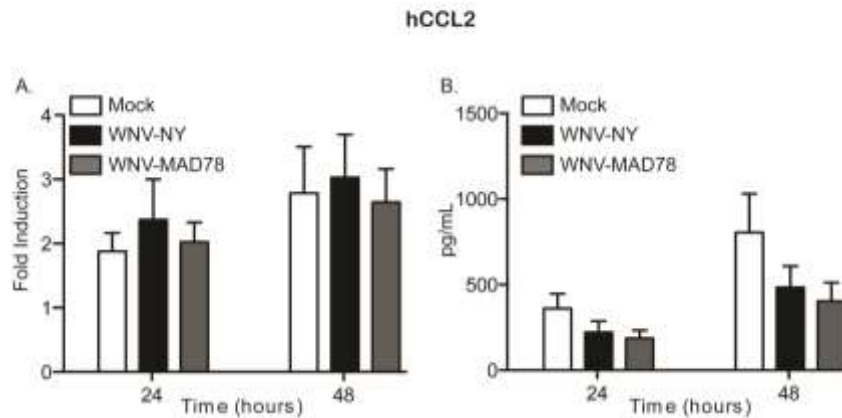


Figure 27. CCL2 expression in WNV-infected HBMECs. Total RNA (A) and culture supernatants (B) were recovered from mock-infected HBMECs or HBMECs infected with WNV-NY or WNV-MAD78 (MOI=0.1). (A) CCL2 mRNA levels in mock and WNV-infected HBMECs were determined by qRT-PCR. Values represent the average (+/- standard error) fold increase compared to mock-infected HBMECs at 1 h post-infection from at least 3 separate experiments. (B) Levels of CCL2 present in the HBMEC-infected supernatants were determined by ELISA. Values represent the average (+/- standard error) from at least 3 separate experiments.

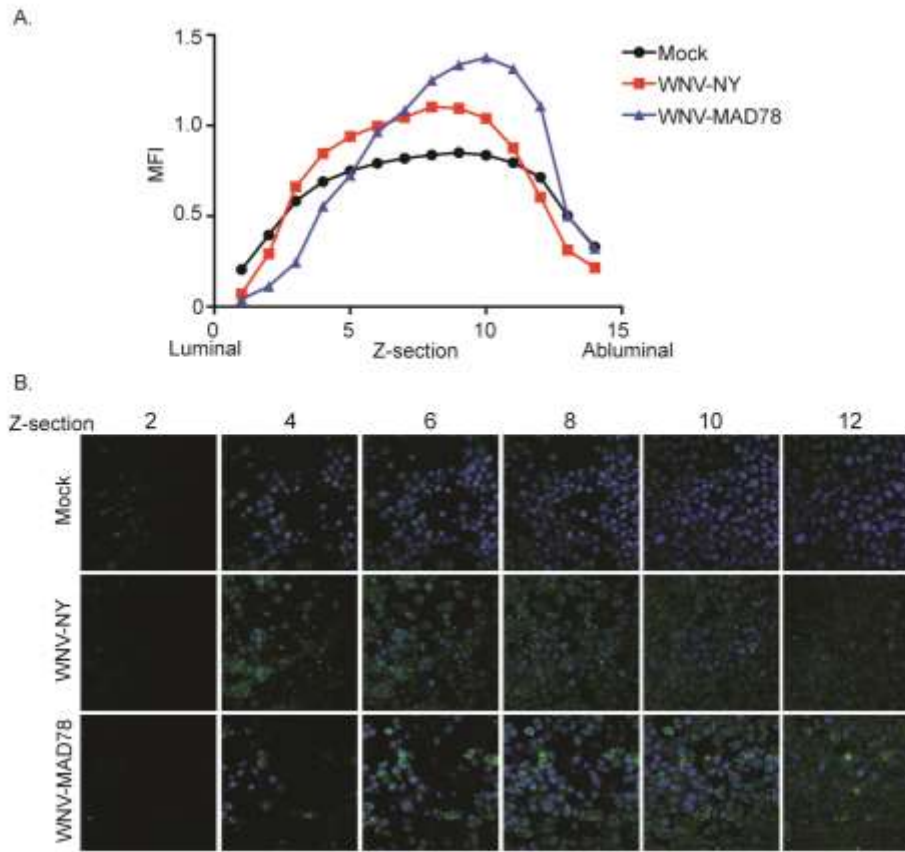


Figure 28. Localization and quantification of CCL2 within WNV-infected HBMECs. HBMECs cultured on transwell inserts were either mock-infected, or infected with WNV-NY or WNV-MAD78 (MOI=0.1). Cell monolayers were fixed at 48 h post-infection and probed for CCL2 using CCL2 polyclonal antisera followed by a DyLight-488 conjugated secondary antibody (green). Nuclei were visualized using Hoechst stain (blue) and used as a reference point for location within the stack. Z-stacks were captured using confocal microscopy and quantification of each stack was determined using ImageJ. Mean fluorescence intensity (MFI) quantification of Z-sections (A) and images of Z sections (B) are representative of 3 independent experiments.

Unlike CCL2, CCL5 mRNA expression was upregulated ~6000-fold in both WNV-NY- and WNV-MAD78- infected HBMECs compared to mock-treated HBMECs (**Figure 29A**, $P < 0.005$). However, in WNV-MAD78-infected cultures, the level of secreted CCL5 was significantly higher (3.5-fold, $P < 0.05$) compared to WNV-NY-infected cultures (**Figure 29B**) and higher levels of CCL5 were detected throughout the WNV-MAD78-infected monolayer compared to WNV-NY (**Figure 30A & B**), suggesting that CCL5 is also regulated at the post-transcriptional level within these cells. Together our findings suggest that neuropathogenic and nonneuropathogenic strains of WNV induce differential proinflammatory chemokine responses in brain endothelial cells.

CCL5 and CCL2 expression in WNV-infected astrocytes. Astrocytes play a central role in mediating neuroinflammation in response to many viruses, including WNV (46, 75, 162, 209, 282). Therefore, we also examined CCL2 and CCL5 expression in primary human brain cortical astrocytes (HBCAs). As observed in HBMECs, CCL2 was constitutively expressed in HBCAs and WNV infection did not alter the level of secreted CCL2 (**Figure 31A**). In contrast to HBMECs, HBCAs secreted significantly more CCL5 in response to WNV-NY than WNV-MAD78 (**Figure 31B**, $P < 0.005$). As we have previously demonstrated that HBCAs are more permissive to infection with WNV-NY compared to WNV-MAD78 (117), the higher levels of CCL5 detected WNV-NY-infected HBCAs -

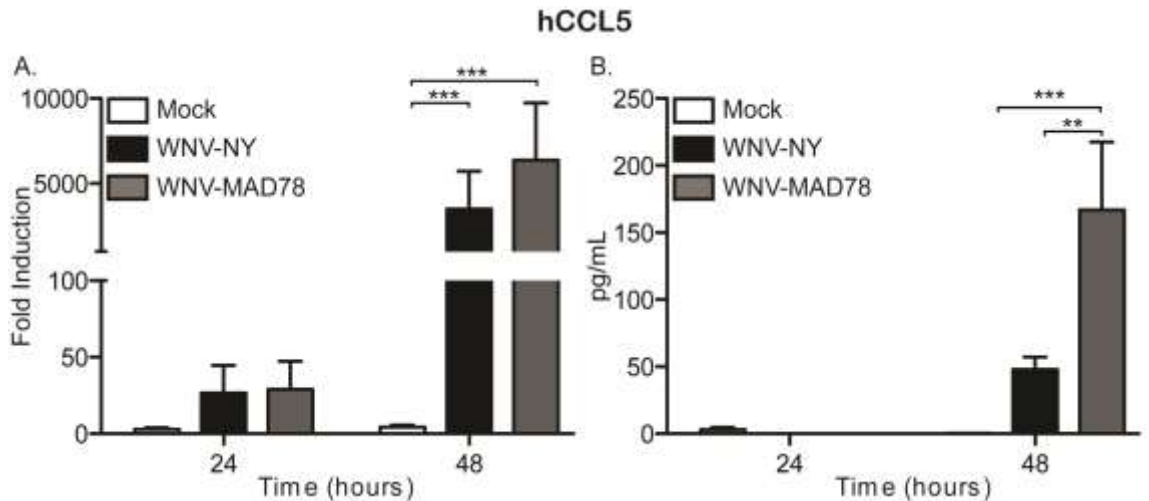


Figure 29. CCL5 expression in WNV-infected HBMECs. Total RNA (A) and culture supernatants (B) were recovered from mock-infected HBMECs or HBMECs infected with WNV-NY or WNV-MAD78 (MOI=0.1). (A) CCL5 mRNA levels in mock and WNV-infected HBMECs were determined by qRT-PCR. Values represent the average (+/- standard error) fold increase compared to mock-infected HBMECs at 1 h post-infection from at least 3 separate experiments. (B) Levels of CCL5 present in the HBMEC-infected supernatants were determined by ELISA. Values represent the average (+/- standard error) from at least 3 separate experiments. One-way Anova was performed to determine significance **p<0.01, ***p<0.005.

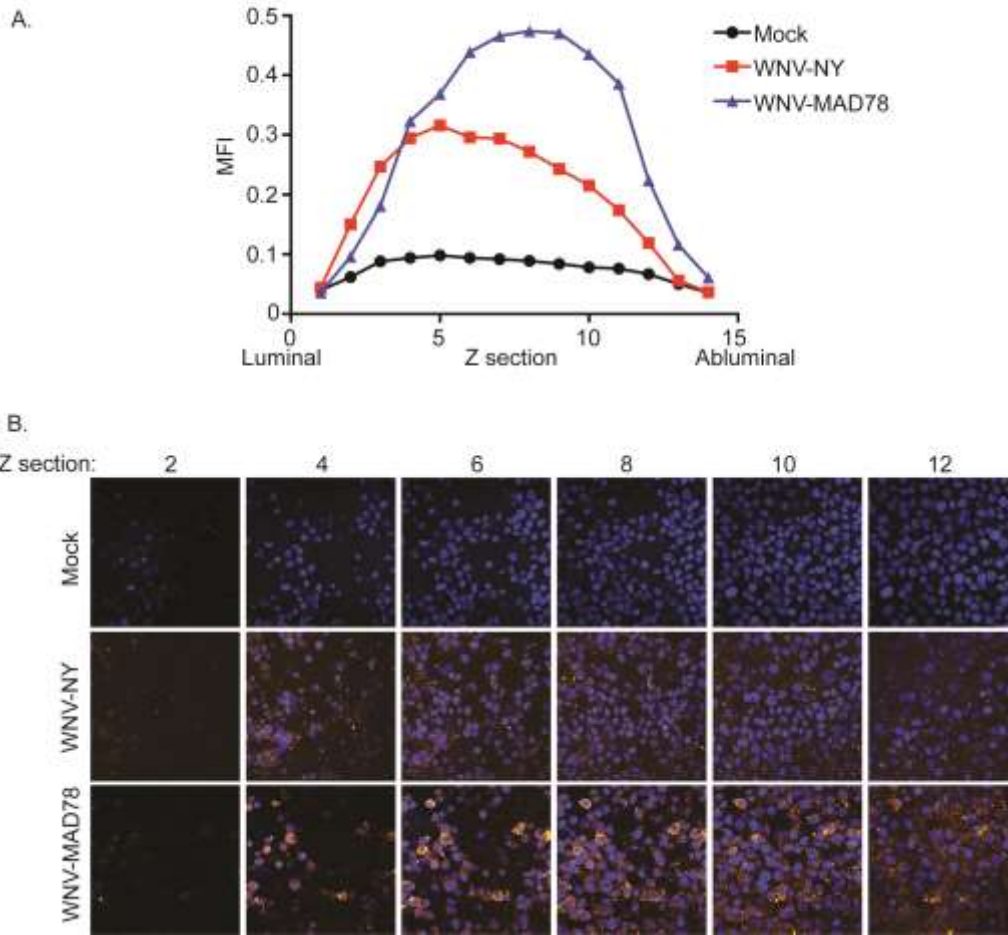


Figure 30. Localization and quantification of CCL5 within WNV-infected HBMECs. HBMECs cultured on transwell inserts were either mock-infected or infected with WNV-NY or WNV-MAD78 (MOI=0.1). Cell monolayers were fixed at 48 h post-infection and probed for CCL5 using CCL5 polyclonal antisera followed by an Alexafluor 633 conjugated secondary antibody (orange). Nuclei were visualized using Hoechst stain (blue) and used as a reference point for location within the stack. Z-stacks were captured using confocal microscopy and quantification of each stack was determined using ImageJ. Mean fluorescence intensity (MFI) quantification of Z-sections (A) and images of Z-sections (B) are representative of 3 independent experiments.

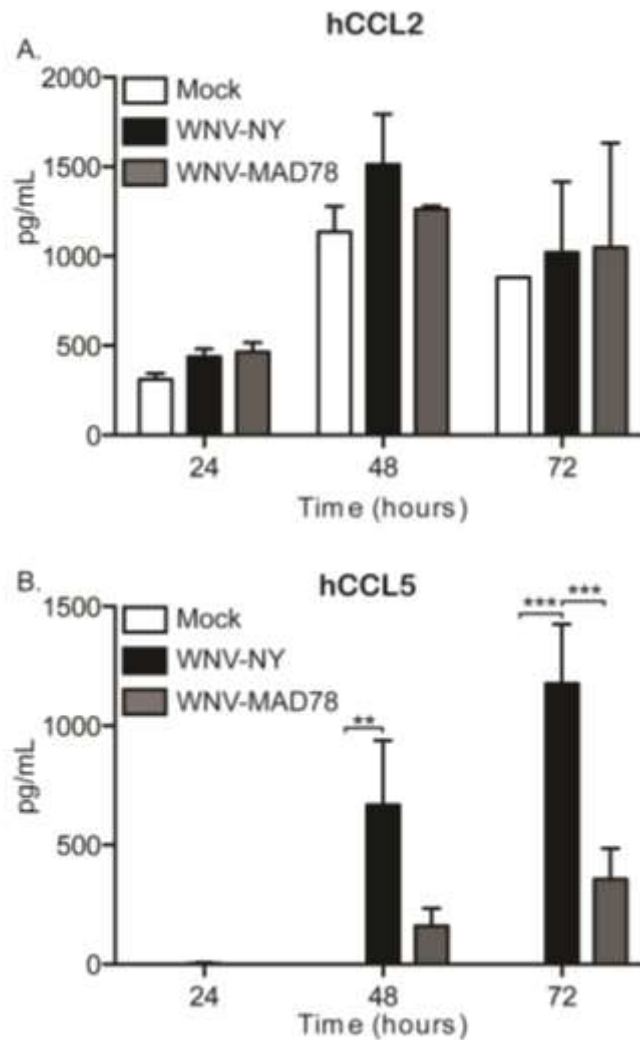


Figure 31. CCL2 and CCL5 expression in WNV-infected HBCAs. Culture supernatants were recovered from mock-infected HBCAs or HBCAs infected with WNV-NY or WNV-MAD78 (MOI=0.01) and levels of secreted CCL2 (A) or CCL5 (B) were determined by ELISA. Values represent an average (+/- standard error) from at least 3 independent experiments. One-way Anova was performed to determine significance ** $p < 0.01$, *** $p < 0.005$.

were likely due to the enhanced ability of WNV-NY to spread from cell to cell within the HBCA monolayer compared to WNV-MAD78. Indeed, WNV-MAD78 and WNV-NY-infected HBCAs secreted similar levels of CCL5 per infected cell (~0.146pg/infected cell for WNV-NY, ~0.547pg/infected cell for WNV-MAD78). These data suggest that the expression of chemokines in astrocytes may play a role in WNV-mediated neuroinflammation.

Chemokine expression in a co-culture model of the BBB. Endothelial cells bind and internalize chemokines produced by cells within the extravascular space (183). As such, the chemokine response to WNV infection in astrocytes may alter the expression of chemokines within the endothelial cell monolayer. Thus, we examined CCL2 and CCL5 localization within HBMECs cultured on a transwell support containing HBCAs cultured in the bottom chamber (**Figures 32 & 33**). In contrast to HBMEC monolayers alone, CCL2 and CCL5 appeared to accumulate to higher levels WNV-NY-infected HBMEC monolayers compared to mock and WNV-MAD78-infected HBMEC monolayers. Thus, astrocytes alter chemokine gradient profiles established in endothelial cell monolayers in response WNV infection.

Effect of WNV infection on the integrity of an *in vitro* model of the BBB. In addition to attracting leukocytes, chemokines can directly disrupt the cell-to-cell junctions necessary for maintaining the integrity of the endothelial monolayer (219). Therefore, we compared the permeability of WNV-NY- and

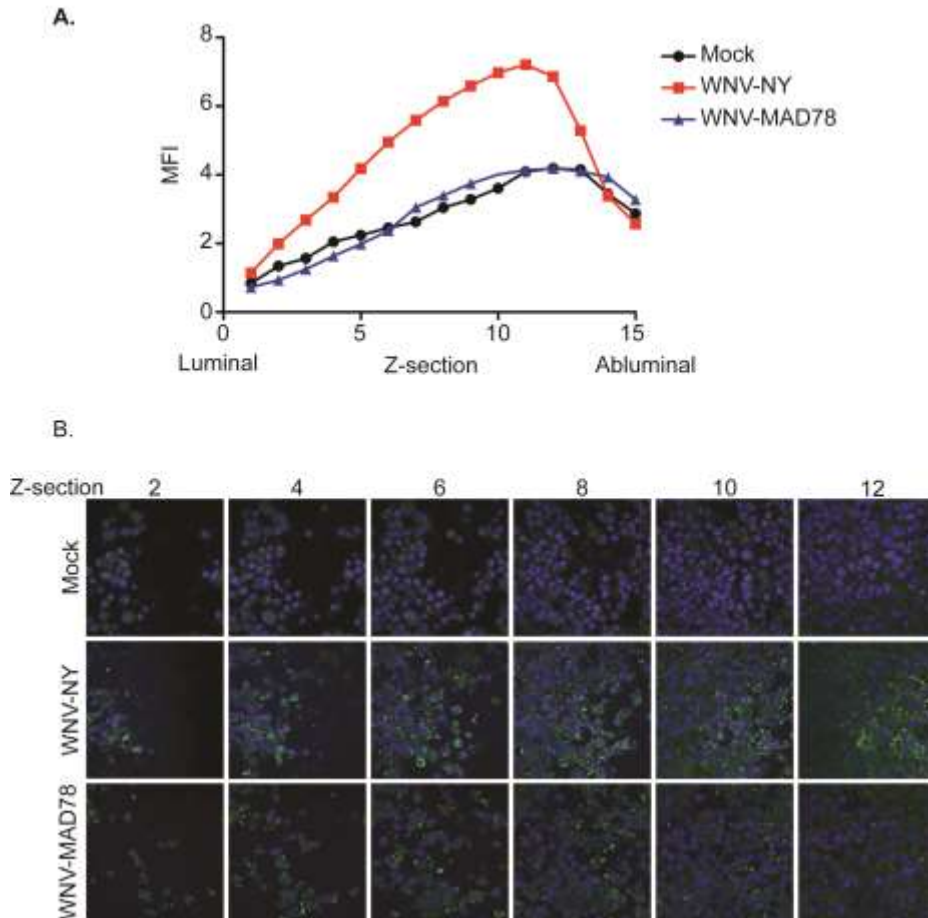


Figure 32. CCL2 localization within the HBMEC monolayer of an *in vitro* model of the BBB. HBMECs cultured on transwell inserts containing HBCAs plated in the abluminal chamber were mock-infected or infected with either WNV-NY or WNV-MAD78 (MOI=0.1). HBMEC monolayers were fixed at 72 h post-infection and CCL2 detected using polyclonal antisera to CCL2 followed by a Dylight-488 conjugated secondary antibody (green). Nuclei were visualized using Hoechst stain (blue) and were used as a reference point for location within the stack. Z-stacks were captured using confocal microscopy and quantification of each stack was determined using ImageJ. Mean fluorescence intensity (MFI) quantification of Z-sections (A) and images of Z-sections (B) are representative of 3 independent experiments.

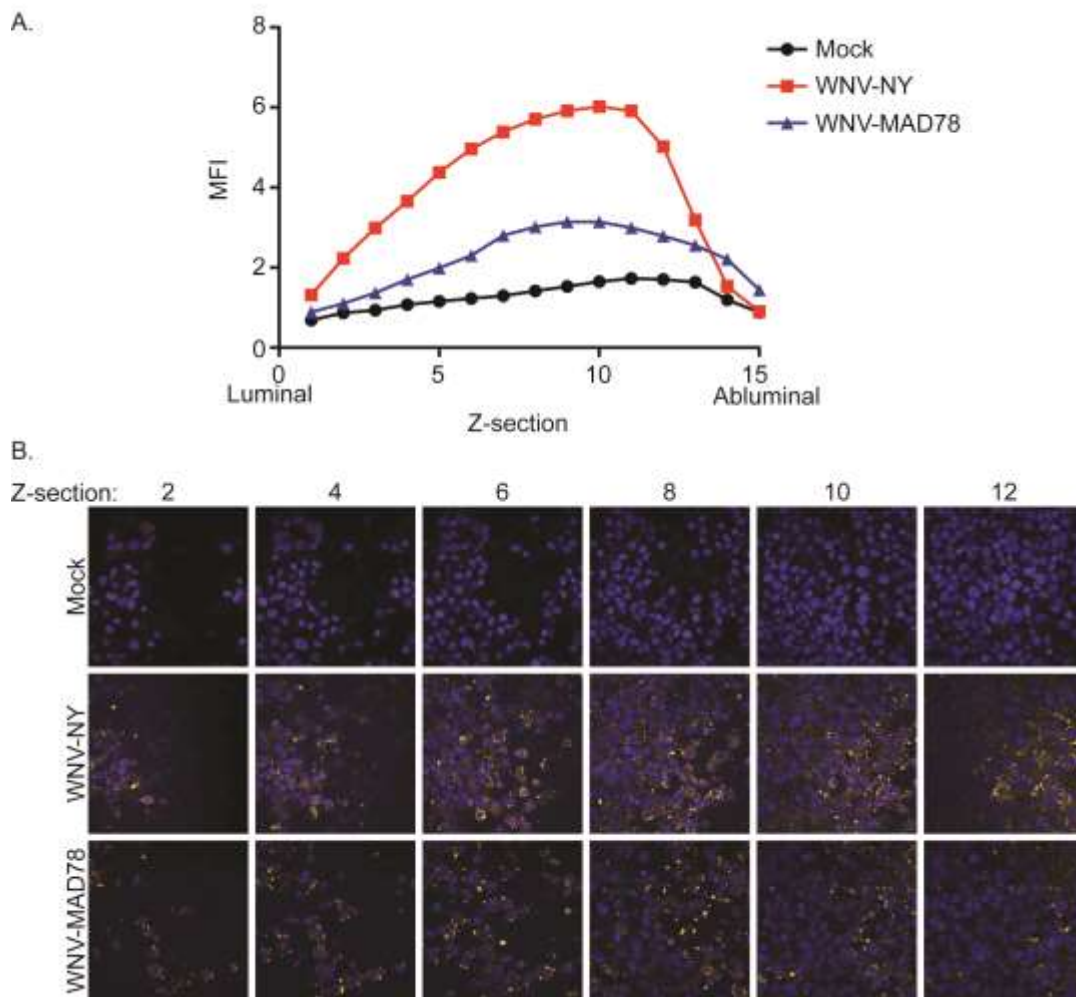


Figure 33. CCL5 localization within the HBMEC monolayer of an *in vitro* model of the BBB. Fixed HBMECs from Figure 6 were also probed with CCL5 polyclonal antisera followed by an Alexafluor-633 conjugated secondary antibody (orange). Nuclei were visualized using Hoechst stain (blue) and were used as a reference point for location within the stack. Z-stacks were captured using confocal microscopy and quantification of each stack was determined using ImageJ. Mean fluorescence intensity (MFI) quantification of Z-sections (A) and images of Z-sections (B) are representative of 3 independent experiments.

WNV-MAD78-infected HBMEC monolayers in the presence and absence of HBCAs. The integrity of the HBMEC monolayer was monitored by quantitating the level of FITC-labeled dextran translocation in mock-, WNV-NY- and WNV-MAD78- infected cultures (**Figure 34 A & B**). As expected, ~70% of the FITC-dextran was detected in the lower chamber of control wells lacking cells and HBMEC monolayers treated with EDTA to disrupt tight junctions. In contrast, only 5-10% of the FITC-dextran was detected in the lower chamber of mock-, WNV-NY- and WNV-MAD78-infected cultures, indicating that the HBMEC monolayer remained intact during infection and the presence of HBCAs did not alter FITC-dextran transmigration. These data suggest that the endothelial monolayer remains intact throughout the initial course of WNV infection, despite the establishment of CCL2 and CCL5 gradients.

WNV-NY-infected HBCAs express higher levels of CAMs compared to WNV-MAD78-infected HBCAs

Since both WNV-infected HBMECs and HBCAs upregulated expression of chemokines, we examined the expression of the next set of molecules to play a role in diapedesis, cell adhesion molecules (CAMs) in both cell lines. HBMECs constitutively expressed ICAM and VCAM at low levels, but expression of either did not increase during WNV infection (**Figure 35 A**). In contrast, WNV-infected HBCAs expressed higher levels of VCAM than mock treated HBCAs, and ICAM expression did not increase during WNV infection (**Figure 35 B**). This suggests

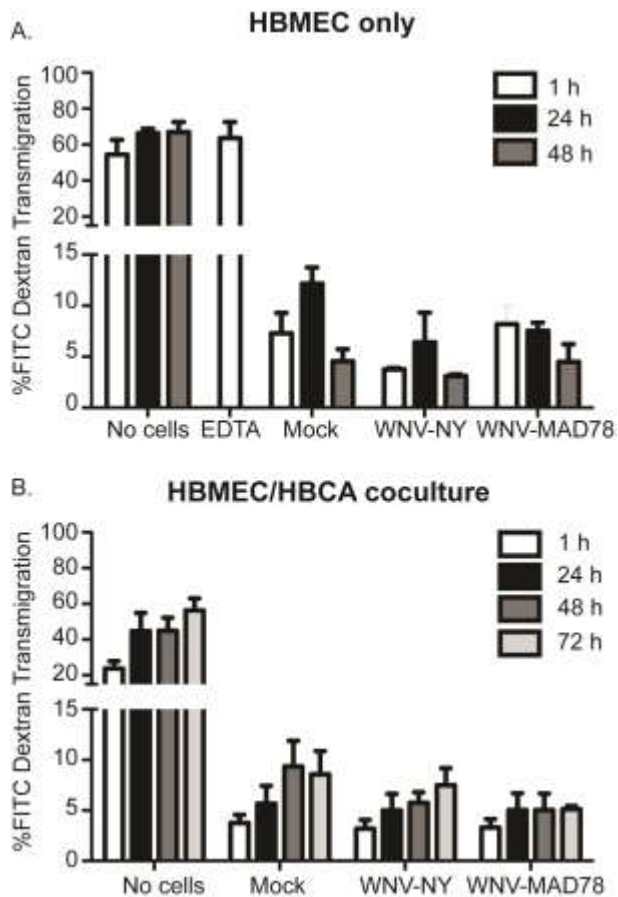


Figure 34. Effect of WNV infection on the permeability of the HBMEC monolayer. HBMECs grown in the absence (A) or presence (B) of HBCAs were infected with WNV-NY or WNV-MAD78 (MOI=0.1) or mock-infected and FITC-dextran (100 μ M) was added to the upper, luminal chamber at the indicated times (h). Cultures were incubated for 1 h and the amount of FITC-dextran present in the lower, abluminal, chamber was determined. Translocation of FITC-dextran across control inserts lacking cells and monolayers treated with 5mM EDTA was also determined. Values are an average (+/- standard error) from at least 2 independent experiments with permeability assays performed in triplicate.

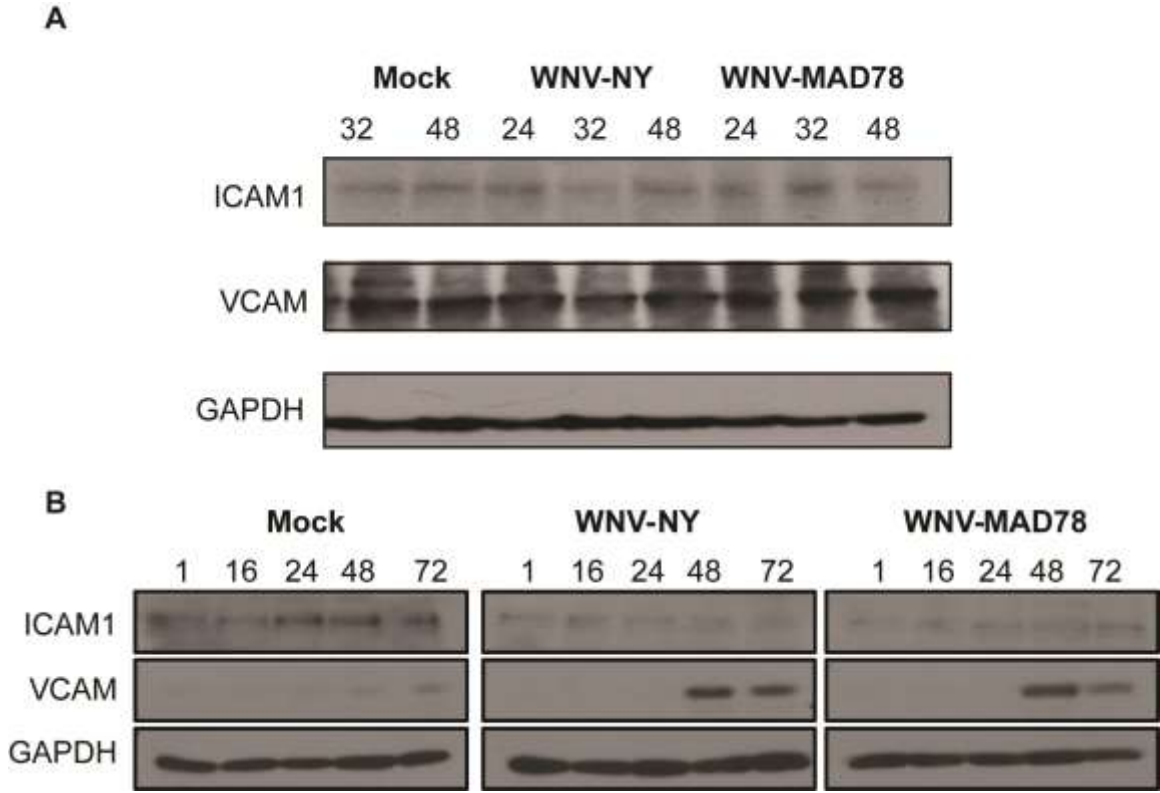


Figure 35. Expression of cell adhesion molecules (CAMs) in HBMECs and HBCAs. (A) HBMECs were either mock-treated, or inoculated with WNV-NY or WNV-MAD78 (MOI=0.1). At time indicated, cells were washed 2x with PBS, lysed in RIPA buffer, and run on SDS PAGE gels. Blots were then probed with the indicated antibodies. (B) HBCAs were either mock-treated, or inoculated with WNV-NY or WNV-MAD78 (MOI=0.01). At time indicated, cells were washed 2x with PBS, lysed in RIPA buffer, and run on SDS PAGE gels. Blots were then probed with the indicated antibodies. All blots presented are representative of at least 2 independent experiments.

that HBCAs may play an active role in extravasation events during WNV infection at the BBB.

WNV-NY and WNV-MAD78 replicate to low levels in THP1 cells

In addition to replication in endothelial cells, replication in hematopoietic cells and traversal of infected hematopoietic cells through the BBB into the CNS is a proposed model for the initial incursion of WNV into the CNS (15, 57, 268, 291, 292, 295). Thus, we examined replication kinetics for both WNV-NY and WNV-MAD78 in THP1s, a human monocyte cell line. WNV-NY and WNV-MAD78 replicated to low levels in THP1s (**Figure 36**). However, infectious particle production never increased compared to the initial amount of virus introduced into the cells. Thus, WNV is either replicating to low levels to maintain a basal level of infectious particle production, or stabilizing the virus and preventing viral clearance. In addition, the peak viral titers for both strains were lower compared to multiple cell lines of the BBB (117). WNV-infected mouse macrophages also display low levels of replication (253). Together, these data suggest that initial replication in hematopoietic cells is unlikely to account for observed differences in neuropathology among strains of WNV.

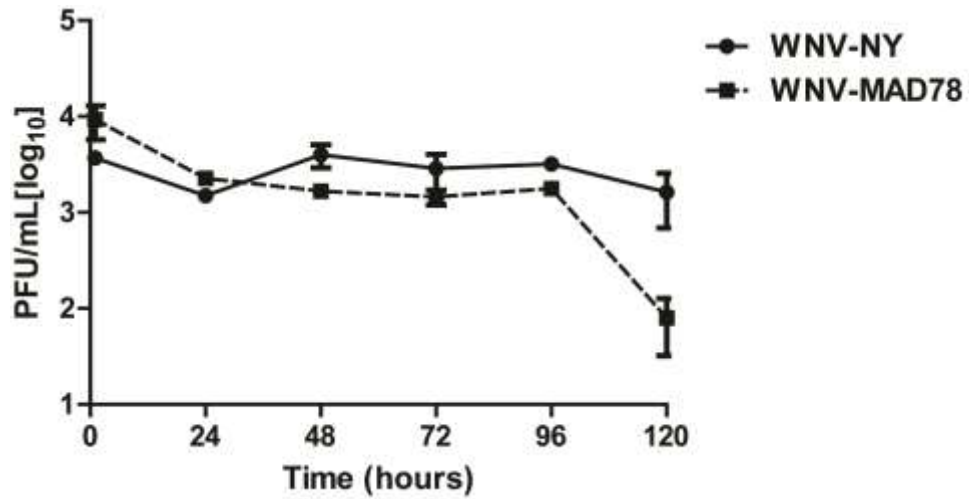


Figure 36. WNV-NY and WNV-MAD78 replication in THP-1 cells. THP-1s were inoculated with either WNV-NY or WNV-MAD78 (MOI=0.1). At indicated time points, cell supernatants were clarified and plaque assays performed on Vero cells. Data presented is an average (+/- standard error) of at least 2 independent experiments.

In vitro models of WNV infection and neuroinflammation at the BBB represent functional model systems

The extravasation process of leukocytes from the blood into infected tissue is a multistep process, including attachment, rolling, and diapedesis through the endothelial cell layer. WNV-MAD78-infected HBMECs express higher levels of CCL5 compared to WNV-NY-infected HBMECs. To assess if the upregulation of CCL5 is functional, fluorescently labeled THP-1 monocytes were incubated with mock-infected, WNV-infected, or TNF α -treated (100ng/mL) HBMEC monolayers (**Figure 37 A**). WNV-MAD78-infected HBMEC monolayers exhibited increased attachment of labeled monocytes compared to WNV-NY-infected or mock-infected monolayers. TNF α -treated HBMEC monolayers exhibited the highest level of attachment, as these levels of treatment have been shown to activate endothelium in several in vitro model systems (167). Since WNV-NY-infected HBCAs secrete higher levels of CCL5 than WNV-MAD78-infected HBCAs, and VCAM expression was increased during WNV infection, we assessed the effect of HBCAs on the extravasation process. When fluorescently labeled THP-1 cells were added to cocultures containing WNV-infected HBMECs in a suspended transwell chamber with HBCAs plated in the bottom chamber, we observed that WNV-NY infected co-cultures exhibited increased fluorescence in the bottom chamber compared to mock- or WNV-MAD78-infected co-cultures, although the increase observed was not statistically significant (**Figure 37 B**).

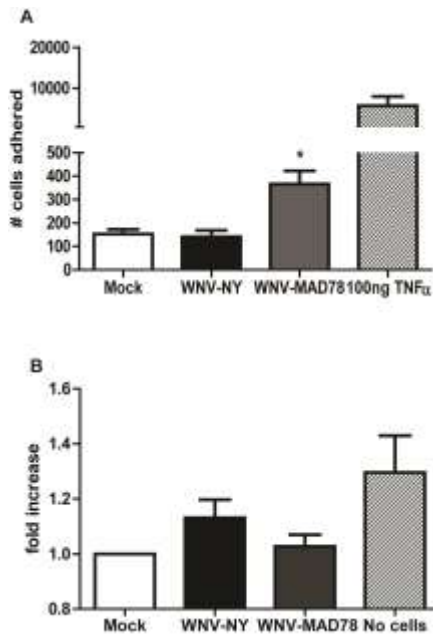


Figure 37. Attachment and diapedesis of monocytes in BBB models.

(A) Adherence of monocytes to HBMECs. HBMECs were infected with WNV-NY or WNV-MAD78 (MOI=0.1). At 48 hr post-infection, HBMECs were incubated with fluorescently labeled monocytes for 1 hr at 37°C. HBMECs were washed extensively and bound monocytes were visualized and counted using an Olympus fluorescent microscope. Results are an average of three independent experiments. (B) Diapedesis of monocytes through HBMEC monolayer in coculture model of the BBB. HBMECs were cultured on transwell inserts with HBCAs cultured in the bottom well as indicated in the materials and methods. HBMECs were inoculated (MOI=0.1) and 72h post inoculation, fluorescently-labeled THP1 cells were added to the luminal compartment. 6 hours post incubation, 2% Triton-X was added to the abluminal chamber, collected, and the absorbance read. All readings were then normalized to the total fluorescence

present in the mock wells. Data presented are an average (\pm standard error) of at least 3 independent experiments.

Together, these data suggest that initially, monocytes may attach to WNV-MAD78-infected endothelium more efficiently than WNV-NY-infected endothelium. Yet as infection progresses through the BBB into astrocytes, infection of astrocytes may influence monocyte extravasation and cause an increase in homing monocytes for WNV-NY-infection compared to WNV-MAD78 infection.

Discussion

While necessary for viral clearance within the CNS, infiltrating immune cells at the BBB also contribute to the severe pathologies observed during WNV infection. Several proinflammatory cytokines and chemokines have been detected within brains of WNV-infected mice (15, 131, 152, 246, 253, 280), yet little is known about how distinct cell types other than neurons within the CNS contribute to the kinetics of WNV neuroinflammation. Because endothelial cells and astrocytes comprise the interface between the circulatory system and the CNS, and likely constitute one of the sites of WNV neuroinvasion (117, 284, 285), understanding how these cell types respond to WNV infection may provide insight into the regulation of the initial neuroinflammatory response. In this study, we demonstrate the effects of proinflammatory cytokines on viral replication in endothelial cells and assess the roles different cell types at the BBB may play in attachment and extravasation of leukocytes across the BBB during WNV infection. Additionally, we describe the innate intracellular antiviral response to

both pathogenic and nonpathogenic strains at the BBB, and observed that both strains are equivalent in their capacities to initiate the antiviral response in HBMECs and HBCAs. We also examined the expression profiles of CCL2 and CCL5 in brain microvascular endothelial cells and astrocytes to describe the role of the BBB in WNV-mediated neuroinflammation. Although WNV-NY and WNV-MAD78 induced similar upregulation of CCL5 mRNA in HBMECs, WNV-MAD78-infected HBMECs secreted higher levels of CCL5 compared to WNV-NY-infected HBMECs. In contrast, higher levels of secreted CCL5 were detected in WNV-NY-infected HBCAs compared to WNV-MAD78-infected HBCAs. Moreover, HBCAs produced substantially higher levels of CCL5 overall compared to HBMECs. This expression pattern for CCL5 is consistent with a previous report that detected similar levels of CCL5 mRNA in the brains of mice infected with nonneuropathogenic and neuropathogenic strains of WNV at an early time post-infection; however, significantly higher levels of CCL5 mRNA were detected in mice infected with the neuropathogenic strain at a later time point (246). In contrast to CCL5 expression, WNV infection did not upregulate CCL2 expression in either brain microvascular endothelial cells or astrocytes, suggesting that the increased levels of CCL2 in the brains of WNV infected mice is due to upregulation of expression in other cell types within the CNS, such as neurons, and/or infiltrating leukocytes themselves.

While soluble chemokine gradients control the recruitment of leukocytes into the parenchyma of the CNS, immobilized chemokine fields mediate the initial migration of immune cells across the BBB (40, 183). Therefore, we also

assessed CCL2 and CCL5 expression patterns within WNV-infected HBMEC monolayers in both the presence and absence of HBCAs. WNV-MAD78 infection of HBMEC monolayers alone expressed higher levels of CCL5 compared to WNV-NY infection, suggesting that brain endothelial cells infected with WNV-MAD78 may be more efficient at attracting circulating immune cells to the BBB after initial infection. However, inclusion of HBCAs within the culture system substantially altered the chemokine expression profile within HBMECs. As endothelial cells are highly efficient at binding and internalizing chemokines produced by extravascular cells (68), secreted CCL5 produced by WNV-NY-infected astrocytes likely contributed to the enhanced chemokine gradient induced in the co-culture model system. Since chemokine gradient establishment leads to binding and traversal of leukocytes, the progression of WNV infection from endothelial cells into astrocytes may influence the kinetics and amplitude leukocytes infiltration into the CNS. Thus, to assess functionality of chemokine expression in both the HBMEC monolayer and coculture models, we examined attachment and extravasation of monocytes during WNV infection. While WNV-MAD78 infected HBMECs promoted increased adhesion of monocytes to the HBMEC monolayer, when HBCAs were added to the model system, extravasation was more pronounced in WNV-NY-infected monolayers compared to WNV-MAD78-infected monolayers. Taken together, these data suggest that WNV-induced neuroinflammation within the BBB is modulated as infection progresses throughout the CNS.

In addition to establishing gradients to attract circulating leukocytes, chemokines have been shown to disrupt the cell-to-cell junctions necessary for the maintenance of the BBB (219). Thus, chemokine secretion during WNV infection could contribute to the disruption of the BBB, resulting in the unregulated infiltration of leukocytes into the CNS. However, our data suggests that WNV replication in an *in vitro* model of the BBB does not affect the integrity of the endothelial monolayer. Thus, the initial infiltration of leukocytes into the CNS is likely due to active recruitment of immune cells by chemokines immobilized on the endothelial surface rather than passive migration due to loss of integrity of the BBB. Furthermore, the maintenance of the integrity of the endothelial cell monolayer suggests that leukocytes utilize transcellular traversal as opposed to paracellular traversal during the initial diapedesis of leukocytes across the WNV-infected endothelial monolayer. However, other factors, such as the secretion of matrix metalloproteases (MMPs) by astrocytes (284) and/or infiltrating leukocytes or direct damage caused by infiltrating leukocytes, likely contribute to disruption of the BBB that is observed at later times post-infection (57, 222, 292). However, it is not likely that infected leukocytes precede replication in endothelial cells at the BBB, since WNV replicates to lower levels in leukocytes than in endothelial cells. Infected leukocytes may exacerbate neuropathogenesis as they are actively recruited to the CNS from the periphery. Thus, the breakdown of the BBB at this later stage of infection may serve to facilitate a second round of viral entry into the brain by allowing the unrestricted

entry of free virus from the blood stream and/or the recruitment of infected leukocytes to the CNS.

Our data suggests that pathogenic and nonpathogenic strains of WNV differentially induce chemokine expression and gradient profiles at the BBB, which may result in altered kinetics of leukocyte infiltration. During the initial infection of the brain endothelial cells, the enhanced chemokine gradient produced in response to WNV-MAD78 may stimulate the rapid recruitment of circulating leukocytes to the BBB, thereby restricting viral replication within the brain endothelium. Additionally, reduced replication (117) and a blunted inflammatory response to WNV-MAD78 in astrocytes would result in limited leukocyte infiltration later during infection, thereby minimizing the potential for leukocyte-mediated neuropathology. In contrast, pathogenic strains of WNV, such as WNV-NY, may delay the active recruitment of leukocytes to infected endothelium until WNV-NY has replicated to high levels within astrocytes, providing a window of opportunity for pathogenic strains to spread to highly susceptible neurons prior to the en masse infiltration of leukocytes. Together, these data suggest that the establishment of chemokine gradients at the BBB in response to WNV infection is a complex process that evolves as the infection progresses through the various layers of the CNS and is differentially regulated by strains that vary in their capacity to cause neuropathogenicity. Therefore, a greater understanding of how various chemokines are involved in this process may aid in developing therapies to limit WNV-mediated neuroinflammation and thus pathogenesis.

Acknowledgements

We thank Amy Beaven (Imaging facility at the University of Maryland) for assistance with the acquisition and analysis of the confocal microscopy data.

Chapter 6- Antiviral responses and detection of virus in mice inoculated with a nonneuropathogenic strain of WNV compared to a neuropathogenic strain of WNV

Abstract

West Nile virus (WNV) neuropathogenesis results from neuronal death by both viral replication in neurons and bystander effects of the immune response during infection. The degree of WNV neuropathogenesis is highly strain dependent. Although the level of viremia may influence neuropathogenesis, additional obstacles for nonneuropathogenic strains may be present at the blood-brain barrier (BBB). Therefore, we monitored the kinetics of virus infection and the host antiviral response in a mouse model of WNV infection that simulated viremia using a neuropathogenic (WNV-NY) and a nonneuropathogenic (WNV-MAD78) strain of WNV. Mice intravenously inoculated with WNV-MAD78 exhibited increased survival compared to mice inoculated with WNV-NY, suggesting that high levels of virus alone does not dictate neuropathogenesis. WNV-NY was readily detected in the spleen and brain as early as 48 hours post inoculation, reaching peak levels at 120 hours post inoculation. In contrast, WNV-MAD78 was only detected in the spleen and only at 8 and 24 hours post inoculation. Despite being unable to detect virus consistently, chemokines were upregulated in the brains of mice infected with either strain of WNV at 120 hours post infection. However, greater chemokine upregulation was observed in mice inoculated with WNV-NY compared to WNV-MAD78. Together, these data

suggest that an additional barrier exists for nonneuropathogenic strains of WNV at the BBB, and that chemokine responses occur after WNV initiates infection in the CNS.

Introduction

Since its introduction into the Western hemisphere in 1999, the flavivirus, West Nile virus (WNV), has become the most common cause of arthropod-borne severe neurological disease {webpage, #7067}. Historically, WNV has been associated with a mild febrile illness, though extremely rare cases noted severe neurological disease. With the emergence of newer strains of WNV in the Western hemisphere in the late 1990s, severe neurological disease has become widespread. Symptoms of WNV-induced neurological disease include acute flaccid paralysis, encephalitis, and meningitis, with some patients never fully recovering from these symptoms. The mechanisms underlying this increase in neuropathogenesis caused by certain strains are unclear. In vitro identification of factors contributing to differential replication in model systems must be validated in vivo to apply to disease models.

Disease pathology in the CNS during WNV infection is a result of neuronal death. Nevertheless, prior replication of WNV in other cell types comprising the CNS, especially at the BBB, is necessary prior to exposure of neurons to virus in the natural course of infection. WNV replication in the mouse model occurs at several sites, including the skin, blood, spleen, kidney, lymph nodes, heart, and lungs, with the highest levels identified in the CNS (63-65) .

While several studies with neuropathogenic WNV have been performed in mice, replication kinetics of infections with nonneuropathogenic strains of WNV is not as well documented.

In addition to virus replication-induced neuronal death, the inflammatory response to infection in the CNS contributes to WNV neuropathogenesis. Thus, many chemokines, chemokine receptors, and cytokines play a role in WNV neuropathogenesis, including TNF α , IL-22, IL-23, type-1 IFN, CCR2, CCR5, CXCL10, and CXCL1/2 (15, 93, 127, 152, 253, 280, 291). During WNV infection, the innate immune response induces production of type-1 IFN and proinflammatory cytokines in both the serum and several organs, including the CNS (227). Therefore, the blood-brain barrier (BBB) may be exposed to proinflammatory cytokines prior to the virus. While other pathogens have been shown to induce cytokine secretion, which disrupts the BBB via antiviral responses from infected peripheral cells, this does not appear to be the case for WNV. However, secretion of cytokines in response to WNV replication functions to attract leukocytes to the site of infection for viral clearance (280). The process of leukocyte attraction and viral clearance is a multi-step event, and it is unclear how different immune factors contribute to a balanced immune response within the CNS. Likewise, the kinetics of the innate immune response during WNV infection in vivo and which cell types are involved is unclear.

A prominent hypothesis in the field is that nonneuropathogenic strains of WNV do not reach high enough levels of viremia to initiate replication in distal organs. In this model, nonpathogenic strains are restricted to the initial site of

infection and therefore are unable to access the CNS and cause neuropathogenesis. To test this hypothesis, we designed in vivo experiments in which the initial peripheral infection of WNV was bypassed by introducing equivalent levels of a neuropathogenic strain, WNV-NY, or a nonneuropathogenic strain, WNV-MAD78, directly into the blood stream. In our mouse model, survival was higher in WNV-MAD78-inoculated mice compared to WNV-NY inoculated mice, suggesting an additional barrier for nonneuropathogenic strains of WNV exists beyond viremia. High levels of WNV-NY and increased CCL2 expression were detected in the brains of mice 5 days after inoculation. In contrast, CCL2 expression in the brain was only modestly increased in mice 5 days after WNV-MAD78 inoculation. Together, our data suggests that WNV-MAD78 is restricted in its ability to replicate in the CNS and induce a robust chemokine response, which limits its capacity to induce neuropathogenesis in a viremic mouse model.

Results

WNV-NY causes greater lethality than WNV-MAD78 in intravenously-inoculated mice.

Most, if not all, strains of WNV are neurovirulent in mice when inoculated via an intracranial route. However, many strains rarely cause neuropathogenesis following peripheral inoculation, possibly due to an inability of these strains to reach high levels in the blood (23). To determine if the level of viremia is the only

determining factor in WNV-induced neuropathology, mice were inoculated via the tail vein with either WNV-NY or WNV-MAD78 at levels representative of viremia in a mammalian model (10^4 PFU) (**Figure 38**). Fewer mice survived when inoculated with WNV-NY than with WNV-MAD78, suggesting additional factors restrict WNV-MAD78 neuropathogenesis in the animal model. Considering that WNV-MAD78 survival is decreased when directly inoculated into the CNS compared to inoculation into the bloodstream, these factors likely represent a barrier of entry into the CNS.

Detection of WNV in intravenously-inoculated mice

Because WNV neuropathogenesis is a result of neuronal death, we determined presence of replicating virus within the CNS in the viremic mouse model (**Table 4, Figure 39**). Viral RNA was detected in the brains of WNV-NY-infected mice as early as 48 hours post infection, with maximum viral replication detected in the brain at 120 hours post inoculation (**Figure 39**). In contrast, viral RNA was not detected in the brains of WNV-MAD78-infected mice. We also examined replication in the blood and spleen, since some models suggest that viral replication in leukocytes initiates CNS infection. We detected viral RNA in the spleens at early times post infection for both WNV-NY- and WNV-MAD78-infected mice. Infectious WNV-MAD78 was not detected in the blood via plaque assay, but WNV-NY was present at 24, 48, and 72 hours post infection. Taken

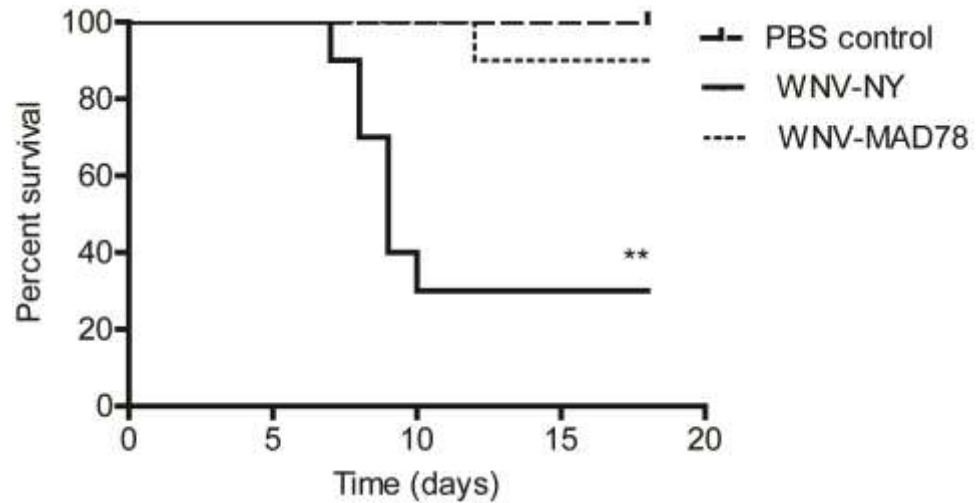


Figure 38. Survival analysis of mice infected with WNV-NY and WNV-MAD78. Four week old Swiss Webster mice were intravenously infected with 10^4 pfu of either WNV-NY (n=10) or WNV-MAD78 (n=10) via the tail vein, or sham inoculated with PBS (n=7). Survival was assessed twice daily as described in materials and methods.

Viral strain	Location	8 hpi	24 hpi	48 hpi	96 hpi	120 hpi
WNV-NY	Serum*	0/3	6/6 [†]	6/6 [†]	0/3	0/6
	Spleen ^{‡Δ}	0/3 ^{Δ‡}	0/3 ^{Δ‡}	3/3 ^{†*}	3/3 ^{†*}	3/3 ^{†*Δ}
	Brain ^{**‡Δ}	0/3 [‡]	0/6 ^{Δ‡}	2/6 ^{††‡Δ‡}	1/3 ^{†‡}	3/3 ^{†*Δ}
WNV-	Serum*	0/2	0/5	0/5	0/2	0/2
MAD78						
	Spleen ^{*‡Δ}	2/2 ^{††Δ‡}	2/2 ^{††‡}	0/2 ^{Δ‡}	1/2 ^{††Δ}	0/2 ^{Δ‡}
	Brain ^{**‡Δ}	0/2 ^{Δ‡}	0/5 ^{Δ‡}	0/5 ^{Δ‡}	0/2 [‡]	0/2 ^{Δ‡}

Table 4. Virus location in mice infected via tail vein injection.

†Value determined using plaque assay

††Value determined using nested PCR

†††Value determined using integrated PCR using RT-PCR and plaque assay

*Samples were assayed using plaque assays

‡ Samples were assayed using nested PCR

Δ Samples assayed using integrated RT-PCR and plaque assays

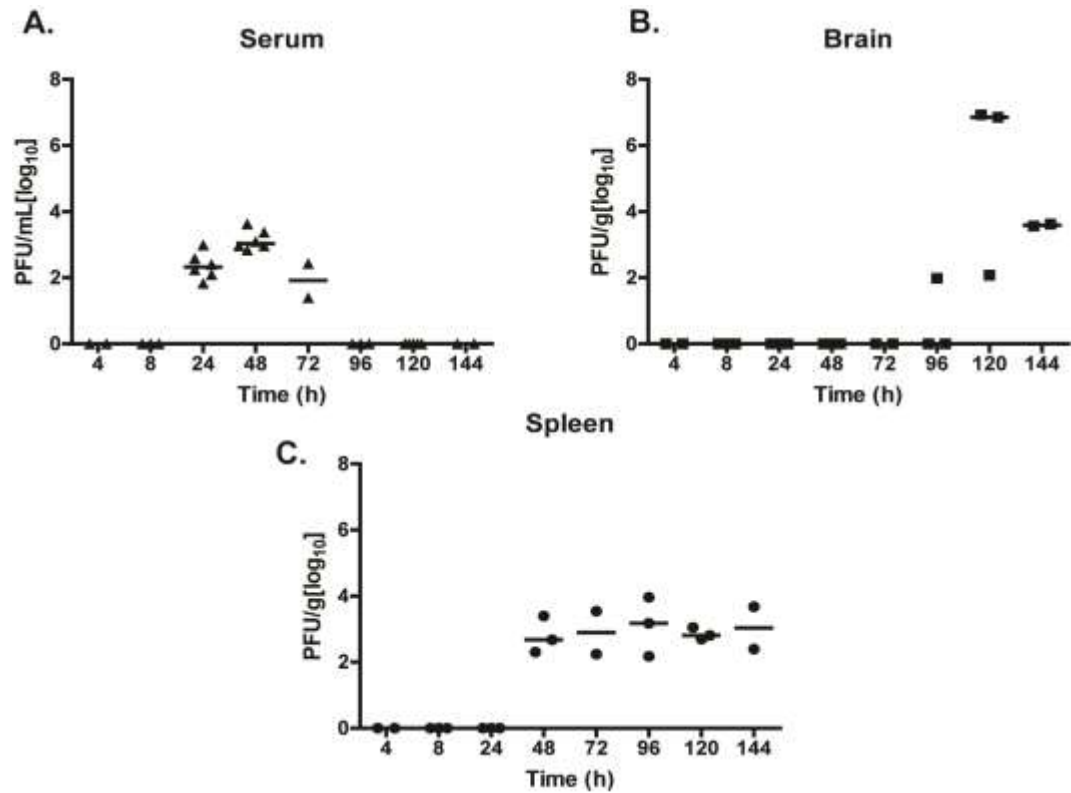


Figure 39. Detection of infectious WNV-NY in intravenously-inoculated mice. Mice inoculated with WNV-NY were sacrificed at the indicated times and serum, spleen, and brain were collected as described in materials and methods. Homogenates of tissues were then subject to plaque assay. Data represented is the median titer of the total number of animals assayed (ranging from n=2 to n=6 per timepoint).

together, our findings suggest that WNV-NY propagates more frequently in the blood and brain than WNV-MAD78. Thus, WNV-MAD78 may be cleared more efficiently from the blood and less likely to enter the brain than WNV-NY during intravenous inoculation.

In addition to viral replication, differential immune responses to WNV infection may contribute to the strain-specific pathologies observed during WNV infection. Because we did not detect WNV-MAD78 in the blood via plaque assay, we hypothesized that this virus may not induce the adaptive immune response due to insufficient levels of stimulating pathogen. However, when we measured the levels of neutralizing antibodies present in the serum at day 4 post-inoculation, similar levels of neutralizing antibodies were present in serum of WNV-MAD78- and WNV-NY-infected mice (**Figure 40**). Thus, both strains stimulated an initial antibody response early after infection, despite different levels of WNV present in the blood. Thus, detection of viral replication methods may not be sensitive enough to explain observed neuropathologies, since virus must be present for a response to occur.

Cytokine and chemokine levels in blood and brains of WNV-inoculated mice

To determine if differential cytokine production in the blood prior to infection in the CNS in response to different WNV strains, we measured the

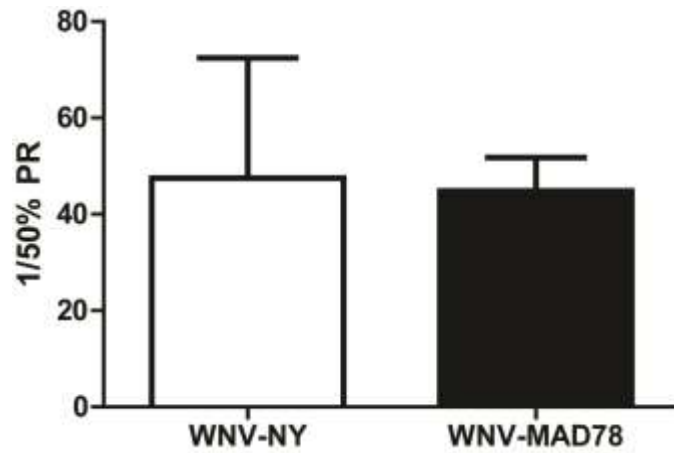


Figure 40. Plaque reduction Neutralization test. Serum from WNV-infected mice at 96h post inoculation was mixed with WNV and titrated on Vero cells. Plaque reduction was considered when >50% of plaques were reduced compared to control wells.

levels of several proinflammatory cytokines in the serum of mice infected with WNV-NY or WNV-MAD78 (**Figure 41 A**) early during infection. Neither strain significantly induced IL-6 or TNF α , at 8, 24 or 48 hours after infection (data not shown). However, similar levels of IL-12 were detected in the serum of WNV-NY- and WNV-MAD78-inoculated mice at 8, 24, and 48 hours post infection. Thus, proinflammatory cytokine levels were not differentially expressed in the blood of WNV-NY and WNV-MAD78 infected mice. Therefore, the proinflammatory responses in the blood did not correspond to the differential neuropathology of these strains.

In addition to proinflammatory cytokines in the serum, we also examined expression of chemokines CXCL2, CCL2, and CCL5 in the brain and spleen (**Figure 41 B**). While there was moderately higher chemokine expression in the spleens of WNV-MAD78-infected mice compared to WNV-NY-infected mice, the increases were very slight and not reach significance (data not shown). Likewise, chemokine expression was not induced in the brain at 48 h post infection. In contrast, all three chemokines were upregulated in WNV-infected brains at 120 hpi. Similar levels of CCL5 were detected in the brains of WNV-MAD78 and WNV-NY infected mice. However, CCL2 levels were increased in WNV-NY-infected mice compared to WNV-MAD78-infected mice. Thus, upregulation of chemokines in the CNS was detected only at late times during infection.

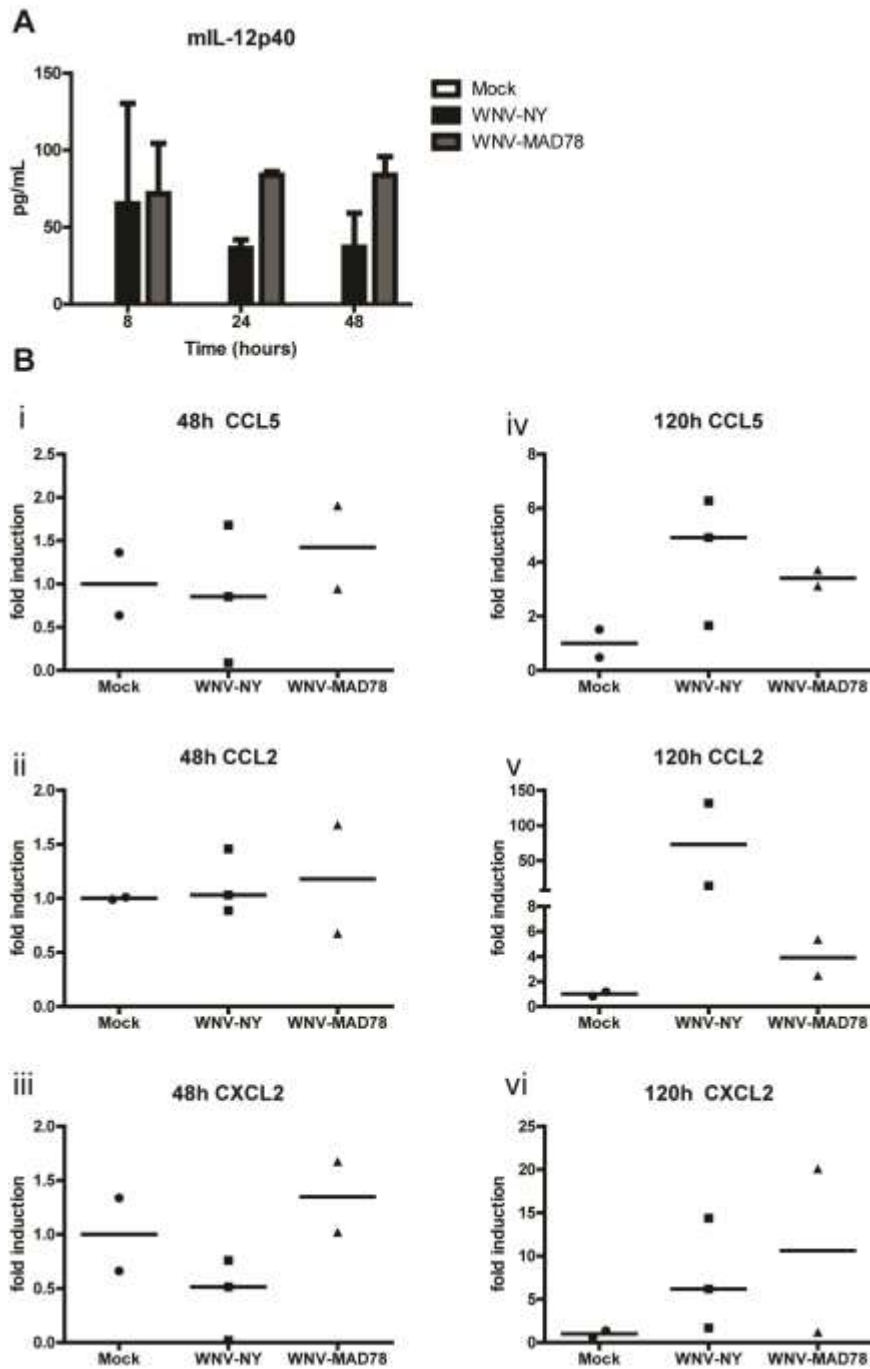


Figure 40- Cytokine and chemokine responses in the blood and brain of WNV-infected mice. (A) Serum from inoculated mice was collected and subjected to ELISA as described in materials and methods. Values presented are

an average (+/- standard error) of at least 2 independent experiments. (B) Brain homogenates were collected at the time indicated and viral RNA was collected and subjected to real time qRT-PCR with primers specific to (i, iv) CCL5, (ii, v) CCL2, or (iii, vi) CXCL2 as described in materials and methods. Data presented is relative to GAPDH expression of the same samples normalized to mock-infected mice. Values represent the median of at least 2 animals.

Discussion

Nonneuropathogenic strains of WNV are restricted when mice are inoculated in the periphery, but if virus is directly inoculated into the CNS, neuropathological symptoms are observed. One current hypothesis addressing the differential capabilities of strains of WNV to induce neuropathology suggests that nonneuropathogenic strains of WNV are restricted in the periphery and do not reach high enough levels in the blood to enter the CNS. Therefore, we hypothesized that neuropathogenesis may occur regardless of strain inoculated if equivalent, high levels of virus were introduced intravenously. Thus, we introduced viremic levels of either a neuropathogenic strain (WNV-NY) or a nonneuropathogenic strain (WNV-MAD78) directly into the blood of mice. Still, mice inoculated with WNV-NY exhibited lower survival than mice inoculated with WNV-MAD78. Thus, there is another factor that contributes to WNV neuropathogenesis in addition to achieving a high level of viremia during infection.

To describe the restriction for neuropathogenesis of WNV-MAD78 *in vivo*, we assessed presence of virus and cytokine expression in several sites permissive to WNV infection. In mice inoculated intravenously, WNV-MAD78 was only detected in the spleen at early times post inoculation. However, at 5 days post inoculation, increased levels of CCL2 and CCL5 were observed in the brains of mice inoculated with WNV-MAD78. In mice inoculated intravenously with WNV-NY, virus was detected in all locations examined, including the CNS at low levels as early as day 2 after infection, and consistently at day 5 post

inoculation. Despite upregulation of CCL2 and CCL5 in brains of mice inoculated with either WNV-NY and WNV-MAD78 at five days post inoculation, no significant increase in chemokines was detected for either virus in the spleens. A slight increase in IL-12 was observed in the blood of mice inoculated with either WNV-NY and WNV-MAD78. The lack of other proinflammatory cytokines and the similar levels of cytokines expressed for both strains suggests that proinflammatory cytokine expression in the blood may not account for the differential capability to induce neuropathology. Together, these data suggest that viral replication precedes high levels of expression of proinflammatory chemokines in the brain, indicating that WNV may enter the brain before initiation of the proinflammatory response. The specific chemokines examined, CXCL2, CCL2, and CCL5, are expressed in early stages during WNV infection in the CNS, and are necessary for the initial infiltration of leukocytes into infected tissues (7, 15, 88, 92, 152, 246). Therefore, determining which tissues initially express these chemokines demonstrates the cell types responsible for supporting early viral replication and the activation of the antiviral response to WNV infection.

Mice inoculated intravenously with WNV-MAD78 expressed increased levels of chemokines in the CNS despite being unable to detect infectious virus. Although less robust than the response in mice inoculated with WNV-NY, the chemokine response in the brain of mice inoculated with WNV-MAD78 suggests that virus may enter into the CNS and initiate infection. Likewise, a detectable response in the blood with the PRNT (**Figure 39**) suggests that active infection,

albeit to low levels, may be present in mice inoculated with WNV-MAD78. We consistently observed ~90% survival in mice inoculated intravenously with WNV-MAD78. Other studies performed with WNV-MAD78 inoculation in the periphery consistently observe 100% survival, regardless of mouse strain or dose of virus used (127, 253, 269). Thus, our assays may not be sensitive enough to detect the low levels of viral replication occurring in mice inoculated with WNV-MAD78. Alternatively, the kinetics of replication of WNV-MAD78 may be delayed compared to that of WNV-NY in the sites of replication examined. Therefore, virus for WNV-MAD78-infected mice may not be detectable until later times during infection, which were not assessed in the experiments performed.

Our observations in chemokine expression for WNV-MAD78, a nonpathogenic, lineage 2 strain, are similar to observations for a moderately pathogenic lineage 1 strain (246). Thus most, if not all, strains of WNV may initiate replication in the CNS, but replication for nonneuropathogenic strains may be limited within the CNS. Further, we detected an upregulation of chemokine expression for nonneuropathogenic strains in the CNS; however, the response may be more tightly regulated than chemokines expressed in mice inoculated with neuropathogenic WNV. WNV-MAD78 restriction in inducing neuropathologies may therefore be attributed to the limitation of viral replication and spread through successfully controlled infiltration of inflammatory leukocytes. In addition to the restriction for cell-to-cell spread within cell types of the CNS (117), a controlled inflammatory process may promote a successfully regulated immune response for mice inoculated with WNV-MAD78. In contrast, mice

inoculated with WNV-NY experience a more robust, less regulated response due to higher levels of viral replication (117) and chemokine expression (Chapter 5) within cell types of the CNS compared to nonneuropathogenic strains. The capacity for strains of Semliki Forest virus to induce neuropathology also lies beyond the BBB. Neuroinvasion occurs in all SFV infections through the hematogenous route, and nonpathogenic strains are further limited within the CNS itself (77, 260), illustrating that restriction in the CNS of viral infection and spread is a likely cause of restriction for nonpathogenic viral infections in the CNS.

Because neither WNV-NY nor WNV-MAD78 induced a proinflammatory cytokine response in the blood prior to virus detection in the brain, it is unlikely that the disruption of the BBB by proinflammatory cytokines is responsible for the incursion of WNV into the CNS. Others (267) and we can detect pathogenic WNV in the CNS as early as 48h after inoculation in the periphery. The ability to detect neuropathogenic WNV at 48h in the CNS is consistent with the kinetics of viral replication in a coculture model of the BBB (117). Thus, it is likely that WNV traversal of the BBB via replication in endothelial cells is nondiscriminant, and neuropathogenicity is not determined simply by access to the CNS. Further replication in astrocytes and neurons, and the immune responses responsible for limiting infection and initiating the innate immune response in these cell types, may then contribute to neuropathogenicity. Herein, we observed that, although rare, mice inoculated via the tail vein with WNV-MAD78 exhibited symptoms of neuropathogenesis, supporting data suggesting that many or all strains of WNV

may initially invade the CNS. However, nonneuropathogenic strains of WNV are restricted in their replication in cell types of the CNS. Once accessing astrocytes and neurons, increased replication of neuropathogenic strains of WNV in either of these cell types may induce a more robust proinflammatory response, leading to increased neuropathology. Additional *in vivo* studies with detailed analyses identifying individual cell types that are infected are necessary to assess if this is the mechanism of incursion. In addition, more extensive experiments are necessary for distinguishing between the kinetics of neuropathogenic and nonneuropathogenic strains within the CNS. Together, these data support a model where WNV-MAD78 may initiate replication in the CNS. After replicating to low levels, an immune response may then be initiated in the CNS that is tightly regulated and may restrict viral replication and spread prior to massive neuronal cell death and uncontrolled infiltration of immune cells. Further characterization of this model system may provide insight into how controlled immune responses to viral infection develop within the CNS, and how to manipulate immune responses to decrease neurological symptoms for neuropathogenic viral infection.

Discussion of Dissertation research

Neurotropic viruses are responsible for encephalitis, neurological disorders, and chronic illnesses worldwide (27, 277). Traditionally, neuroscience has focused on examination of pathogen triggered actions and reactions within neurons. Yet recent studies indicate that non-neuronal cell types in the CNS, including trafficking immune cells, glia, and endothelial cells, play an essential role in the physiological and immunological responses to viral infection within the CNS (254). As a virus with the potential to cause neuropathogenesis, West Nile virus (WNV) continues to be a public health threat. Naturally occurring strains of WNV vary greatly in their capability to cause neuropathogenesis. Thus, comparing replication of these strains within the CNS provides an excellent model for determining factors, both host and viral, that contribute to neuropathogenesis cause by viral infection. In addition, several labs have established mouse models for WNV infection, allowing for observations made in cell culture models to be examined in vivo.

Here, we analyzed WNV replication and the innate antiviral immune responses to infection in several cell types representing the various components of the CNS. Initially, we observed that a nonneuropathogenic strain of WNV, WNV-MAD78, was delayed at initiating replication and restricted in cell-to-cell spread in astrocytes compared to a neuropathogenic strain, WNV-NY, identifying astrocytes as a possible site of regulation for viral infection in the CNS (Chapter 3). Further, this restriction was independent of type-1 IFN. However, inhibition of enzymes that play a role in viral particle maturation led to

increased particle production for nonneuropathogenic WNV in astrocytes. In addition, replication of a recombinant virus with the structural components from nonneuropathogenic WNV was restricted to similar levels as nonneuropathogenic WNV in astrocytes (Chapter 4). Thus, we suggest that all strains of WNV may replicate well in the endothelium and enter into the CNS, but are limited in astrocytes by the strain-specific differences in the structural proteins that comprise the virion.

Replication of other viruses in endothelial cells, including high and low pathogenic Semliki Forest virus displayed similar results (77, 260), suggesting that traversal from the blood into the CNS may not always correlate with neuropathogenesis. Indeed, mice inoculated intracranially with WNV-MAD78 experience delayed and reduced mortality compared to mice inoculated with WNV-NY (253), suggesting that a component within the CNS restricts WNV-MAD78-induced neuropathology. Our data demonstrates that this restriction is not at the level of replication within neurons. Therefore, we examined additional cells types within the CNS. Since WNV may enter into the CNS via the hematogenous route, cell types of the BBB were plausible candidates for limiting nonneuropathogenic WNV infection. Thus, we examined replication of WNV-NY and WNV-MAD78 in endothelial cells and astrocytes, which are cell types that comprise the BBB. Both strains replicated to equivalent levels in endothelial cells, and initially infected astrocytes at equivalent levels. However, in astrocytes, WNV-MAD78 was restricted in both initiating viral replication as well as cell-to-cell spread compared to WNV-NY. These data suggest that astrocytes may be a

unique physiological site of restriction for WNV infection. Since astrocytes reside within the CNS, all strains of WNV may be neuroinvasive, and a restriction for neuropathogenesis may reside within the CNS.

The restriction for WNV-MAD78 replication and cell-to-cell spread in astrocytes was independent of type-1 IFN. Moreover, type-1 IFN levels were significantly higher in WNV-NY-infected astrocytes compared to WNV-MAD78-infected astrocytes. While secretion of type-I IFN did restrict WNV-NY replication in astrocytes to some degree, it is well documented that neurons are highly responsive to type-1 IFN (289) and prolonged exposure to type-1 IFN induces apoptosis (61). Therefore, in the context of the CNS, secretion of type-I IFN by astrocytes may be neurotoxic and contribute to neuropathogenesis. This hypothesis is consistent with the observation that bystander neuronal cell death occurs in mice infected with a highly pathogenic strain of WNV (32) and in vitro studies demonstrating that WNV-infected astrocytes secrete neurotoxic factors (282). Further in vitro and in vivo analyses are necessary to determine what cells within the CNS secrete type-1 IFN in response to WNV infection, and the role of secreted IFN in bystander cell death during WNV infection within the CNS.

Our data suggests that viral and host factors other than IFN were responsible for restricting WNV-MAD78 cell-to-cell spread in astrocytes. Other viruses that replicate in astrocytes are limited by several factors, including astrocyte activation and reactive nitrogen species (RNS) (209). Likewise, a recent study demonstrated that exosomes may transport antiviral effector proteins to neighboring cells (281). However, we demonstrated that WNV-

MAD78-infected astrocytes did not secrete an inhibitory factor. In addition, cell-to-cell spread was not the result of increased activation of astrocytes as assessed by GFAP expression (data not shown), a classical indicator of neurological distress and ischemia (72). Since classical antiviral pathways did not appear to be responsible for the restriction in cell-to-cell spread, we compared the quantity and quality of particles produced by WNV-NY-infected and WNV-MAD78-infected astrocytes. Both the particle:PFU ratio in astrocytes as well as the ratio of infectivity on Vero cells compared to astrocytes were significantly higher for WNV-MAD78 compared to WNV-NY, suggesting that WNV-MAD78 produces higher levels of defective particles in astrocytes compared to WNV-NY.

Others have shown that partially mature particles are still infectious, but at a lower degree compared to more highly processed particles (53). Therefore, we explored the roles of cellular enzymes that contribute to the maturation process of WNV particles. Maturation of WNV particles involves the host protease furin (262). However, furin activity in astrocytes was higher compared to more permissive cell types, such as endothelial cells (Chapter 4). Furthermore, WNV-MAD78-infected astrocytes produced increased levels of infectious particles in astrocytes in the presence of furin inhibitor. Therefore, the infectivity of WNV-MAD78 particles produced in astrocytes inversely correlated with furin activity, suggesting that complete maturation is detrimental for WNV-MAD78 in astrocytes.

To address the viral-specific factors that contribute to cell-to-cell spread in astrocytes, we examined the replication kinetics of chimeric viruses that

exchanged the structural and nonstructural proteins of WNV-NY and WNV-MAD78 in astrocytes. Consistent with our infectivity data, the structural components of WNV-MAD78 limited infectious viral particle production, even when the chimeric virus encoded the nonstructural proteins of WNV-NY. Similarly, chimeric virus consisting of WNV-NY structural proteins replicated to equivalent levels as WNV-NY even with all of the nonstructural proteins from WNV-MAD78. Viral replication for both chimeric viruses was delayed compared to WNV-NY; however, peak viral titers of chimeric viruses closely followed that of the parental strain of the structural proteins they contained. Therefore, we hypothesize that strain-specific variation in the structural proteins that comprise the viral particle is a factor in the restriction in cell-to-cell spread for nonneuropathogenic strains of WNV in astrocytes. Thus, examination of moieties within structural proteins known to contribute to neuropathogenicity was carried out. The glycosylation motif at residues 154-156 of the envelope protein is essential for WNV neuropathogenesis (13, 24, 237). In addition, sugar moieties of several viruses, such as HIV, are essential for attachment and entry into cells (30). However, disruption of the glycosylation site for WNV-NY or addition of the glycosylation site for WNV-MAD78 did not alter the replication kinetics of these chimeric viruses in astrocytes. Further studies performed in astrocytes with the WNV-MAD78 structural: WNV-NY nonstructural chimeric virus will determine whether the lower level of viral replication is due to a restriction in cell-to-cell spread or by another mechanism. Additional chimeric viruses exchanging the structural proteins individually will be used to determine which proteins and

residues play a role in restricting infectious particle production for WNV-MAD78 in astrocytes. These constructs provide novel tools for studying WNV replication at the BBB.

In addition to the viral factors that contribute to cell-to-cell spread, a cellular factor within astrocytes contributes to the delay in infectious particle production for WNV-MAD78-infected astrocytes. We observed a delay in the production of negative strand genomic RNA, suggesting that there may be a delay in the switch from translation of the incoming virus to initiation of negative strand synthesis. The cellular and viral factors involved in regulating this transition remain to be determined.

In order to initiate and maintain constant translation or replication, WNV genomes must circularize. Circularization of the WNV genome involves the interaction between two regions within the 5' and 3' portions of the genome (319). One of these cyclization sites resides within the coding region of the capsid protein, and is necessary for efficient initiation of viral replication (319). Stem-loop structures in the 3'UTR of WNV bind to TIA-1 and TIAR, aiding in circularization for genomic replication (70, 71, 149, 244). Presence of these factors within astrocytes has yet to be examined, and additional astrocyte-specific factors may play a role in binding to the 3'UTR and promoting negative strand synthesis. Since the 3'UTRs of WNV-NY and WNV-MAD78 are significantly different in sequence and possibly structure, binding affinities of these regions to the viral replication complex (VRC) and host factors associated with it may be altered within astrocytes. A chimeric virus consisting of the 5' and

3'UTRs from WNV-NY and the ORF of WNV-MAD78 replicated at a similar rate and to similar levels as WNV-MAD78 in astrocytes (data not shown). However, other proteins in the VRC, including the nonstructural proteins, may bridge the viral UTRs with host transcription factors, and may play a role in initiating viral replication. In addition to cellular proteins, several enzymatic cofactors, such as cations, are necessary for efficient viral propagation and intracellular levels of these cations may vary in different cell types (235). Assessing viral components that contribute to initiating replication and identifying cell-type specific host components that promote assembly of the VRC and the switch from translation to replication is a necessary approach to determine the mechanistic basis for the delay in WNV-MAD78 replication in astrocytes.

In addition to viral replication, neuronal death may occur during WNV infection from the activity of infiltrating immune cells from the periphery. It is well documented that WNV-infected neurons secrete CXCL10 to attract CD8⁺ T cells to the CNS (131). However, little is known about how other cell types within the CNS contribute to neuroinflammation during WNV infection. To determine the contribution of the BBB to neuroinflammation during WNV infection, innate immune responses during WNV infection in cell types of the BBB were assessed. Surprisingly, the antiviral response to WNV in HBMECs and HBMVEs was not sufficient to inhibit viral replication, since peak viral titers remained high throughout infection in both cell types. In both WNV-NY- and WNV-MAD78-infected HBMECs, CCL5 mRNA was elevated at equivalent levels compared to mock-infected cells. However, WNV-MAD78-infected HBMECs expressed higher

levels of intracellular CCL5 and secreted higher levels of CCL5 compared to WNV-NY-infected cultures. This suggests that regulation of CCL5 protein expression may occur post-transcriptionally during WNV infection, possibly by microRNA pathways. Regulation is also possible via protein stability and degradation of CCL5. Since we observed higher levels of CCL5 in WNV-MAD78-infected HBMECs, it is possible that one of the strain-specific differences in the proteins for WNV-NY promotes degradation of antiviral molecules such as CCL5. However, extensive studies will need to be performed to explore the possible pathways regulating CCL5 expression during WNV infection in HBMECs.

Chemokine secretion and establishing chemokine gradients is an initial step in extravasation. However, expression does not confer functionality. Thus, we performed functional assays with both monolayers and transwell cocultures of endothelial cells and astrocytes during WNV infection. Indeed, increased levels of labeled monocytes adhered to WNV-MAD78-infected endothelial cells compared to WNV-NY-infected endothelial cells. Therefore, initiating cellular innate immunity before WNV can reach highly permissive neurons may prevent progression of nonneuropathogenic strains, and thus limit severe neurological disease. As viral replication progressed into astrocytes, higher levels of CCL5 and VCAM were observed in WNV-NY-infected astrocytes compared to WNV-MAD78-infected astrocytes, which correlated with the enhanced levels of WNV-NY replication within the monolayer. We hypothesize that the chemokine induction by WNV-NY-infected astrocytes may lead to increased leukocyte infiltration into the CNS during WNV-NY infection in mice compared to WNV-

MAD78. Although a regulated cellular response, both innate and adaptive, in the CNS is necessary for survival of WNV infection (63-65, 248), there is increasing evidence that it can also contribute to WNV-mediated neuropathology. For example, ICAM is a cellular adhesion molecule necessary for extravasation of leukocytes from the blood into the brain. Mice deficient in ICAM exhibit decreased morbidity and viral load in the CNS compared to wild type mice, suggesting that trafficking of leukocytes may be important for establishing a sustained infection in the CNS (57). Matrix metalloproteinases (MMPs) are expressed by activated leukocytes and contribute to the disruption of cell:cell junctions at the BBB. Mice deficient in MMP9 also exhibit decreased morbidity and viral loads in the CNS compared to wild type mice, suggesting that leukocyte trafficking and disruption of the BBB contributes to WNV-induced neuropathology (292). Finally, mice deficient in DRAK2, an apoptosis-inducing enzyme specifically expressed by activated B and T cells, exhibit decreased morbidity and viral loads in the CNS compared to wild type mice, suggesting that infected T cell trafficking into the CNS may contribute to WNV-induced neuropathology (295). Further, aberrant or overactive immune responses to infection often cause pathology, most notably filoviruses (170). Unregulated immune responses to infection may also contribute to chronic illnesses within the CNS, including multiple sclerosis (27).

Although it has been hypothesized that the cellular response is responsible for the initial neuroinvasion of WNV, (15, 291, 292, 295), replication in monocytes (Chapter 5) as well as other leukocytes and macrophages (253,

295) is not as robust as more permissive cell types, including endothelial cells (117, 285). In addition, viral replication in the CNS is detected (day2-4) prior to the presence of infiltrating leukocytes (day6-8) (212, 250). Thus, WNV neuroinvasion likely occurs prior to the initial attachment and extravasion of leukocytes into the CNS. Since endothelial cells comprise the vasculature, virus detected in the serum may be a result of infected endothelial cells in the periphery in addition to replication in hematopoetic cells. Moreover, viral persistence in the CNS and the inability to clear cytolytic T cells during the late stages of WNV infection leads to increased morbidity. In CD4^{-/-} mice, viral loads in the CNS were persistently high compared to wild type mice despite early high levels of CD8⁺ T cells. However, after acute infection, CD8⁺ T cells were not sustained in CD4^{-/-} mice, suggesting that CD4 T cells are also necessary for clearance of virus in the CNS and survival during WNV infection (257). It is also likely that modulation of the cellular innate response may result from the immune response initiated once viral replication occurs within neurons. Yet in order to replicate within neurons, WNV must traverse endothelial cells and astrocytes. Thus, limitation of nonneuropathogenic strains in astrocytes may provide an essential site for regulating WNV infection, further emphasizing the need to understand the nature of infection within these cells more completely.

In order to support our in vitro hypotheses, we examined WNV infection in a mouse model. By simulating viremia, the peripheral responses were bypassed, exposing the brain endothelium to virus without the requirement for replication in the periphery. Kinetics studies of intravenous inoculation display that inoculation

into the blood is sufficient for delivery of small molecules to the CNS within minutes (140), suggesting that virus inoculated via this route will reach the BBB directly after inoculation. Despite inoculation with high levels of virus in the blood, WNV-MAD78-infected mice exhibited increased survival compared to WNV-NY-infected mice. Although we detected virus only in the spleen for WNV-MAD78-infected mice, the methods we used were not sensitive enough to detect low levels of replication that are likely to occur with WNV-MAD78 infection. Indeed, WNV-MAD78-infected mice displayed neurological pathologies in ~10% of mice, including seizures and paralysis, albeit at delayed kinetics compared to WNV-NY. Thus, WNV-MAD78 may enter into the CNS during intravenous inoculation, but additional factors limit WNV-MAD78-induced neuropathologies. WNV-MAD78 may either be cleared quickly by an early activation of the cellular innate immune response during infection, or limited at sites within the CNS, such as astrocytes. In examining cytokine profiles in the blood, spleen, and brain of both WNV-NY and WNV-MAD78-infected mice, elevated levels were not observed in the spleen or the blood. However, CCL5 was notably higher in the brains of both WNV-NY and WNV-MAD78-infected mice at late times (day 5) post inoculation, and substantially higher levels of CCL2 were observed for WNV-NY. Although CCL2 levels were also elevated for WNV-MAD78-infected mice, WNV-NY-infected mice exhibited a greater increase than WNV-MAD78-infected mice. Virus was detected as early as 48 hours post inoculation in WNV-NY-infected mice, and others have likewise detected virus at early times post infection in other studies (267). Despite the detection of viral replication at early timepoints, increased

cytokine expression was only observed at later time points, suggesting that viral replication in the CNS occurs prior to attraction and infiltration of immune cells. In vivo analysis of viral replication in specific cell types of the CNS may describe a physiological role for astrocytes and other non-neuronal cells during WNV neuropathogenesis. Examination of replication in the CNS of mice inoculated with viral chimeras may further detail viral components necessary for WNV neuropathogenesis.

Taken together, our data contribute to the following model of WNV neuropathogenesis. Mosquitoes introduce WNV either directly into the blood, which is likely to occur in 76% of cases (266), or WNV reaches the blood after trafficking from the epidermal and dermal layers of the skin into the spleen where a second round of replication occurs. Upon entering the blood stream, WNV has access to brain endothelial cells as well as peripheral organs. Both neuropathogenic and nonneuropathogenic strains replicate to equivalent levels in the brain endothelium and progress into astrocytes, which are in direct contact with endothelial cells in vivo. During infection of endothelial cells, nonneuropathogenic strains express high levels of monocyte- chemoattractant chemokines, leading to the activation of the extravasation process. In vivo, the attachment and activation of leukocytes may initiate clearance of virus from the endothelium, further restricting nonneuropathogenic strains of WNV. As replication progresses into the CNS and into astrocytes, nonneuropathogenic strains are delayed in initiating replication and restricted in cell-to-cell spread. High levels of replication in astrocytes of neuropathogenic strains of WNV

induces high levels of proinflammatory cytokines, such as type-1 IFNs, and chemokines, such as CCL5, leading to a robust response from resident leukocytes and leukocytes in the blood. The robust expression of CCL5 by WNV-infected astrocytes may lead to extravasation of more leukocytes than necessary to clear infection. Therefore, the traversal of leukocytes in response to infection initiated in astrocytes may exacerbate pathology, and may include traversal of infected leukocytes, thereby enhancing infection in the CNS. Nonneuropathogenic strains, however, are restricted in infectious particle production in astrocytes, limiting their capability to spread to neurons. Since neurons also express molecules that contribute to the trafficking of leukocytes to the CNS (131), limiting their exposure to nonneuropathogenic strains may limit the antiviral response in neurons and therefore leukocyte trafficking into the CNS. While low levels of leukocyte homing to the infected CNS may promote viral clearance, high levels of immunoreactive cells may lead to unregulated immune responses and neuronal death, or bystander cell death of glial cells. The high levels of replication in astrocytes for neuropathogenic strains of WNV permit further transfer and propagation into neurons. Although additional in vivo data will be necessary to validate this model, our initial studies utilizing intravenous inoculations of high levels of both neuropathogenic and nonneuropathogenic WNV suggest that an additional restriction exists for nonneuropathogenic strains of WNV at the BBB. Observations in neutrophil-depleted mice prior to or directly after infection support this hypothesis; if neutrophils are depleted prior to infection, an increase in pathogenesis is observed, suggesting that early on in

infection, neutrophils are beneficial to the host. However, if depleted after infection, survival of mice increases, suggesting that if infection is established in the CNS, activity of these cells may contribute to pathogenesis, or may lead to a secondary infection of the CNS (15). Further, in macrophage-depleted mice infected with a nonneuropathogenic strain of WNV, mice had a lower survival rate and higher viral loads in the CNS and the periphery compared to controls, demonstrating the active role for macrophages in restricting nonneuropathogenic WNV (26). Finally, IFNAR^{-/-} mice inoculated with nonneuropathogenic WNV have a longer mean time to death (127), suggesting an additional factor to the type-1 IFN response restricts nonneuropathogenic strains. Thus, we propose that all strains of WNV may enter into the CNS. However, the immune responses initiated at the BBB and the restriction in cell-to-cell spread by the structural proteins of nonneuropathogenic strains of WNV limit the transfer of virus to neurons and promote a controlled immune response to infection in the CNS. However, neuropathogenic strains are not restricted at the level of astrocyte replication, and the increased initiation of the cellular immune response in astrocytes may initiate an excessive immune response in the CNS, leading to bystander cell death. Indeed, WNV-NY-infected astrocytes secrete high levels of type-1 IFN, as do infected neurons (144). This model displays a novel role for astrocytes at modulating WNV neuropathogenicity.

Several additional experiments may expand on the presented model. In vivo data supporting and expanding on the immune response during tail vein inoculations of both WNV-NY and WNV-MAD78 will provide a more complete

model of the kinetics of the response to infection at the CNS. Detection of viral antigen present in astrocytes and endothelial cells would provide physiological evidence of replication in both endothelial cells and astrocytes. More detailed analysis on residues and motifs present within the structural proteins of WNV that limit infectious particle production in astrocytes may provide a mechanism of the restriction of nonneuropathogenic WNV in astrocytes. While infectious viral particle production was examined with chimeric viruses, a restriction in cell-to-cell spread still must be confirmed. Thus, there may not be an inherent deficiency in astrocytes for entry by either strain, but in the production of infectious particles. It is possible that the inability to synthesize infectious particles is the cause for the restriction in cell-to-cell spread. In addition, the factors that contribute to the delay in initiating replication was not determined. Both chimeric viruses with structural and nonstructural portions were delayed at initiating infectious particle production. Thus, these viruses may be utilized in further examination of the delay of WNV replication in astrocytes. Overall, the data presented provide novel tools and insights into the varying degrees of neuropathologies induced among strains of WNV. The data presented provides sites within cell types, such as the maturation pathway within astrocytes, as well as within the CNS, where nonpathogenic strains may be restricted, offering possible mechanisms that underlie WNV neuropathology. This knowledge provides novel targets for the development of vaccines through synthesis of chimeric viruses and antiviral drug targets, such as pathways of viral maturation in astrocytes, within the CNS that may help alleviate and prevent WNV neuropathologies.

References

1. **Abbott, N. J.** 2002. Astrocyte-endothelial interactions and blood-brain barrier permeability. *Journal of anatomy* **200**:629-638.
2. **Adolf, G. R.** 1985. Structure and effects of interferon-gamma. *Oncology* **42 Suppl 1**:33-40.
3. **Agarwal, A., and S. Rajan.** 1995. The LMA in intracranial aneurysm surgery. *Canadian journal of anaesthesia = Journal canadien d'anesthesie* **42**:1176-1177.
4. **Akira, S., S. Uematsu, and O. Takeuchi.** 2006. Pathogen recognition and innate immunity. *Cell* **124**:783-801.
5. **Al-Harhi, L.** 2012. Interplay between Wnt/beta-catenin signaling and HIV: virologic and biologic consequences in the CNS. *Journal of neuroimmune pharmacology : the official journal of the Society on NeuroImmune Pharmacology* **7**:731-739.
6. **Alcami, A.** 2003. Viral mimicry of cytokines, chemokines and their receptors. *Nature reviews. Immunology* **3**:36-50.
7. **Allen, S. J., S. E. Crown, and T. M. Handel.** 2007. Chemokine: receptor structure, interactions, and antagonism. *Annual review of immunology* **25**:787-820.

8. **Allison, S. L., J. Schalich, K. Stiasny, C. W. Mandl, C. Kunz, and F. X. Heinz.** 1995. Oligomeric rearrangement of tick-borne encephalitis virus envelope proteins induced by an acidic pH. *Journal of virology* **69**:695-700.
9. **Ancuta, P., A. Moses, and D. Gabuzda.** 2004. Transendothelial migration of CD16⁺ monocytes in response to fractalkine under constitutive and inflammatory conditions. *Immunobiology* **209**:11-20.
10. **Anthony, I. C., and J. E. Bell.** 2008. The Neuropathology of HIV/AIDS. *Int Rev Psychiatry* **20**:15-24.
11. **Appler, K. K., A. N. Brown, B. S. Stewart, M. J. Behr, V. L. Demarest, S. J. Wong, and K. A. Bernard.** 2010. Persistence of West Nile virus in the central nervous system and periphery of mice. *PloS one* **5**:e10649.
12. **Armah, H. B., G. Wang, B. I. Omalu, R. B. Tesh, K. A. Gyure, D. J. Chute, R. D. Smith, P. Dulai, H. V. Vinters, B. K. Kleinschmidt-DeMasters, and C. A. Wiley.** 2007. Systemic distribution of West Nile virus infection: postmortem immunohistochemical study of six cases. *Brain Pathol* **17**:354-362.
13. **Audsley, M., J. Edmonds, W. Liu, V. Mokhonov, E. Mokhonova, E. B. Melian, N. Prow, R. A. Hall, and A. A. Khromykh.** 2011. Virulence determinants between New York 99 and Kunjin strains of West Nile virus. *Virology* **414**:63-73.

14. **Bach, E. A., M. Aguet, and R. D. Schreiber.** 1997. The IFN gamma receptor: a paradigm for cytokine receptor signaling. *Annual review of immunology* **15**:563-591.
15. **Bai, F., K. F. Kong, J. Dai, F. Qian, L. Zhang, C. R. Brown, E. Fikrig, and R. R. Montgomery.** 2010. A paradoxical role for neutrophils in the pathogenesis of West Nile virus. *The Journal of infectious diseases* **202**:1804-1812.
16. **Ballabh, P., A. Braun, and M. Nedergaard.** 2004. The blood-brain barrier: an overview: structure, regulation, and clinical implications. *Neurobiology of disease* **16**:1-13.
17. **Baqar, S., C. G. Hayes, J. R. Murphy, and D. M. Watts.** 1993. Vertical transmission of West Nile virus by *Culex* and *Aedes* species mosquitoes. *The American journal of tropical medicine and hygiene* **48**:757-762.
18. **Barnum, S. R., and A. J. Szalai.** 2005. Complement as a biomarker in multiple sclerosis. *Journal of neuropathology and experimental neurology* **64**:741.
19. **Bartenschlager, R., M. Frese, and T. Pietschmann.** 2004. Novel insights into hepatitis C virus replication and persistence. *Advances in virus research* **63**:71-180.
20. **Bashirova, A. A., T. B. Geijtenbeek, G. C. van Duijnhoven, S. J. van Vliet, J. B. Eilering, M. P. Martin, L. Wu, T. D. Martin, N. Viebig, P. A. Knolle, V. N. KewalRamani, Y. van Kooyk, and M. Carrington.** 2001. A dendritic cell-specific intercellular adhesion molecule 3-grabbing

nonintegrin (DC-SIGN)-related protein is highly expressed on human liver sinusoidal endothelial cells and promotes HIV-1 infection. *The Journal of experimental medicine* **193**:671-678.

21. **Bearer, E. L., X. O. Breakefield, D. Schuback, T. S. Reese, and J. H. LaVail.** 2000. Retrograde axonal transport of herpes simplex virus: evidence for a single mechanism and a role for tegument. *Proceedings of the National Academy of Sciences of the United States of America* **97**:8146-8150.
22. **Beasley, D. W., C. T. Davis, J. Estrada-Franco, R. Navarro-Lopez, A. Campomanes-Cortes, R. B. Tesh, S. C. Weaver, and A. D. Barrett.** 2004. Genome sequence and attenuating mutations in West Nile virus isolate from Mexico. *Emerging infectious diseases* **10**:2221-2224.
23. **Beasley, D. W., L. Li, M. T. Suderman, and A. D. Barrett.** 2002. Mouse neuroinvasive phenotype of West Nile virus strains varies depending upon virus genotype. *Virology* **296**:17-23.
24. **Beasley, D. W., M. C. Whiteman, S. Zhang, C. Y. Huang, B. S. Schneider, D. R. Smith, G. D. Gromowski, S. Higgs, R. M. Kinney, and A. D. Barrett.** 2005. Envelope protein glycosylation status influences mouse neuroinvasion phenotype of genetic lineage 1 West Nile virus strains. *Journal of virology* **79**:8339-8347.
25. **Becher, P., M. Konig, D. J. Paton, and H. J. Thiel.** 1995. Further characterization of border disease virus isolates: evidence for the

- presence of more than three species within the genus pestivirus. *Virology* **209**:200-206.
26. **Ben-Nathan, D., I. Huitinga, S. Lustig, N. van Rooijen, and D. Kober.** 1996. West Nile virus neuroinvasion and encephalitis induced by macrophage depletion in mice. *Archives of virology* **141**:459-469.
 27. **Bennett, J. L., and O. Stuve.** 2009. Update on inflammation, neurodegeneration, and immunoregulation in multiple sclerosis: therapeutic implications. *Clinical neuropharmacology* **32**:121-132.
 28. **Benveniste, E. N., V. T. Nguyen, and D. R. Wesemann.** 2004. Molecular regulation of CD40 gene expression in macrophages and microglia. *Brain, behavior, and immunity* **18**:7-12.
 29. **Berger, E. A.** 1998. HIV entry and tropism. When one receptor is not enough. *Advances in experimental medicine and biology* **452**:151-157.
 30. **Blumenthal, R., S. Durell, and M. Viard.** 2012. HIV entry and envelope glycoprotein-mediated fusion. *The Journal of biological chemistry* **287**:40841-40849.
 31. **Botha, E. M., W. Markotter, M. Wolfaardt, J. T. Paweska, R. Swanepoel, G. Palacios, L. H. Nel, and M. Venter.** 2008. Genetic determinants of virulence in pathogenic lineage 2 West Nile virus strains. *Emerging infectious diseases* **14**:222-230.
 32. **Brien, J. D., S. Daffis, H. M. Lazear, H. Cho, M. S. Suthar, M. Gale, Jr., and M. S. Diamond.** 2011. Interferon regulatory factor-1 (IRF-1) shapes

- both innate and CD8(+) T cell immune responses against West Nile virus infection. *PLoS pathogens* **7**:e1002230.
33. **Brown, A. M., and B. R. Ransom.** 2007. Astrocyte glycogen and brain energy metabolism. *Glia* **55**:1263-1271.
 34. **Brown, A. N., K. A. Kent, C. J. Bennett, and K. A. Bernard.** 2007. Tissue tropism and neuroinvasion of West Nile virus do not differ for two mouse strains with different survival rates. *Virology* **368**:422-430.
 35. **Bsibsi, M., C. Persoon-Deen, R. W. Verwer, S. Meeuwsen, R. Ravid, and J. M. Van Noort.** 2006. Toll-like receptor 3 on adult human astrocytes triggers production of neuroprotective mediators. *Glia* **53**:688-695.
 36. **Bsibsi, M., R. Ravid, D. Gveric, and J. M. van Noort.** 2002. Broad expression of Toll-like receptors in the human central nervous system. *Journal of neuropathology and experimental neurology* **61**:1013-1021.
 37. **Busch, M. P., D. J. Wright, B. Custer, L. H. Tobler, S. L. Stramer, S. H. Kleinman, H. E. Prince, C. Bianco, G. Foster, L. R. Petersen, G. Nemo, and S. A. Glynn.** 2006. West Nile virus infections projected from blood donor screening data, United States, 2003. *Emerging infectious diseases* **12**:395-402.
 38. **Bushong, E. A., M. E. Martone, Y. Z. Jones, and M. H. Ellisman.** 2002. Protoplasmic astrocytes in CA1 stratum radiatum occupy separate anatomical domains. *The Journal of neuroscience : the official journal of the Society for Neuroscience* **22**:183-192.

39. **Byrne, S. N., G. M. Halliday, L. J. Johnston, and N. J. King.** 2001. Interleukin-1beta but not tumor necrosis factor is involved in West Nile virus-induced Langerhans cell migration from the skin in C57BL/6 mice. *The Journal of investigative dermatology* **117**:702-709.
40. **Carman, C. V.** 2009. Mechanisms for transcellular diapedesis: probing and pathfinding by 'invadosome-like protrusions'. *Journal of cell science* **122**:3025-3035.
41. **Carman, C. V., and T. A. Springer.** 2004. A transmigratory cup in leukocyte diapedesis both through individual vascular endothelial cells and between them. *The Journal of cell biology* **167**:377-388.
42. **Castle, E., U. Leidner, T. Nowak, G. Wengler, and G. Wengler.** 1986. Primary structure of the West Nile flavivirus genome region coding for all nonstructural proteins. *Virology* **149**:10-26.
43. **Castle, E., T. Nowak, U. Leidner, G. Wengler, and G. Wengler.** 1985. Sequence analysis of the viral core protein and the membrane-associated proteins V1 and NV2 of the flavivirus West Nile virus and of the genome sequence for these proteins. *Virology* **145**:227-236.
44. **Ceccaldi, P. E., M. Lucas, and P. Despres.** 2004. New insights on the neuropathology of West Nile virus. *FEMS microbiology letters* **233**:1-6.
45. **Chapagain, M. L., S. Verma, F. Mercier, R. Yanagihara, and V. R. Nerurkar.** 2007. Polyomavirus JC infects human brain microvascular endothelial cells independent of serotonin receptor 2A. *Virology* **364**:55-63.

46. **Cheeran, M. C., S. Hu, W. S. Sheng, A. Rashid, P. K. Peterson, and J. R. Lokensgard.** 2005. Differential responses of human brain cells to West Nile virus infection. *Journal of neurovirology* **11**:512-524.
47. **Chevalier, G., E. Suberbielle, C. Monnet, V. Duplan, G. Martin-Blondel, F. Farrugia, G. Le Masson, R. Liblau, and D. Gonzalez-Dunia.** 2011. Neurons are MHC class I-dependent targets for CD8 T cells upon neurotropic viral infection. *PLoS pathogens* **7**:e1002393.
48. **Cho, H., and M. S. Diamond.** 2012. Immune responses to West Nile virus infection in the central nervous system. *Viruses* **4**:3812-3830.
49. **Chu, J. J., and M. L. Ng.** 2004. Infectious entry of West Nile virus occurs through a clathrin-mediated endocytic pathway. *Journal of virology* **78**:10543-10555.
50. **Chu, J. J., and M. L. Ng.** 2004. Interaction of West Nile virus with alpha v beta 3 integrin mediates virus entry into cells. *The Journal of biological chemistry* **279**:54533-54541.
51. **Chui, R., and K. Dorovini-Zis.** 2010. Regulation of CCL2 and CCL3 expression in human brain endothelial cells by cytokines and lipopolysaccharide. *Journal of neuroinflammation* **7**:1.
52. **Clemens, M. J., and C. M. Vaquero.** 1978. Inhibition of protein synthesis by double-stranded RNA in reticulocyte lysates: evidence for activation of an endoribonuclease. *Biochemical and biophysical research communications* **83**:59-68.

53. **Colpitts, T. M., I. Rodenhuis-Zybert, B. Moesker, P. Wang, E. Fikrig, and J. M. Smit.** 2011. prM-antibody renders immature West Nile virus infectious in vivo. *The Journal of general virology* **92**:2281-2285.
54. **Daffis, S., M. A. Samuel, M. S. Suthar, M. Gale, Jr., and M. S. Diamond.** 2008. Toll-like receptor 3 has a protective role against West Nile virus infection. *Journal of virology* **82**:10349-10358.
55. **Daffis, S., M. A. Samuel, M. S. Suthar, B. C. Keller, M. Gale, Jr., and M. S. Diamond.** 2008. Interferon regulatory factor IRF-7 induces the antiviral alpha interferon response and protects against lethal West Nile virus infection. *Journal of virology* **82**:8465-8475.
56. **Daffis, S., M. S. Suthar, M. Gale, Jr., and M. S. Diamond.** 2009. Measure and countermeasure: type I IFN (IFN-alpha/beta) antiviral response against West Nile virus. *Journal of innate immunity* **1**:435-445.
57. **Dai, J., P. Wang, F. Bai, T. Town, and E. Fikrig.** 2008. Icam-1 participates in the entry of west nile virus into the central nervous system. *Journal of virology* **82**:4164-4168.
58. **Dar, A. C., T. E. Dever, and F. Sicheri.** 2005. Higher-order substrate recognition of eIF2alpha by the RNA-dependent protein kinase PKR. *Cell* **122**:887-900.
59. **Darnell, J. E., Jr., I. M. Kerr, and G. R. Stark.** 1994. Jak-STAT pathways and transcriptional activation in response to IFNs and other extracellular signaling proteins. *Science* **264**:1415-1421.

60. **Davis, C. W., H. Y. Nguyen, S. L. Hanna, M. D. Sanchez, R. W. Doms, and T. C. Pierson.** 2006. West Nile virus discriminates between DC-SIGN and DC-SIGNR for cellular attachment and infection. *Journal of virology* **80**:1290-1301.
61. **Dedoni, S., M. C. Olanas, and P. Onali.** 2010. Interferon-beta induces apoptosis in human SH-SY5Y neuroblastoma cells through activation of JAK-STAT signaling and down-regulation of PI3K/Akt pathway. *Journal of neurochemistry* **115**:1421-1433.
62. **Deng, J., K. Hua, S. S. Lesser, and J. B. Harp.** 2000. Activation of signal transducer and activator of transcription-3 during proliferative phases of 3T3-L1 adipogenesis. *Endocrinology* **141**:2370-2376.
63. **Diamond, M. S., B. Shrestha, A. Marri, D. Mahan, and M. Engle.** 2003. B cells and antibody play critical roles in the immediate defense of disseminated infection by West Nile encephalitis virus. *Journal of virology* **77**:2578-2586.
64. **Diamond, M. S., B. Shrestha, E. Mehlhop, E. Sitati, and M. Engle.** 2003. Innate and adaptive immune responses determine protection against disseminated infection by West Nile encephalitis virus. *Viral immunology* **16**:259-278.
65. **Diamond, M. S., E. M. Sitati, L. D. Friend, S. Higgs, B. Shrestha, and M. Engle.** 2003. A critical role for induced IgM in the protection against West Nile virus infection. *The Journal of experimental medicine* **198**:1853-1862.

66. **Dietzschold, B., M. Schnell, and H. Koprowski.** 2005. Pathogenesis of rabies. *Current topics in microbiology and immunology* **292**:45-56.
67. **Dorrbecker, B., G. Dobler, M. Spiegel, and F. T. Hufert.** 2010. Tick-borne encephalitis virus and the immune response of the mammalian host. *Travel medicine and infectious disease* **8**:213-222.
68. **Ebnet, K., M. M. Simon, and S. Shaw.** 1996. Regulation of chemokine gene expression in human endothelial cells by proinflammatory cytokines and *Borrelia burgdorferi*. *Annals of the New York Academy of Sciences* **797**:107-117.
69. **Elghonemy, S., W. G. Davis, and M. A. Brinton.** 2005. The majority of the nucleotides in the top loop of the genomic 3' terminal stem loop structure are cis-acting in a West Nile virus infectious clone. *Virology* **331**:238-246.
70. **Emara, M. M., and M. A. Brinton.** 2007. Interaction of TIA-1/TIAR with West Nile and dengue virus products in infected cells interferes with stress granule formation and processing body assembly. *Proceedings of the National Academy of Sciences of the United States of America* **104**:9041-9046.
71. **Emara, M. M., H. Liu, W. G. Davis, and M. A. Brinton.** 2008. Mutation of mapped TIA-1/TIAR binding sites in the 3' terminal stem-loop of West Nile virus minus-strand RNA in an infectious clone negatively affects genomic RNA amplification. *Journal of virology* **82**:10657-10670.

72. **Eng, L. F., and R. S. Ghirnikar.** 1994. GFAP and astrogliosis. *Brain Pathol* **4**:229-237.
73. **Engle, M. J., and M. S. Diamond.** 2003. Antibody prophylaxis and therapy against West Nile virus infection in wild-type and immunodeficient mice. *Journal of virology* **77**:12941-12949.
74. **Erbel, P., N. Schiering, A. D'Arcy, M. Renatus, M. Kroemer, S. P. Lim, Z. Yin, T. H. Keller, S. G. Vasudevan, and U. Hommel.** 2006. Structural basis for the activation of flaviviral NS3 proteases from dengue and West Nile virus. *Nature structural & molecular biology* **13**:372-373.
75. **Eugenin, E. A., J. E. Clements, M. C. Zink, and J. W. Berman.** 2011. Human immunodeficiency virus infection of human astrocytes disrupts blood-brain barrier integrity by a gap junction-dependent mechanism. *The Journal of neuroscience : the official journal of the Society for Neuroscience* **31**:9456-9465.
76. **Falgout, B., M. Pethel, Y. M. Zhang, and C. J. Lai.** 1991. Both nonstructural proteins NS2B and NS3 are required for the proteolytic processing of dengue virus nonstructural proteins. *Journal of virology* **65**:2467-2475.
77. **Fazakerley, J. K.** 2002. Pathogenesis of Semliki Forest virus encephalitis. *Journal of neurovirology* **8 Suppl 2**:66-74.
78. **Fields, B.** 2007. *Virology*, vol. 1. Lippincott Williams and Wilkins, Philadelphia, PA, USA.

79. **Fitzgerald, K. A., E. M. Palsson-McDermott, A. G. Bowie, C. A. Jefferies, A. S. Mansell, G. Brady, E. Brint, A. Dunne, P. Gray, M. T. Harte, D. McMurray, D. E. Smith, J. E. Sims, T. A. Bird, and L. A. O'Neill.** 2001. Mal (MyD88-adaptor-like) is required for Toll-like receptor-4 signal transduction. *Nature* **413**:78-83.
80. **Fitzgerald, K. A., D. C. Rowe, B. J. Barnes, D. R. Caffrey, A. Visintin, E. Latz, B. Monks, P. M. Pitha, and D. T. Golenbock.** 2003. LPS-TLR4 signaling to IRF-3/7 and NF-kappaB involves the toll adaptors TRAM and TRIF. *The Journal of experimental medicine* **198**:1043-1055.
81. **Fredericksen, B. L., and M. Gale, Jr.** 2006. West Nile virus evades activation of interferon regulatory factor 3 through RIG-I-dependent and -independent pathways without antagonizing host defense signaling. *Journal of virology* **80**:2913-2923.
82. **Fredericksen, B. L., B. C. Keller, J. Fornek, M. G. Katze, and M. Gale, Jr.** 2008. Establishment and maintenance of the innate antiviral response to West Nile Virus involves both RIG-I and MDA5 signaling through IPS-1. *Journal of virology* **82**:609-616.
83. **Fredericksen, B. L., M. Smith, M. G. Katze, P. Y. Shi, and M. Gale, Jr.** 2004. The host response to West Nile Virus infection limits viral spread through the activation of the interferon regulatory factor 3 pathway. *Journal of virology* **78**:7737-7747.
84. **Furr, S. R., M. Moerdyk-Schauwecker, V. Z. Grdzlishvili, and I. Marriott.** 2010. RIG-I mediates nonsegmented negative-sense RNA virus-

induced inflammatory immune responses of primary human astrocytes. *Glia* **58**:1620-1629.

85. **Gasque, P., Y. D. Dean, E. P. McGreal, J. VanBeek, and B. P. Morgan.** 2000. Complement components of the innate immune system in health and disease in the CNS. *Immunopharmacology* **49**:171-186.
86. **Geijtenbeek, T. B., and S. I. Gringhuis.** 2009. Signalling through C-type lectin receptors: shaping immune responses. *Nature reviews. Immunology* **9**:465-479.
87. **Getts, D. R., I. Matsumoto, M. Muller, M. T. Getts, J. Radford, B. Shrestha, I. L. Campbell, and N. J. King.** 2007. Role of IFN-gamma in an experimental murine model of West Nile virus-induced seizures. *Journal of neurochemistry* **103**:1019-1030.
88. **Getts, D. R., R. L. Terry, M. T. Getts, M. Muller, S. Rana, B. Shrestha, J. Radford, N. Van Rooijen, I. L. Campbell, and N. J. King.** 2008. Ly6c+ "inflammatory monocytes" are microglial precursors recruited in a pathogenic manner in West Nile virus encephalitis. *The Journal of experimental medicine* **205**:2319-2337.
89. **Gibson, D. G., L. Young, R. Y. Chuang, J. C. Venter, C. A. Hutchison, 3rd, and H. O. Smith.** 2009. Enzymatic assembly of DNA molecules up to several hundred kilobases. *Nature methods* **6**:343-345.
90. **Gillet, J. P., P. Derer, and H. Tsiang.** 1986. Axonal transport of rabies virus in the central nervous system of the rat. *Journal of neuropathology and experimental neurology* **45**:619-634.

91. **Girard, Y. A., V. Popov, J. Wen, V. Han, and S. Higgs.** 2005. Ultrastructural study of West Nile virus pathogenesis in *Culex pipiens quinquefasciatus* (Diptera: Culicidae). *Journal of medical entomology* **42**:429-444.
92. **Glass, W. G., J. K. Lim, R. Cholera, A. G. Pletnev, J. L. Gao, and P. M. Murphy.** 2005. Chemokine receptor CCR5 promotes leukocyte trafficking to the brain and survival in West Nile virus infection. *The Journal of experimental medicine* **202**:1087-1098.
93. **Glass, W. G., D. H. McDermott, J. K. Lim, S. Lekhong, S. F. Yu, W. A. Frank, J. Pape, R. C. Cheshier, and P. M. Murphy.** 2006. CCR5 deficiency increases risk of symptomatic West Nile virus infection. *The Journal of experimental medicine* **203**:35-40.
94. **Gold, R., C. Linington, and H. Lassmann.** 2006. Understanding pathogenesis and therapy of multiple sclerosis via animal models: 70 years of merits and culprits in experimental autoimmune encephalomyelitis research. *Brain : a journal of neurology* **129**:1953-1971.
95. **Goldenberg, M. M.** 2012. Multiple sclerosis review. *P & T : a peer-reviewed journal for formulary management* **37**:175-184.
96. **Goldstein, G. W.** 1988. Endothelial cell-astrocyte interactions. A cellular model of the blood-brain barrier. *Annals of the New York Academy of Sciences* **529**:31-39.

97. **Gollins, S. W., and J. S. Porterfield.** 1985. Flavivirus infection enhancement in macrophages: an electron microscopic study of viral cellular entry. *The Journal of general virology* **66 (Pt 9)**:1969-1982.
98. **Gollins, S. W., and J. S. Porterfield.** 1986. The uncoating and infectivity of the flavivirus West Nile on interaction with cells: effects of pH and ammonium chloride. *The Journal of general virology* **67 (Pt 9)**:1941-1950.
99. **Grab, D. J., G. Perides, J. S. Dumler, K. J. Kim, J. Park, Y. V. Kim, O. Nikolskaia, K. S. Choi, M. F. Stins, and K. S. Kim.** 2005. *Borrelia burgdorferi*, host-derived proteases, and the blood-brain barrier. *Infection and immunity* **73**:1014-1022.
100. **Grabowski, J., S. L. Salzstein, G. R. Sadler, and S. Blair.** 2008. Intracystic papillary carcinoma: a review of 917 cases. *Cancer* **113**:916-920.
101. **Gralinski, L. E., S. L. Ashley, S. D. Dixon, and K. R. Spindler.** 2009. Mouse adenovirus type 1-induced breakdown of the blood-brain barrier. *Journal of virology* **83**:9398-9410.
102. **Guo, J. T., J. Hayashi, and C. Seeger.** 2005. West Nile virus inhibits the signal transduction pathway of alpha interferon. *Journal of virology* **79**:1343-1350.
103. **Hahn, C. S., J. M. Dalrymple, J. H. Strauss, and C. M. Rice.** 1987. Comparison of the virulent Asibi strain of yellow fever virus with the 17D vaccine strain derived from it. *Proceedings of the National Academy of Sciences of the United States of America* **84**:2019-2023.

104. **Halassa, M. M., T. Fellin, H. Takano, J. H. Dong, and P. G. Haydon.** 2007. Synaptic islands defined by the territory of a single astrocyte. *The Journal of neuroscience : the official journal of the Society for Neuroscience* **27**:6473-6477.
105. **Halevy, M., Y. Akov, D. Ben-Nathan, D. Kobiler, B. Lachmi, and S. Lustig.** 1994. Loss of active neuroinvasiveness in attenuated strains of West Nile virus: pathogenicity in immunocompetent and SCID mice. *Archives of virology* **137**:355-370.
106. **Hanna, S. L., T. C. Pierson, M. D. Sanchez, A. A. Ahmed, M. M. Murtadha, and R. W. Doms.** 2005. N-linked glycosylation of west nile virus envelope proteins influences particle assembly and infectivity. *Journal of virology* **79**:13262-13274.
107. **Harton, J. A., M. W. Linhoff, J. Zhang, and J. P. Ting.** 2002. Cutting edge: CATERPILLER: a large family of mammalian genes containing CARD, pyrin, nucleotide-binding, and leucine-rich repeat domains. *J Immunol* **169**:4088-4093.
108. **Hasebe, R., T. Suzuki, Y. Makino, M. Igarashi, S. Yamanouchi, A. Maeda, M. Horiuchi, H. Sawa, and T. Kimura.** 2010. Transcellular transport of West Nile virus-like particles across human endothelial cells depends on residues 156 and 159 of envelope protein. *BMC microbiology* **10**:165.
109. **Hayashi, Y., M. Nomura, S. Yamagishi, S. Harada, J. Yamashita, and H. Yamamoto.** 1997. Induction of various blood-brain barrier properties in

non-neural endothelial cells by close apposition to co-cultured astrocytes. *Glia* **19**:13-26.

110. **Hayes, E. B., N. Komar, R. S. Nasci, S. P. Montgomery, D. R. O'Leary, and G. L. Campbell.** 2005. Epidemiology and transmission dynamics of West Nile virus disease. *Emerging infectious diseases* **11**:1167-1173.
111. **Heinz, F. X.** 2003. Molecular aspects of TBE virus research. *Vaccine* **21 Suppl 1**:S3-S10.
112. **Honda, K., H. Yanai, A. Takaoka, and T. Taniguchi.** 2005. Regulation of the type I IFN induction: a current view. *International immunology* **17**:1367-1378.
113. **Hornig, T., G. M. Barton, and R. Medzhitov.** 2001. TIRAP: an adapter molecule in the Toll signaling pathway. *Nature immunology* **2**:835-841.
114. <http://www.who.int/mediacentre/factsheets/fs164/en/>, posting date. [Online.]
115. **Huang, S. H., and A. Y. Jong.** 2001. Cellular mechanisms of microbial proteins contributing to invasion of the blood-brain barrier. *Cellular microbiology* **3**:277-287.
116. **Hubalek, Z., and J. Halouzka.** 1999. West Nile fever--a reemerging mosquito-borne viral disease in Europe. *Emerging infectious diseases* **5**:643-650.
117. **Hussmann, K. L., M. A. Samuel, K. S. Kim, M. S. Diamond, and B. L. Fredericksen.** 2013. Differential replication of pathogenic and

- nonpathogenic strains of West Nile virus within astrocytes. *Journal of virology* **87**:2814-2822.
118. **Iadecola, C.** 2004. Neurovascular regulation in the normal brain and in Alzheimer's disease. *Nature reviews. Neuroscience* **5**:347-360.
 119. **Inohara, N., and G. Nunez.** 2001. The NOD: a signaling module that regulates apoptosis and host defense against pathogens. *Oncogene* **20**:6473-6481.
 120. **Isaacs, A., and J. Lindenmann.** 1957. Virus interference. I. The interferon. *Proc R Soc Lond B Biol Sci* **147**:258-267.
 121. **Isaacs, A., J. Lindenmann, and R. C. Valentine.** 1957. Virus interference. II. Some properties of interferon. *Proc R Soc Lond B Biol Sci* **147**:268-273.
 122. **Johnson, R. T., D. S. Burke, M. Elwell, C. J. Leake, A. Nisalak, C. H. Hoke, and W. Lorsomrudee.** 1985. Japanese encephalitis: immunocytochemical studies of viral antigen and inflammatory cells in fatal cases. *Annals of neurology* **18**:567-573.
 123. **Johnston, L. J., G. M. Halliday, and N. J. King.** 2000. Langerhans cells migrate to local lymph nodes following cutaneous infection with an arbovirus. *The Journal of investigative dermatology* **114**:560-568.
 124. **Kang, D. C., R. V. Gopalkrishnan, Q. Wu, E. Jankowsky, A. M. Pyle, and P. B. Fisher.** 2002. mda-5: An interferon-inducible putative RNA helicase with double-stranded RNA-dependent ATPase activity and

- melanoma growth-suppressive properties. *Proceedings of the National Academy of Sciences of the United States of America* **99**:637-642.
125. **Kanneganti, T. D.** 2010. Central roles of NLRs and inflammasomes in viral infection. *Nature reviews. Immunology* **10**:688-698.
126. **Kansas, G. S.** 1996. Selectins and their ligands: current concepts and controversies. *Blood* **88**:3259-3287.
127. **Keller, B. C., B. L. Fredericksen, M. A. Samuel, R. E. Mock, P. W. Mason, M. S. Diamond, and M. Gale, Jr.** 2006. Resistance to alpha/beta interferon is a determinant of West Nile virus replication fitness and virulence. *Journal of virology* **80**:9424-9434.
128. **Khromykh, A. A., P. L. Sedlak, and E. G. Westaway.** 2000. cis- and trans-acting elements in flavivirus RNA replication. *Journal of virology* **74**:3253-3263.
129. **Kim, K. S.** 2008. Mechanisms of microbial traversal of the blood-brain barrier. *Nature reviews. Microbiology* **6**:625-634.
130. **Kimelberg, H. K., and M. Nedergaard.** 2010. Functions of astrocytes and their potential as therapeutic targets. *Neurotherapeutics : the journal of the American Society for Experimental NeuroTherapeutics* **7**:338-353.
131. **Klein, R. S., E. Lin, B. Zhang, A. D. Luster, J. Tollett, M. A. Samuel, M. Engle, and M. S. Diamond.** 2005. Neuronal CXCL10 directs CD8+ T-cell recruitment and control of West Nile virus encephalitis. *Journal of virology* **79**:11457-11466.

132. **Klenk, K., J. Snow, K. Morgan, R. Bowen, M. Stephens, F. Foster, P. Gordy, S. Beckett, N. Komar, D. Gubler, and M. Bunning.** 2004. Alligators as West Nile virus amplifiers. *Emerging infectious diseases* **10**:2150-2155.
133. **Klimstra, W. B., E. M. Nangle, M. S. Smith, A. D. Yurochko, and K. D. Ryman.** 2003. DC-SIGN and L-SIGN can act as attachment receptors for alphaviruses and distinguish between mosquito cell- and mammalian cell-derived viruses. *Journal of virology* **77**:12022-12032.
134. **Kojouharoff, G., W. Hans, F. Obermeier, D. N. Mannel, T. Andus, J. Scholmerich, V. Gross, and W. Falk.** 1997. Neutralization of tumour necrosis factor (TNF) but not of IL-1 reduces inflammation in chronic dextran sulphate sodium-induced colitis in mice. *Clinical and experimental immunology* **107**:353-358.
135. **Konishi, E., and P. W. Mason.** 1993. Proper maturation of the Japanese encephalitis virus envelope glycoprotein requires cosynthesis with the premembrane protein. *Journal of virology* **67**:1672-1675.
136. **Kopf, M., M. F. Bachmann, and B. J. Marsland.** 2010. Averting inflammation by targeting the cytokine environment. *Nature reviews. Drug discovery* **9**:703-718.
137. **Koschinski, A., G. Wengler, G. Wengler, and H. Repp.** 2003. The membrane proteins of flaviviruses form ion-permeable pores in the target membrane after fusion: identification of the pores and analysis of their

- possible role in virus infection. *The Journal of general virology* **84**:1711-1721.
138. **Kramer, L. D., and K. A. Bernard.** 2001. West Nile virus infection in birds and mammals. *Annals of the New York Academy of Sciences* **951**:84-93.
139. **Kumar, M., K. Roe, B. Orillo, D. A. Muruve, V. R. Nerurkar, M. Gale, Jr., and S. Verma.** 2013. Inflammasome adaptor protein Apoptosis-associated speck-like protein containing CARD (ASC) is critical for the immune response and survival in west Nile virus encephalitis. *Journal of virology* **87**:3655-3667.
140. **Kumar, P., H. Wu, J. L. McBride, K. E. Jung, M. H. Kim, B. L. Davidson, S. K. Lee, P. Shankar, and N. Manjunath.** 2007. Transvascular delivery of small interfering RNA to the central nervous system. *Nature* **448**:39-43.
141. **Lanciotti, R. S., G. D. Ebel, V. Deubel, A. J. Kerst, S. Murri, R. Meyer, M. Bowen, N. McKinney, W. E. Morrill, M. B. Crabtree, L. D. Kramer, and J. T. Roehrig.** 2002. Complete genome sequences and phylogenetic analysis of West Nile virus strains isolated from the United States, Europe, and the Middle East. *Virology* **298**:96-105.
142. **Laudanna, C., J. Y. Kim, G. Constantin, and E. Butcher.** 2002. Rapid leukocyte integrin activation by chemokines. *Immunological reviews* **186**:37-46.
143. **Laurent-Rolle, M., E. F. Boer, K. J. Lubick, J. B. Wolfenbarger, A. B. Carmody, B. Rockx, W. Liu, J. Ashour, W. L. Shupert, M. R. Holbrook,**

- A. D. Barrett, P. W. Mason, M. E. Bloom, A. Garcia-Sastre, A. A. Khromykh, and S. M. Best.** 2010. The NS5 protein of the virulent West Nile virus NY99 strain is a potent antagonist of type I interferon-mediated JAK-STAT signaling. *Journal of virology* **84**:3503-3515.
144. **Lazear, H. M., A. K. Pinto, M. R. Vogt, M. Gale, Jr., and M. S. Diamond.** 2011. Beta interferon controls West Nile virus infection and pathogenesis in mice. *Journal of virology* **85**:7186-7194.
145. **Leis, A. A., J. Fratkin, D. S. Stokic, T. Harrington, R. M. Webb, and S. A. Slavinski.** 2003. West Nile poliomyelitis. *The Lancet infectious diseases* **3**:9-10.
146. **Leis, A. A., D. S. Stokic, R. M. Webb, S. A. Slavinski, and J. Fratkin.** 2003. Clinical spectrum of muscle weakness in human West Nile virus infection. *Muscle & nerve* **28**:302-308.
147. **Lemaitre, C., N. Orange, P. Saglio, N. Saint, J. Gagnon, and G. Molle.** 1996. Characterization and ion channel activities of novel antibacterial proteins from the skin mucosa of carp (*Cyprinus carpio*). *European journal of biochemistry / FEBS* **240**:143-149.
148. **Ley, K., C. Laudanna, M. I. Cybulsky, and S. Nourshargh.** 2007. Getting to the site of inflammation: the leukocyte adhesion cascade updated. *Nature reviews. Immunology* **7**:678-689.
149. **Li, W., Y. Li, N. Kedersha, P. Anderson, M. Emara, K. M. Swiderek, G. T. Moreno, and M. A. Brinton.** 2002. Cell proteins TIA-1 and TIAR interact with the 3' stem-loop of the West Nile virus complementary minus-

- strand RNA and facilitate virus replication. *Journal of virology* **76**:11989-12000.
150. **Lim, J. K., A. Lisco, D. H. McDermott, L. Huynh, J. M. Ward, B. Johnson, H. Johnson, J. Pape, G. A. Foster, D. Kryzstof, D. Follmann, S. L. Stramer, L. B. Margolis, and P. M. Murphy.** 2009. Genetic variation in OAS1 is a risk factor for initial infection with West Nile virus in man. *PLoS pathogens* **5**:e1000321.
151. **Lim, J. K., and P. M. Murphy.** 2011. Chemokine control of West Nile virus infection. *Experimental cell research* **317**:569-574.
152. **Lim, J. K., C. J. Obara, A. Rivollier, A. G. Pletnev, B. L. Kelsall, and P. M. Murphy.** 2011. Chemokine receptor Ccr2 is critical for monocyte accumulation and survival in West Nile virus encephalitis. *J Immunol* **186**:471-478.
153. **Lim, P. Y., M. J. Behr, C. M. Chadwick, P. Y. Shi, and K. A. Bernard.** 2011. Keratinocytes are cell targets of West Nile virus in vivo. *Journal of virology* **85**:5197-5201.
154. **Lindenbach, B. D., and C. M. Rice.** 1999. Genetic interaction of flavivirus nonstructural proteins NS1 and NS4A as a determinant of replicase function. *Journal of virology* **73**:4611-4621.
155. **Lindenbach, B. D., and C. M. Rice.** 1997. trans-Complementation of yellow fever virus NS1 reveals a role in early RNA replication. *Journal of virology* **71**:9608-9617.

156. **Liu, T. H., L. C. Liang, C. C. Wang, H. C. Liu, and W. J. Chen.** 2008. The blood-brain barrier in the cerebrum is the initial site for the Japanese encephalitis virus entering the central nervous system. *Journal of neurovirology* **14**:514-521.
157. **Liu, W. J., H. B. Chen, X. J. Wang, H. Huang, and A. A. Khromykh.** 2004. Analysis of adaptive mutations in Kunjin virus replicon RNA reveals a novel role for the flavivirus nonstructural protein NS2A in inhibition of beta interferon promoter-driven transcription. *Journal of virology* **78**:12225-12235.
158. **Liu, W. J., X. J. Wang, D. C. Clark, M. Lobigs, R. A. Hall, and A. A. Khromykh.** 2006. A single amino acid substitution in the West Nile virus nonstructural protein NS2A disables its ability to inhibit alpha/beta interferon induction and attenuates virus virulence in mice. *Journal of virology* **80**:2396-2404.
159. **Loeb, K. R., and A. L. Haas.** 1992. The interferon-inducible 15-kDa ubiquitin homolog conjugates to intracellular proteins. *The Journal of biological chemistry* **267**:7806-7813.
160. **Loov, C., L. Hillered, T. Ebendal, and A. Erlandsson.** 2012. Engulfing astrocytes protect neurons from contact-induced apoptosis following injury. *PloS one* **7**:e33090.
161. **Lorenz, I. C., S. L. Allison, F. X. Heinz, and A. Helenius.** 2002. Folding and dimerization of tick-borne encephalitis virus envelope proteins prM and E in the endoplasmic reticulum. *Journal of virology* **76**:5480-5491.

162. **Louboutin, J. P., and D. S. Strayer.** 2012. Blood-brain barrier abnormalities caused by HIV-1 gp120: mechanistic and therapeutic implications. *TheScientificWorldJournal* **2012**:482575.
163. **Lozach, P. Y., H. Lortat-Jacob, A. de Lacroix de Lavalette, I. Staropoli, S. Foug, A. Amara, C. Houles, F. Fieschi, O. Schwartz, J. L. Virelizier, F. Arenzana-Seisdedos, and R. Altmeyer.** 2003. DC-SIGN and L-SIGN are high affinity binding receptors for hepatitis C virus glycoprotein E2. *The Journal of biological chemistry* **278**:20358-20366.
164. **Lustig, S., H. D. Danenberg, Y. Kafri, D. Kobilier, and D. Ben-Nathan.** 1992. Viral neuroinvasion and encephalitis induced by lipopolysaccharide and its mediators. *The Journal of experimental medicine* **176**:707-712.
165. **Ma, L., C. T. Jones, T. D. Groesch, R. J. Kuhn, and C. B. Post.** 2004. Solution structure of dengue virus capsid protein reveals another fold. *Proceedings of the National Academy of Sciences of the United States of America* **101**:3414-3419.
166. **Macdonald, J., J. Tonry, R. A. Hall, B. Williams, G. Palacios, M. S. Ashok, O. Jabado, D. Clark, R. B. Tesh, T. Briese, and W. I. Lipkin.** 2005. NS1 protein secretion during the acute phase of West Nile virus infection. *Journal of virology* **79**:13924-13933.
167. **Mackay, F., H. Loetscher, D. Stueber, G. Gehr, and W. Lesslauer.** 1993. Tumor necrosis factor alpha (TNF-alpha)-induced cell adhesion to human endothelial cells is under dominant control of one TNF receptor type, TNF-R55. *The Journal of experimental medicine* **177**:1277-1286.

168. **Mackenzie, J. M., M. K. Jones, and P. R. Young.** 1996. Immunolocalization of the dengue virus nonstructural glycoprotein NS1 suggests a role in viral RNA replication. *Virology* **220**:232-240.
169. **Mackenzie, J. M., and E. G. Westaway.** 2001. Assembly and maturation of the flavivirus Kunjin virus appear to occur in the rough endoplasmic reticulum and along the secretory pathway, respectively. *Journal of virology* **75**:10787-10799.
170. **Mahanty, S., and M. Bray.** 2004. Pathogenesis of filoviral haemorrhagic fevers. *The Lancet infectious diseases* **4**:487-498.
171. **Malathi, K., B. Dong, M. Gale, Jr., and R. H. Silverman.** 2007. Small self-RNA generated by RNase L amplifies antiviral innate immunity. *Nature* **448**:816-819.
172. **Marie, I., J. Svab, and A. G. Hovanessian.** 1990. The binding of the 69- and 100-kD forms of 2',5'-oligoadenylate synthetase to different polynucleotides. *Journal of interferon research* **10**:571-578.
173. **Marie, I., J. Svab, N. Robert, J. Galabru, and A. G. Hovanessian.** 1990. Differential expression and distinct structure of 69- and 100-kDa forms of 2-5A synthetase in human cells treated with interferon. *The Journal of biological chemistry* **265**:18601-18607.
174. **Martina, B. E., P. Koraka, and A. D. Osterhaus.** 2009. Dengue virus pathogenesis: an integrated view. *Clinical microbiology reviews* **22**:564-581.

175. **Mathieu, C., C. Pohl, J. Szecsi, S. Trajkovic-Bodennec, S. Devergnas, H. Raoul, F. L. Cosset, D. Gerlier, T. F. Wild, and B. Horvat.** 2011. Nipah virus uses leukocytes for efficient dissemination within a host. *Journal of virology* **85**:7863-7871.
176. **Medigeshi, G. R., A. J. Hirsch, D. N. Streblow, J. Nikolich-Zugich, and J. A. Nelson.** 2008. West Nile virus entry requires cholesterol-rich membrane microdomains and is independent of alphavbeta3 integrin. *Journal of virology* **82**:5212-5219.
177. **Mehlhop, E., A. Fuchs, M. Engle, and M. S. Diamond.** 2009. Complement modulates pathogenesis and antibody-dependent neutralization of West Nile virus infection through a C5-independent mechanism. *Virology* **393**:11-15.
178. **Mehlhop, E., S. Nelson, C. A. Jost, S. Gorlatov, S. Johnson, D. H. Fremont, M. S. Diamond, and T. C. Pierson.** 2009. Complement protein C1q reduces the stoichiometric threshold for antibody-mediated neutralization of West Nile virus. *Cell host & microbe* **6**:381-391.
179. **Melchjorsen, J., L. N. Sorensen, and S. R. Paludan.** 2003. Expression and function of chemokines during viral infections: from molecular mechanisms to in vivo function. *Journal of leukocyte biology* **74**:331-343.
180. **Melian, E. B., E. Hinzman, T. Nagasaki, A. E. Firth, N. M. Wills, A. S. Nouwens, B. J. Blitvich, J. Leung, A. Funk, J. F. Atkins, R. Hall, and A. A. Khromykh.** 2010. NS1' of flaviviruses in the Japanese encephalitis

virus serogroup is a product of ribosomal frameshifting and plays a role in viral neuroinvasiveness. *Journal of virology* **84**:1641-1647.

181. **Meylan, E., K. Burns, K. Hofmann, V. Blancheteau, F. Martinon, M. Kelliher, and J. Tschopp.** 2004. RIP1 is an essential mediator of Toll-like receptor 3-induced NF-kappa B activation. *Nature immunology* **5**:503-507.
182. **Michallet, M. C., E. Meylan, M. A. Ermolaeva, J. Vazquez, M. Rebsamen, J. Curran, H. Poeck, M. Bscheider, G. Hartmann, M. Konig, U. Kalinke, M. Pasparakis, and J. Tschopp.** 2008. TRADD protein is an essential component of the RIG-like helicase antiviral pathway. *Immunity* **28**:651-661.
183. **Middleton, J., A. M. Patterson, L. Gardner, C. Schmutz, and B. A. Ashton.** 2002. Leukocyte extravasation: chemokine transport and presentation by the endothelium. *Blood* **100**:3853-3860.
184. **Moreland, L. W., L. W. Heck, Jr., and W. J. Koopman.** 1997. Biologic agents for treating rheumatoid arthritis. Concepts and progress. *Arthritis and rheumatism* **40**:397-409.
185. **Morrey, J. D., A. L. Olsen, V. Siddharthan, N. E. Motter, H. Wang, B. S. Taro, D. Chen, D. Ruffner, and J. O. Hall.** 2008. Increased blood-brain barrier permeability is not a primary determinant for lethality of West Nile virus infection in rodents. *The Journal of general virology* **89**:467-473.
186. **Morrey, J. D., V. Siddharthan, H. Wang, J. O. Hall, R. T. Skirpstunas, A. L. Olsen, J. L. Nordstrom, S. Koenig, S. Johnson, and M. S. Diamond.** 2008. West Nile virus-induced acute flaccid paralysis is

prevented by monoclonal antibody treatment when administered after infection of spinal cord neurons. *Journal of neurovirology* **14**:152-163.

187. **Morris, M. M., H. Dyson, D. Baker, L. S. Harbige, J. K. Fazakerley, and S. Amor.** 1997. Characterization of the cellular and cytokine response in the central nervous system following Semliki Forest virus infection. *Journal of neuroimmunology* **74**:185-197.
188. **Munoz-Jordan, J. L., M. Laurent-Rolle, J. Ashour, L. Martinez-Sobrido, M. Ashok, W. I. Lipkin, and A. Garcia-Sastre.** 2005. Inhibition of alpha/beta interferon signaling by the NS4B protein of flaviviruses. *Journal of virology* **79**:8004-8013.
189. **Murray, K., C. Walker, E. Herrington, J. A. Lewis, J. McCormick, D. W. Beasley, R. B. Tesh, and S. Fisher-Hoch.** 2010. Persistent infection with West Nile virus years after initial infection. *The Journal of infectious diseases* **201**:2-4.
190. **Muylaert, I. R., R. Galler, and C. M. Rice.** 1997. Genetic analysis of the yellow fever virus NS1 protein: identification of a temperature-sensitive mutation which blocks RNA accumulation. *Journal of virology* **71**:291-298.
191. **Nedergaard, M., B. Ransom, and S. A. Goldman.** 2003. New roles for astrocytes: redefining the functional architecture of the brain. *Trends in neurosciences* **26**:523-530.
192. **Nelson, S., C. A. Jost, Q. Xu, J. Ess, J. E. Martin, T. Oliphant, S. S. Whitehead, A. P. Durbin, B. S. Graham, M. S. Diamond, and T. C.**

- Pierson.** 2008. Maturation of West Nile virus modulates sensitivity to antibody-mediated neutralization. *PLoS pathogens* **4**:e1000060.
193. **Netea, M. G., B. J. Kullberg, and J. W. Van der Meer.** 2000. Circulating cytokines as mediators of fever. *Clinical infectious diseases : an official publication of the Infectious Diseases Society of America* **31 Suppl 5**:S178-184.
194. **Nowak, T., and G. Wengler.** 1987. Analysis of disulfides present in the membrane proteins of the West Nile flavivirus. *Virology* **156**:127-137.
195. **O'Shea, J. J.** 1997. Jaks, STATs, cytokine signal transduction, and immunoregulation: are we there yet? *Immunity* **7**:1-11.
196. **Oglesbee, M., and S. Niewiesk.** 2011. Measles virus neurovirulence and host immunity. *Future virology* **6**:85-99.
197. **Omalu, B. I., A. A. Shakir, G. Wang, W. I. Lipkin, and C. A. Wiley.** 2003. Fatal fulminant pan-meningo-polioencephalitis due to West Nile virus. *Brain Pathol* **13**:465-472.
198. **Oshiumi, H., M. Matsumoto, K. Funami, T. Akazawa, and T. Seya.** 2003. TICAM-1, an adaptor molecule that participates in Toll-like receptor 3-mediated interferon-beta induction. *Nature immunology* **4**:161-167.
199. **Papa, A., T. Bakonyi, K. Xanthopoulou, A. Vazquez, A. Tenorio, and N. Nowotny.** 2011. Genetic characterization of West Nile virus lineage 2, Greece, 2010. *Emerging infectious diseases* **17**:920-922.
200. **Papa, A., K. Danis, A. Baka, A. Bakas, G. Dougas, T. Lytras, G. Theocharopoulos, D. Chrysagis, E. Vassiliadou, F. Kamaria, A. Liona,**

- K. Mellou, G. Saroglou, and T. Panagiotopoulos.** 2010. Ongoing outbreak of West Nile virus infections in humans in Greece, July-August 2010. *Euro surveillance : bulletin Europeen sur les maladies transmissibles = European communicable disease bulletin* **15**.
201. **Papa, A., K. Xanthopoulou, S. Gewehr, and S. Mourelatos.** 2011. Detection of West Nile virus lineage 2 in mosquitoes during a human outbreak in Greece. *Clinical microbiology and infection : the official publication of the European Society of Clinical Microbiology and Infectious Diseases* **17**:1176-1180.
202. **Parham, P.** 1995. Antigen presentation by class I major histocompatibility complex molecules: a context for thinking about HLA-G. *Am J Reprod Immunol* **34**:10-19.
203. **Pedersen, I. M., G. Cheng, S. Wieland, S. Volinia, C. M. Croce, F. V. Chisari, and M. David.** 2007. Interferon modulation of cellular microRNAs as an antiviral mechanism. *Nature* **449**:919-922.
204. **Penn, R. G., J. Guarner, J. J. Sejvar, H. Hartman, R. D. McComb, D. L. Nevins, J. Bhatnagar, and S. R. Zaki.** 2006. Persistent neuroinvasive West Nile virus infection in an immunocompromised patient. *Clinical infectious diseases : an official publication of the Infectious Diseases Society of America* **42**:680-683.
205. **Perry, A. K., G. Chen, D. Zheng, H. Tang, and G. Cheng.** 2005. The host type I interferon response to viral and bacterial infections. *Cell research* **15**:407-422.

206. **Pestka, S.** 1997. The interferon receptors. *Seminars in oncology* **24**:S9-18-S19-40.
207. **Plevka, P., A. J. Battisti, J. Junjhon, D. C. Winkler, H. A. Holdaway, P. Keelapang, N. Sittisombut, R. J. Kuhn, A. C. Steven, and M. G. Rossmann.** 2011. Maturation of flaviviruses starts from one or more icosahedrally independent nucleation centres. *EMBO reports* **12**:602-606.
208. **Pogodina, V. V., M. P. Frolova, G. V. Malenko, G. I. Fokina, G. V. Koreshkova, L. L. Kiseleva, N. G. Bochkova, and N. M. Ralph.** 1983. Study on West Nile virus persistence in monkeys. *Archives of virology* **75**:71-86.
209. **Pozner, R. G., S. Collado, C. Jaquenod de Giusti, A. E. Ure, M. E. Biedma, V. Romanowski, M. Schattner, and R. M. Gomez.** 2008. Astrocyte response to Junin virus infection. *Neuroscience letters* **445**:31-35.
210. **Proudfoot, A. E., T. M. Handel, Z. Johnson, E. K. Lau, P. LiWang, I. Clark-Lewis, F. Borlat, T. N. Wells, and M. H. Kosco-Vilbois.** 2003. Glycosaminoglycan binding and oligomerization are essential for the in vivo activity of certain chemokines. *Proceedings of the National Academy of Sciences of the United States of America* **100**:1885-1890.
211. **Purtha, W. E., K. A. Chachu, H. W. t. Virgin, and M. S. Diamond.** 2008. Early B-cell activation after West Nile virus infection requires alpha/beta interferon but not antigen receptor signaling. *Journal of virology* **82**:10964-10974.

212. **Ramos, H. J., M. C. Lanteri, G. Blahnik, A. Negash, M. S. Suthar, M. M. Brassil, K. Sodhi, P. M. Treuting, M. P. Busch, P. J. Norris, and M. Gale, Jr.** 2012. IL-1beta signaling promotes CNS-intrinsic immune control of West Nile virus infection. *PLoS pathogens* **8**:e1003039.
213. **Ransohoff, R. M., P. Kivisakk, and G. Kidd.** 2003. Three or more routes for leukocyte migration into the central nervous system. *Nature reviews. Immunology* **3**:569-581.
214. **Redzic, Z.** 2011. Molecular biology of the blood-brain and the blood-cerebrospinal fluid barriers: similarities and differences. *Fluids and barriers of the CNS* **8**:3.
215. **Reith, W., S. LeibundGut-Landmann, and J. M. Waldburger.** 2005. Regulation of MHC class II gene expression by the class II transactivator. *Nature reviews. Immunology* **5**:793-806.
216. **Rios, J. J., J. G. Fleming, U. K. Bryant, C. N. Carter, J. C. Huber, M. T. Long, T. E. Spencer, and D. L. Adelson.** 2010. OAS1 polymorphisms are associated with susceptibility to West Nile encephalitis in horses. *PLoS one* **5**:e10537.
217. **Risau, W.** 1991. Induction of blood-brain barrier endothelial cell differentiation. *Annals of the New York Academy of Sciences* **633**:405-419.
218. **Risau, W., and H. Wolburg.** 1990. Development of the blood-brain barrier. *Trends in neurosciences* **13**:174-178.

219. **Roberts, T. K., E. A. Eugenin, L. Lopez, I. A. Romero, B. B. Weksler, P. O. Couraud, and J. W. Berman.** 2012. CCL2 disrupts the adherens junction: implications for neuroinflammation. *Laboratory investigation; a journal of technical methods and pathology* **92**:1213-1233.
220. **Roberts, W. K., M. J. Clemens, and I. M. Kerr.** 1976. Interferon-induced inhibition of protein synthesis in L-cell extracts: an ATP-dependent step in the activation of an inhibitor by double-stranded RNA. *Proceedings of the National Academy of Sciences of the United States of America* **73**:3136-3140.
221. **Roberts, W. K., A. Hovanessian, R. E. Brown, M. J. Clemens, and I. M. Kerr.** 1976. Interferon-mediated protein kinase and low-molecular-weight inhibitor of protein synthesis. *Nature* **264**:477-480.
222. **Roe, K., M. Kumar, S. Lum, B. Orillo, V. R. Nerurkar, and S. Verma.** 2012. West Nile virus-induced disruption of the blood-brain barrier in mice is characterized by the degradation of the junctional complex proteins and increase in multiple matrix metalloproteinases. *The Journal of general virology* **93**:1193-1203.
223. **Ruzek, D., J. Salat, S. K. Singh, and J. Kopecky.** 2011. Breakdown of the blood-brain barrier during tick-borne encephalitis in mice is not dependent on CD8+ T-cells. *PloS one* **6**:e20472.
224. **Sadler, A. J., and B. R. Williams.** 2008. Interferon-inducible antiviral effectors. *Nature reviews. Immunology* **8**:559-568.

225. **Samarajiwa, S. A., S. Forster, K. Auchetti, and P. J. Hertzog.** 2009. INTERFEROME: the database of interferon regulated genes. *Nucleic acids research* **37**:D852-857.
226. **Samuel, M. A., and M. S. Diamond.** 2005. Alpha/beta interferon protects against lethal West Nile virus infection by restricting cellular tropism and enhancing neuronal survival. *Journal of virology* **79**:13350-13361.
227. **Samuel, M. A., and M. S. Diamond.** 2006. Pathogenesis of West Nile Virus infection: a balance between virulence, innate and adaptive immunity, and viral evasion. *Journal of virology* **80**:9349-9360.
228. **Samuel, M. A., J. D. Morrey, and M. S. Diamond.** 2007. Caspase 3-dependent cell death of neurons contributes to the pathogenesis of West Nile virus encephalitis. *Journal of virology* **81**:2614-2623.
229. **Samuel, M. A., H. Wang, V. Siddharthan, J. D. Morrey, and M. S. Diamond.** 2007. Axonal transport mediates West Nile virus entry into the central nervous system and induces acute flaccid paralysis. *Proceedings of the National Academy of Sciences of the United States of America* **104**:17140-17145.
230. **Samuel, M. A., K. Whitby, B. C. Keller, A. Marri, W. Barchet, B. R. Williams, R. H. Silverman, M. Gale, Jr., and M. S. Diamond.** 2006. PKR and RNase L contribute to protection against lethal West Nile Virus infection by controlling early viral spread in the periphery and replication in neurons. *Journal of virology* **80**:7009-7019.

231. **Sangster, M. Y., D. B. Heliam, J. S. MacKenzie, and G. R. Shellam.** 1993. Genetic studies of flavivirus resistance in inbred strains derived from wild mice: evidence for a new resistance allele at the flavivirus resistance locus (Flv). *Journal of virology* **67**:340-347.
232. **Sangster, M. Y., J. S. Mackenzie, and G. R. Shellam.** 1998. Genetically determined resistance to flavivirus infection in wild *Mus musculus domesticus* and other taxonomic groups in the genus *Mus*. *Archives of virology* **143**:697-715.
233. **Sant, A. J., and A. McMichael.** 2012. Revealing the role of CD4(+) T cells in viral immunity. *The Journal of experimental medicine* **209**:1391-1395.
234. **Saura, J.** 2007. Microglial cells in astroglial cultures: a cautionary note. *Journal of neuroinflammation* **4**:26.
235. **Scherbik, S. V., and M. A. Brinton.** 2010. Virus-induced Ca²⁺ influx extends survival of west nile virus-infected cells. *Journal of virology* **84**:8721-8731.
236. **Scherbik, S. V., B. M. Stockman, and M. A. Brinton.** 2007. Differential expression of interferon (IFN) regulatory factors and IFN-stimulated genes at early times after West Nile virus infection of mouse embryo fibroblasts. *Journal of virology* **81**:12005-12018.
237. **Scherret, J. H., J. S. Mackenzie, A. A. Khromykh, and R. A. Hall.** 2001. Biological significance of glycosylation of the envelope protein of Kunjin virus. *Annals of the New York Academy of Sciences* **951**:361-363.

238. **Schluns, K. S., and L. Lefrancois.** 2003. Cytokine control of memory T-cell development and survival. *Nature reviews. Immunology* **3**:269-279.
239. **Schneider, C. A., W. S. Rasband, and K. W. Eliceiri.** 2012. NIH Image to ImageJ: 25 years of image analysis. *Nature methods* **9**:671-675.
240. **Schneider-Schaulies, J., V. Meulen, and S. Schneider-Schaulies.** 2003. Measles infection of the central nervous system. *Journal of neurovirology* **9**:247-252.
241. **Seifert, G., K. Schilling, and C. Steinhauser.** 2006. Astrocyte dysfunction in neurological disorders: a molecular perspective. *Nature reviews. Neuroscience* **7**:194-206.
242. **Sejvar, J. J.** 2007. The long-term outcomes of human West Nile virus infection. *Clinical infectious diseases : an official publication of the Infectious Diseases Society of America* **44**:1617-1624.
243. **Sejvar, J. J., L. E. Davis, E. Szabados, and A. C. Jackson.** 2010. Delayed-onset and recurrent limb weakness associated with West Nile virus infection. *Journal of neurovirology* **16**:93-100.
244. **Shi, P. Y., W. Li, and M. A. Brinton.** 1996. Cell proteins bind specifically to West Nile virus minus-strand 3' stem-loop RNA. *Journal of virology* **70**:6278-6287.
245. **Shi, P. Y., M. Tilgner, M. K. Lo, K. A. Kent, and K. A. Bernard.** 2002. Infectious cDNA clone of the epidemic west nile virus from New York City. *Journal of virology* **76**:5847-5856.

246. **Shirato, K., T. Kimura, T. Mizutani, H. Kariwa, and I. Takashima.** 2004. Different chemokine expression in lethal and non-lethal murine West Nile virus infection. *Journal of medical virology* **74**:507-513.
247. **Shrestha, B., and M. S. Diamond.** 2007. Fas ligand interactions contribute to CD8⁺ T-cell-mediated control of West Nile virus infection in the central nervous system. *Journal of virology* **81**:11749-11757.
248. **Shrestha, B., and M. S. Diamond.** 2004. Role of CD8⁺ T cells in control of West Nile virus infection. *Journal of virology* **78**:8312-8321.
249. **Shrestha, B., D. Gottlieb, and M. S. Diamond.** 2003. Infection and injury of neurons by West Nile encephalitis virus. *Journal of virology* **77**:13203-13213.
250. **Shrestha, B., A. K. Pinto, S. Green, I. Bosch, and M. S. Diamond.** 2012. CD8⁺ T cells use TRAIL to restrict West Nile virus pathogenesis by controlling infection in neurons. *Journal of virology* **86**:8937-8948.
251. **Shrestha, B., M. A. Samuel, and M. S. Diamond.** 2006. CD8⁺ T cells require perforin to clear West Nile virus from infected neurons. *Journal of virology* **80**:119-129.
252. **Shrestha, B., T. Wang, M. A. Samuel, K. Whitby, J. Craft, E. Fikrig, and M. S. Diamond.** 2006. Gamma interferon plays a crucial early antiviral role in protection against West Nile virus infection. *Journal of virology* **80**:5338-5348.
253. **Shrestha, B., B. Zhang, W. E. Purtha, R. S. Klein, and M. S. Diamond.** 2008. Tumor necrosis factor alpha protects against lethal West Nile virus

- infection by promoting trafficking of mononuclear leukocytes into the central nervous system. *Journal of virology* **82**:8956-8964.
254. **Shrikant, P., and E. N. Benveniste.** 1996. The central nervous system as an immunocompetent organ: role of glial cells in antigen presentation. *J Immunol* **157**:1819-1822.
255. **Siddharthan, V., H. Wang, N. E. Motter, J. O. Hall, R. D. Skinner, R. T. Skirpstunas, and J. D. Morrey.** 2009. Persistent West Nile virus associated with a neurological sequela in hamsters identified by motor unit number estimation. *Journal of virology* **83**:4251-4261.
256. **Sitati, E., E. E. McCandless, R. S. Klein, and M. S. Diamond.** 2007. CD40-CD40 ligand interactions promote trafficking of CD8+ T cells into the brain and protection against West Nile virus encephalitis. *Journal of virology* **81**:9801-9811.
257. **Sitati, E. M., and M. S. Diamond.** 2006. CD4+ T-cell responses are required for clearance of West Nile virus from the central nervous system. *Journal of virology* **80**:12060-12069.
258. **SMITHBURN, K. C., HUGHES, T.P., BURKE, A.W. and PAUL, J.H. .** 1940. A neurotropic virus isolated from the blood of a native of Uganda. *American Journal of Tropical Medicine and Hygiene* **20**:471-492.
259. **Sofroniew, M. V., and H. V. Vinters.** 2010. Astrocytes: biology and pathology. *Acta neuropathologica* **119**:7-35.
260. **Soilu-Hanninen, M., J. P. Eralinna, V. Hukkanen, M. Roytta, A. A. Salmi, and R. Salonen.** 1994. Semliki Forest virus infects mouse brain

- endothelial cells and causes blood-brain barrier damage. *Journal of virology* **68**:6291-6298.
261. **Springer, T. A.** 1994. Traffic signals for lymphocyte recirculation and leukocyte emigration: the multistep paradigm. *Cell* **76**:301-314.
262. **Stadler, K., S. L. Allison, J. Schlich, and F. X. Heinz.** 1997. Proteolytic activation of tick-borne encephalitis virus by furin. *Journal of virology* **71**:8475-8481.
263. **Stewart, B. S., V. L. Demarest, S. J. Wong, S. Green, and K. A. Bernard.** 2011. Persistence of virus-specific immune responses in the central nervous system of mice after West Nile virus infection. *BMC immunology* **12**:6.
264. **Stins, M. F., J. Badger, and K. Sik Kim.** 2001. Bacterial invasion and transcytosis in transfected human brain microvascular endothelial cells. *Microbial pathogenesis* **30**:19-28.
265. **Stins, M. F., F. Gilles, and K. S. Kim.** 1997. Selective expression of adhesion molecules on human brain microvascular endothelial cells. *Journal of neuroimmunology* **76**:81-90.
266. **Styer, L. M., K. A. Kent, R. G. Albright, C. J. Bennett, L. D. Kramer, and K. A. Bernard.** 2007. Mosquitoes inoculate high doses of West Nile virus as they probe and feed on live hosts. *PLoS pathogens* **3**:1262-1270.
267. **Styer, L. M., P. Y. Lim, K. L. Louie, R. G. Albright, L. D. Kramer, and K. A. Bernard.** 2011. Mosquito saliva causes enhancement of West Nile virus infection in mice. *Journal of virology* **85**:1517-1527.

268. **Sultana, H., G. Neelakanta, H. G. Foellmer, R. R. Montgomery, J. F. Anderson, R. A. Koski, R. M. Medzhitov, and E. Fikrig.** 2012. Semaphorin 7A contributes to West Nile virus pathogenesis through TGF-beta1/Smad6 signaling. *J Immunol* **189**:3150-3158.
269. **Suthar, M. S., M. M. Brassil, G. Blahnik, and M. Gale, Jr.** 2012. Infectious clones of novel lineage 1 and lineage 2 West Nile virus strains WNV-TX02 and WNV-Madagascar. *Journal of virology* **86**:7704-7709.
270. **Suthar, M. S., D. Y. Ma, S. Thomas, J. M. Lund, N. Zhang, S. Daffis, A. Y. Rudensky, M. J. Bevan, E. A. Clark, M. K. Kaja, M. S. Diamond, and M. Gale, Jr.** 2010. IPS-1 is essential for the control of West Nile virus infection and immunity. *PLoS pathogens* **6**:e1000757.
271. **Szretter, K. J., J. D. Brien, L. B. Thackray, H. W. Virgin, P. Cresswell, and M. S. Diamond.** 2011. The interferon-inducible gene viperin restricts West Nile virus pathogenesis. *Journal of virology* **85**:11557-11566.
272. **Szretter, K. J., S. Daffis, J. Patel, M. S. Suthar, R. S. Klein, M. Gale, Jr., and M. S. Diamond.** 2010. The innate immune adaptor molecule MyD88 restricts West Nile virus replication and spread in neurons of the central nervous system. *Journal of virology* **84**:12125-12138.
273. **Szretter, K. J., B. P. Daniels, H. Cho, M. D. Gainey, W. M. Yokoyama, M. Gale, Jr., H. W. Virgin, R. S. Klein, G. C. Sen, and M. S. Diamond.** 2012. 2'-O methylation of the viral mRNA cap by West Nile virus evades ifit1-dependent and -independent mechanisms of host restriction in vivo. *PLoS pathogens* **8**:e1002698.

274. **Szretter, K. J., M. A. Samuel, S. Gilfillan, A. Fuchs, M. Colonna, and M. S. Diamond.** 2009. The immune adaptor molecule SARM modulates tumor necrosis factor alpha production and microglia activation in the brainstem and restricts West Nile Virus pathogenesis. *Journal of virology* **83**:9329-9338.
275. **Takaoka, A., H. Yanai, S. Kondo, G. Duncan, H. Negishi, T. Mizutani, S. Kano, K. Honda, Y. Ohba, T. W. Mak, and T. Taniguchi.** 2005. Integral role of IRF-5 in the gene induction programme activated by Toll-like receptors. *Nature* **434**:243-249.
276. **Takeuchi, O., and S. Akira.** 2010. Pattern recognition receptors and inflammation. *Cell* **140**:805-820.
277. **Tan le, V., H. R. van Doorn, H. D. Nghia, T. T. Chau, T. P. Tu le, M. de Vries, M. Canuti, M. Deijis, M. F. Jebbink, S. Baker, J. E. Bryant, N. T. Tham, B. K. NT, M. F. Boni, T. Q. Loi, T. Phuong le, J. T. Verhoeven, M. Crusat, R. E. Jeeninga, C. Schultsz, N. V. Chau, T. T. Hien, L. van der Hoek, J. Farrar, and M. D. de Jong.** 2013. Identification of a new cyclovirus in cerebrospinal fluid of patients with acute central nervous system infections. *mBio* **4**:e00231-00213.
278. **Tautz, N., G. Meyers, and H. J. Thiel.** 1998. Pathogenesis of mucosal disease, a deadly disease of cattle caused by a pestivirus. *Clinical and diagnostic virology* **10**:121-127.
279. **Topp, K. S., L. B. Meade, and J. H. LaVail.** 1994. Microtubule polarity in the peripheral processes of trigeminal ganglion cells: relevance for the

- retrograde transport of herpes simplex virus. *The Journal of neuroscience : the official journal of the Society for Neuroscience* **14**:318-325.
280. **Town, T., F. Bai, T. Wang, A. T. Kaplan, F. Qian, R. R. Montgomery, J. F. Anderson, R. A. Flavell, and E. Fikrig.** 2009. Toll-like receptor 7 mitigates lethal West Nile encephalitis via interleukin 23-dependent immune cell infiltration and homing. *Immunity* **30**:242-253.
281. **Tumne, A., V. S. Prasad, Y. Chen, D. B. Stolz, K. Saha, D. M. Ratner, M. Ding, S. C. Watkins, and P. Gupta.** 2009. Noncytotoxic suppression of human immunodeficiency virus type 1 transcription by exosomes secreted from CD8+ T cells. *Journal of virology* **83**:4354-4364.
282. **van Marle, G., J. Antony, H. Ostermann, C. Dunham, T. Hunt, W. Halliday, F. Maingat, M. D. Urbanowski, T. Hobman, J. Peeling, and C. Power.** 2007. West Nile virus-induced neuroinflammation: glial infection and capsid protein-mediated neurovirulence. *Journal of virology* **81**:10933-10949.
283. **van Sorge, N. M., D. Quach, M. A. Gurney, P. M. Sullam, V. Nizet, and K. S. Doran.** 2009. The group B streptococcal serine-rich repeat 1 glycoprotein mediates penetration of the blood-brain barrier. *The Journal of infectious diseases* **199**:1479-1487.
284. **Verma, S., M. Kumar, U. Gurjav, S. Lum, and V. R. Nerurkar.** 2010. Reversal of West Nile virus-induced blood-brain barrier disruption and tight junction proteins degradation by matrix metalloproteinases inhibitor. *Virology* **397**:130-138.

285. **Verma, S., Y. Lo, M. Chapagain, S. Lum, M. Kumar, U. Gurjav, H. Luo, A. Nakatsuka, and V. R. Nerurkar.** 2009. West Nile virus infection modulates human brain microvascular endothelial cells tight junction proteins and cell adhesion molecules: Transmigration across the in vitro blood-brain barrier. *Virology* **385**:425-433.
286. **Vogel, P., W. M. Kell, D. L. Fritz, M. D. Parker, and R. J. Schoepp.** 2005. Early events in the pathogenesis of eastern equine encephalitis virus in mice. *The American journal of pathology* **166**:159-171.
287. **von Andrian, U. H., and T. R. Mempel.** 2003. Homing and cellular traffic in lymph nodes. *Nature reviews. Immunology* **3**:867-878.
288. **Voskuhl, R. R., R. S. Peterson, B. Song, Y. Ao, L. B. Morales, S. Tiwari-Woodruff, and M. V. Sofroniew.** 2009. Reactive astrocytes form scar-like perivascular barriers to leukocytes during adaptive immune inflammation of the CNS. *The Journal of neuroscience : the official journal of the Society for Neuroscience* **29**:11511-11522.
289. **Wang, J., and I. L. Campbell.** 2005. Innate STAT1-dependent genomic response of neurons to the antiviral cytokine alpha interferon. *Journal of virology* **79**:8295-8302.
290. **Wang, L., H. Zhang, F. Zhong, and J. Lu.** 2004. A toll-like receptor-based two-hybrid assay for detecting protein--protein interactions on live eukaryotic cells. *Journal of immunological methods* **292**:175-186.
291. **Wang, P., F. Bai, L. A. Zenewicz, J. Dai, D. Gate, G. Cheng, L. Yang, F. Qian, X. Yuan, R. R. Montgomery, R. A. Flavell, T. Town, and E. Fikrig.**

2012. IL-22 signaling contributes to West Nile encephalitis pathogenesis. *PloS one* **7**:e44153.
292. **Wang, P., J. Dai, F. Bai, K. F. Kong, S. J. Wong, R. R. Montgomery, J. A. Madri, and E. Fikrig.** 2008. Matrix metalloproteinase 9 facilitates West Nile virus entry into the brain. *Journal of virology* **82**:8978-8985.
293. **Wang, S., T. Q. Le, N. Kurihara, J. Chida, Y. Cisse, M. Yano, and H. Kido.** 2010. Influenza virus-cytokine-protease cycle in the pathogenesis of vascular hyperpermeability in severe influenza. *The Journal of infectious diseases* **202**:991-1001.
294. **Wang, S., M. B. Voisin, K. Y. Larbi, J. Dangerfield, C. Scheiermann, M. Tran, P. H. Maxwell, L. Sorokin, and S. Nourshargh.** 2006. Venular basement membranes contain specific matrix protein low expression regions that act as exit points for emigrating neutrophils. *The Journal of experimental medicine* **203**:1519-1532.
295. **Wang, S., T. Welte, M. McGargill, T. Town, J. Thompson, J. F. Anderson, R. A. Flavell, E. Fikrig, S. M. Hedrick, and T. Wang.** 2008. Drak2 contributes to West Nile virus entry into the brain and lethal encephalitis. *J Immunol* **181**:2084-2091.
296. **Wang, T., Y. Gao, E. Scully, C. T. Davis, J. F. Anderson, T. Welte, M. Ledizet, R. Koski, J. A. Madri, A. Barrett, Z. Yin, J. Craft, and E. Fikrig.** 2006. Gamma delta T cells facilitate adaptive immunity against West Nile virus infection in mice. *J Immunol* **177**:1825-1832.

297. **Wang, T., T. Town, L. Alexopoulou, J. F. Anderson, E. Fikrig, and R. A. Flavell.** 2004. Toll-like receptor 3 mediates West Nile virus entry into the brain causing lethal encephalitis. *Nature medicine* **10**:1366-1373.
298. **Wang, Y., M. Lobigs, E. Lee, A. Koskinen, and A. Mullbacher.** 2006. CD8(+) T cell-mediated immune responses in West Nile virus (Sarafend strain) encephalitis are independent of gamma interferon. *The Journal of general virology* **87**:3599-3609.
299. **Wang, Y., M. Lobigs, E. Lee, and A. Mullbacher.** 2003. CD8+ T cells mediate recovery and immunopathology in West Nile virus encephalitis. *Journal of virology* **77**:13323-13334.
300. **Wang, Y., M. Lobigs, E. Lee, and A. Mullbacher.** 2004. Exocytosis and Fas mediated cytolytic mechanisms exert protection from West Nile virus induced encephalitis in mice. *Immunology and cell biology* **82**:170-173.
301. **Weber, C.** 2003. Novel mechanistic concepts for the control of leukocyte transmigration: specialization of integrins, chemokines, and junctional molecules. *J Mol Med (Berl)* **81**:4-19.
302. **Weingartl, H., S. Czub, J. Copps, Y. Berhane, D. Middleton, P. Marszal, J. Gren, G. Smith, S. Ganske, L. Manning, and M. Czub.** 2005. Invasion of the central nervous system in a porcine host by nipah virus. *Journal of virology* **79**:7528-7534.
303. **Wengler, G., E. Castle, U. Leidner, T. Nowak, and G. Wengler.** 1985. Sequence analysis of the membrane protein V3 of the flavivirus West Nile virus and of its gene. *Virology* **147**:264-274.

304. **Wengler, G., G. Czaya, P. M. Farber, and J. H. Hegemann.** 1991. In vitro synthesis of West Nile virus proteins indicates that the amino-terminal segment of the NS3 protein contains the active centre of the protease which cleaves the viral polyprotein after multiple basic amino acids. *The Journal of general virology* **72 (Pt 4):**851-858.
305. **Wengler, G., and G. Wengler.** 1993. The NS 3 nonstructural protein of flaviviruses contains an RNA triphosphatase activity. *Virology* **197:**265-273.
306. **Westaway, E. G., J. M. Mackenzie, M. T. Kenney, M. K. Jones, and A. A. Khromykh.** 1997. Ultrastructure of Kunjin virus-infected cells: colocalization of NS1 and NS3 with double-stranded RNA, and of NS2B with NS3, in virus-induced membrane structures. *Journal of virology* **71:**6650-6661.
307. **Westaway, E. G., J. M. Mackenzie, and A. A. Khromykh.** 2002. Replication and gene function in Kunjin virus. *Current topics in microbiology and immunology* **267:**323-351.
308. **Whiteman, M. C., L. Li, J. A. Wicker, R. M. Kinney, C. Huang, D. W. Beasley, K. M. Chung, M. S. Diamond, T. Solomon, and A. D. Barrett.** 2010. Development and characterization of non-glycosylated E and NS1 mutant viruses as a potential candidate vaccine for West Nile virus. *Vaccine* **28:**1075-1083.
309. **Wilhelm, I., C. Fazakas, and I. A. Krizbai.** 2011. In vitro models of the blood-brain barrier. *Acta neurobiologiae experimentalis* **71:**113-128.

310. **Winkler, G., F. X. Heinz, and C. Kunz.** 1987. Characterization of a disulphide bridge-stabilized antigenic domain of tick-borne encephalitis virus structural glycoprotein. *The Journal of general virology* **68 (Pt 8):**2239-2244.
311. **Winkler, G., S. E. Maxwell, C. Ruemmler, and V. Stollar.** 1989. Newly synthesized dengue-2 virus nonstructural protein NS1 is a soluble protein but becomes partially hydrophobic and membrane-associated after dimerization. *Virology* **171:**302-305.
312. **Xie, Y., K. J. Kim, and K. S. Kim.** 2004. Current concepts on Escherichia coli K1 translocation of the blood-brain barrier. *FEMS immunology and medical microbiology* **42:**271-279.
313. **Yamamoto, M., S. Sato, K. Mori, K. Hoshino, O. Takeuchi, K. Takeda, and S. Akira.** 2002. Cutting edge: a novel Toll/IL-1 receptor domain-containing adapter that preferentially activates the IFN-beta promoter in the Toll-like receptor signaling. *J Immunol* **169:**6668-6672.
314. **Yamshchikov, G., V. Borisevich, A. Seregin, E. Chaporgina, M. Mishina, V. Mishin, C. W. Kwok, and V. Yamshchikov.** 2004. An attenuated West Nile prototype virus is highly immunogenic and protects against the deadly NY99 strain: a candidate for live WN vaccine development. *Virology* **330:**304-312.
315. **Yang, Y. L., L. F. Reis, J. Pavlovic, A. Aguzzi, R. Schafer, A. Kumar, B. R. Williams, M. Aguet, and C. Weissmann.** 1995. Deficient signaling in

- mice devoid of double-stranded RNA-dependent protein kinase. The EMBO journal **14**:6095-6106.
316. **Ye, J., B. Zhu, Z. F. Fu, H. Chen, and S. Cao.** 2013. Immune evasion strategies of flaviviruses. Vaccine **31**:461-471.
317. **Yoneyama, M., M. Kikuchi, T. Natsukawa, N. Shinobu, T. Imaizumi, M. Miyagishi, K. Taira, S. Akira, and T. Fujita.** 2004. The RNA helicase RIG-I has an essential function in double-stranded RNA-induced innate antiviral responses. Nature immunology **5**:730-737.
318. **Zarbock, A., and K. Ley.** 2008. Mechanisms and consequences of neutrophil interaction with the endothelium. The American journal of pathology **172**:1-7.
319. **Zhang, B., H. Dong, Y. Zhou, and P. Y. Shi.** 2008. Genetic interactions among the West Nile virus methyltransferase, the RNA-dependent RNA polymerase, and the 5' stem-loop of genomic RNA. Journal of virology **82**:7047-7058.
320. **Zhang, M., B. Gaschen, W. Blay, B. Foley, N. Haigwood, C. Kuiken, and B. Korber.** 2004. Tracking global patterns of N-linked glycosylation site variation in highly variable viral glycoproteins: HIV, SIV, and HCV envelopes and influenza hemagglutinin. Glycobiology **14**:1229-1246.
321. **Zhang, W., B. Kaufmann, P. R. Chipman, R. J. Kuhn, and M. G. Rossmann.** 2013. Membrane curvature in flaviviruses. Journal of structural biology **183**:86-94.

322. **Zhang, Y., B. Kaufmann, P. R. Chipman, R. J. Kuhn, and M. G. Rossmann.** 2007. Structure of immature West Nile virus. *Journal of virology* **81**:6141-6145.
323. **Zhao, C., C. Denison, J. M. Huibregtse, S. Gygi, and R. M. Krug.** 2005. Human ISG15 conjugation targets both IFN-induced and constitutively expressed proteins functioning in diverse cellular pathways. *Proceedings of the National Academy of Sciences of the United States of America* **102**:10200-10205.